NEDO-22171
82NED073
CLASS I
JULY 1982

CORE SPRAY SPARGER CRACK ANALYSIS AT BRUNSWICK STEAM ELECTRIC PLANT — UNIT 2

GENERAL ELECTRIC

NEDO-22171
DRF E21-0067
82NED073
Class I
July 1982

CORE SPRAY SPARGER CRACK ANALYSIS
AT
BRUNSWICK STEAM ELECTRIC PLANT
UNIT 2

Approved: R. J. Brandon, Manager
Nuclear Services Engineering
Operation

Approved: for
E. Kiss, Manager
Plant Materials and
Mechanics Section
Nuclear Power Systems
Engineering Department

Approved: for
R. L. Gridley, Manager
Fuel and Services Licensing
Safety and Licensing Operation

IMPORTANT NOTICE REGARDING
CONTENTS OF THIS REPORT
PLEASE READ CAREFULLY

This report was prepared by General Electric solely for Carolina Power & Light (CP&L) for CP&L's use with the U.S. Nuclear Regulatory Commission (USNRC) for the Brunswick Steam Electric Plant Unit 2. The information contained in this report is believed by General Electric to be an accurate and true representation of the facts known, obtained or provided to General Electric at the time this report was prepared.

The only undertakings of the General Electric Company respecting information in this document are contained in the General Electric Company Proposal No. 424-TY706-KBO, Rev 1. ("Core Spray Sparger Crack Contingency Analysis for Carolina Power & Light Co., Brunswick Steam Electric Plant Unit 2", dated May 1982), and CP&L P.O. No. 769128. The use of this information except as defined by said contract or for any purpose other than that for which it is intended, is not authorized; and with respect to any such unauthorized use, neither General Electric Company nor any of the contributors to this document makes any representation or warranty (express or implied) as to the completeness, accuracy or usefulness of the information contained in this document or that such use of such information may not infringe privately owned rights; nor do they assume any responsibility for liability of damage of any kind which may result from such use of such information.

CONTENTS

CONTENTS (Continued)

APPENDICES

TABLES

ILLUSTRATIONS

1. INTRODUCTION AND SUMMARY

One of the scheduled tasks during the Reload 4 refueling and maintenance outage in May, 1982 at the Brunswick Steam Electric Plant Unit 2 was the performance of a visual inspection of the Core Spray Spargers using underwater television cameras. This inspection was conducted as required by and in accordance with IE-Bulletin 80-13 (Reference 1-1).

During the inspection of the core spray spargers, a crack indication was observed on the upper sparger in the heat-affected-zone of the sparger to T-box weld. It is GE's understanding that this crack is approximately 120° in length, 5-10 mils in width. The crack location is shown in Figure 1-1. The discovery of the crack was reported to the NRC by CP&L.

On June 14, 1982 CP&L and GE met with members of the staff to present technical justification to support plant start-up with the core spray sparger in its current condition. This presentation included the technical basis to establish continued structural integrity of the upper core spray sparger for all normal and injection conditions. A discussion of the possible consequences of potential loose pieces from a cracked sparger was also presented. Finally, the effect of a postulated Loss Of Coolant Accident (LOCA) with a cracked core spray sparger was discussed. This information is documented in this report. Supplemental information provided by GE to CP&L on June 15, 1982 for use in continued discussions with the staff is also documented here.

1.1 STRUCTURAL

A structural analysis is presented in Section 2, which describes the potential sources of stress in the spargers resulting from fabrication, installation, normal operation, and operation during postulated LOCA. It is concluded that the structural integrity of the sparger will be maintained for all conditions of operation. In addition, potential causes of cracking are discussed, and it is concluded that the most likely cause is Intergranular Stress Corrosion Cracking (IGSCC).

1.2 LOST PARTS

Because continued sparger structural integrity has been demonstrated, lost parts (loose pieces) are not expected. However, a lost parts analysis has been performed and is presented in Section 3. It is concluded that the probability of unacceptable flow blockage of a fuel assembly or for unacceptable control rod interference is essentially zero. The potential for corrosion or other chemical reaction with reactor materials is essentially zero because the sparger material is designed for in-vessel use. It is also shown that loose pieces are not expected to cause damage to the other reactor pressure vessel internals.

1.3 EFFECT ON LOCA ANALYSIS

Section 4 presents the results of LOCA analyses assuming one cracked core spray sparger. GE believes that the current reload analysis calculations are still valid because coolant injection to the upper plenum is maintained. It is concluded that there is no basis to impose a Maximum Average Planar Linear Heat Generation Rate (MAPLHGR) penalty on Brunswick 2.

1.4 CONCLUSION

A detailed evaluation of the Brunswick 2 core spray sparger cracks has been performed. This evaluation included structural, lost parts and LOCA analyses to determine the impact on plant operation of the cracked sparger. It is concluded that Brunswick 2 can safely operate in this condition and that no operational changes or restrictions are required.

1.5 REFERENCE

1-1 USNRC IE Bulletin No. 80-13, Cracking in Core Spray Spargers, May 12, 1980.

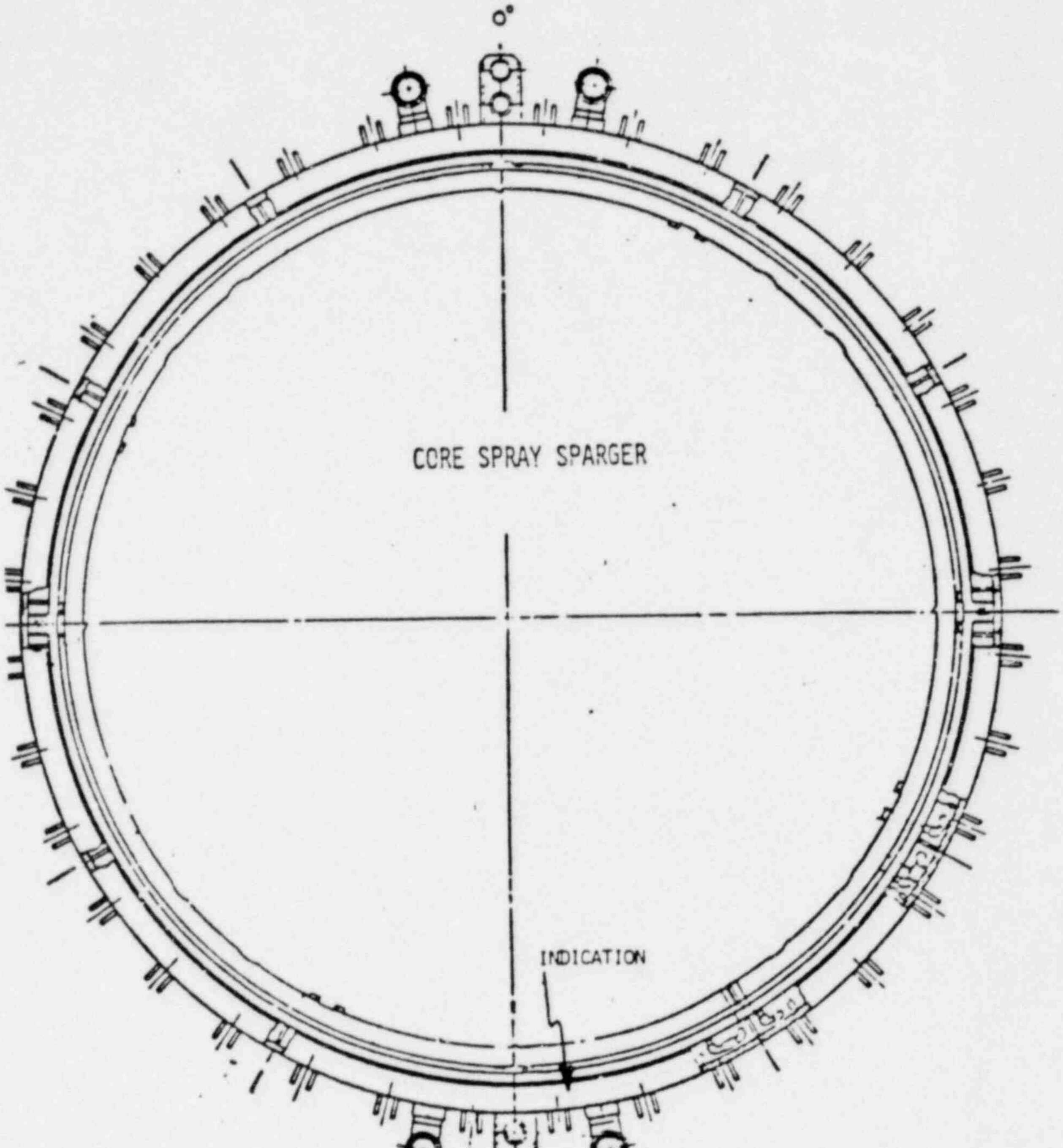

Figure 1-1a. Plan View of Cracked Core Spray Sparger

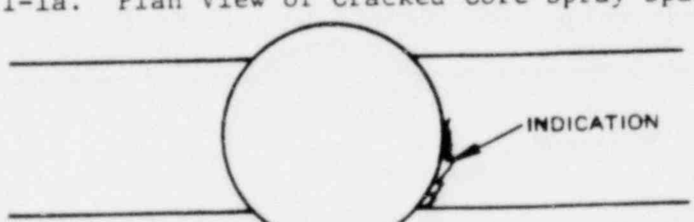

Figure 1-1b. Elevation View of Cracked Core Spray Sparger

2. CORE SPRAY SPARGER STRUCTURAL INTEGRITY

2.1 SPARGER CONFIGURATION

The core spray sparger configuration is shown in Figure 2-1 through 2-5.

The spargers are mounted in the upper shroud, as shown in Figure 2-1. Vertical spacing is 10-1/4 inches between header pipe centerlines. The upper sparger has bottom-mounted nozzles and the lower sparger has top-mounted elbows. The plan view (Figure 2-2) shows that the spargers are asymmetric. The shorter header pipe has an arc length of 80°, and the longer header pipe has an arc length of 100°. The T-boxes for the spargers are located ±10° from the vessel 0° and 180° azimuths.

Figure 2-3 shows the attachment of the T-box to the shroud. The T-box is a 5-in. Schedule 40 section of pipe with an end plate toward the vessel centerline. The 5-in. pipe extends through the shroud wall and is butt-welded to external piping. The T-box pipe is attached to the shroud by the seal ring with the attachment welds to the 5-in. pipe and the exterior surface of the shroud wall. This arrangement (as opposed to direct attachment) eliminates high thermally induced stresses during core spray injection of cold water into the reactor at operating temperature.

The sparger flow nozzles are depicted in Figure 2-4. The Brunswick 2 upper and lower core spray sparger headers use 1-in. shielded VNC nozzles alternating with SPRACO 3101 nozzles.

The 100° header pipe and the 80° header pipe are each supported at three locations. Figure 2-5 shows the support arrangement at locations between the T-box and end supports. The brackets are 1/2-in. thick and are welded to the shroud. The pipe-to-bracket mating surfaces are not welded to allow circumferential relative motion between the header pipe and the shroud during a core spray injection of cold wter into a system at reactor operating temperature. The header pipe is 3-1/2 in. Schedule 40 Type-304 stainless steel.

The street elbows, 90° elbows, orifices, tees and the close nipples (used to connect the elbows and orifice the elbows) are all Type-304 stainless steel.

2.2 FABRICATION SEQUENCE

Fabrication records show that the Brunswick 2 spargers were fabricated as follows:

1. The pipe was bent using a four-roll bending process as shown in Figure 2-6. The rollers have 2 in. radius grooves, and rollers 3 and 4 are adjustable to accommodate the pipe size and to bend the pipe to the required radius. In this case, the design radius is R = 91.25 inches. The maximum strain in the pipe is calculated to be 2.2%.

2. After the pipe is bent to the proper radius, it is placed in the shroud to verify that the pipe fits the shroud as-built conditions. During this fit-up process, the T-box 5-in. pipe is marked for drilling the header pipe holes.

3. After removing the pipe from the shroud, the headers are welded to the T-box.

4. The holes for each nozzle are drilled in the header pipes.

5. Stainless steel orifices are bevel welded at each nozzle opening.

6. The elbows are screwed into the assembly and roughly aimed.

2.3 INSTALLATION SEQUENCE

The sparger is installed in the shroud in the following manner:

1. The brackets are welded to the shroud, thereby positioning and holding the spargers. The T-box is attached to the shroud by

welding the seal ring to the T-box and the shroud. It is assumed that, because of interference between sparger ends, one or more of the spargers would be cold sprung during installation. This operation was not addressed in the fabrication records.

2. The next operation was to aim the nozzle as required by the sparger drawing.

3. The elbows were then tack welded to assure that the threaded connections remain intact.

2.4 PERFORMANCE HISTORY

Brunswick 2 first went critical in March 1975. There have bee- no inadvertent core spray injections. Brunswick 2 does flush the core spray spargers during refueling outages. Water is pumped from condensate storage at a temperature of approximately 70°F into the vessel at a temperature of approximately 200°F. The resulting ΔT is sufficiently low that fatigue is not a concern.

2.5 POTENTIAL SOURCES OF STRESS

The potential sources of stress in the core spray sparger which could result from fabrication, installation, normal plant operation, and operation of the core spray system during postulated loss-of-coolant accidents are presented in this section.

2.5.1 Fabrication Stresses

Residual stresses are developed when an initially straight pipe is subjected to a moment sufficient to cause yielding and later unloaded, as would occur during the fabrication of the core spray spargers. The fabrication operation is idealized in Figure 2-7. The steps involved in the calculation of the residual stresses are:

1. Determine the moment-curvature curve for the pipe assuming simple beam theory.

2. Calculate the applied moment, M_t, corresponding to the final unloaded radius of curvature. Determine the stress distribution associated with this moment.

3. Calculate the elastic stress distribution corresponding to the applied moment ($-M_t$) to describe the unloading.

4. Determine the residual stress in the pipe which is the algebraic sum of the elastic-plastic stresses due to M_t and the elastic stresses due to ($-M_t$).

In calculating the movement-curvature curve for the pipe, thin shell theory was applied and a representative bilinear stress-strain curve (Figure 2-8) was used.

As shown in Figure 2-9, the strain varies linearly through the section, while the stress follows the bilinear curve for angles greater than θ.

The applied moment (M_t) is given by:

$$M_t = 2 \int_0^\theta (E\varepsilon_o \text{ Sin}\phi) (a \sin\phi) (2atd\phi)$$

$$+ 2 \int_\theta^{\pi/2} \{(\varepsilon_o \text{ Sin } \phi - \varepsilon_y) E_t + E\varepsilon_y\} (a \text{ Sin}\phi) (2atd\phi) \qquad (2\text{-}1)$$

where

ε_o = a/R = outside strain

a = radius of pipe

R = radius of curvature

ε_y, σ_y = yield strain

E, E_t = elastic and plastic modulus, respectively

The first term in Equation 2-1 is the contribution from the elastic part of the stress distribution, and the second term corresponds to the plastic portion of the stress distribution.

After integration and rearrangement, Equation 2-1 becomes:

$$M_t = M_o \left[\frac{(1 - E_t/E)}{\pi} \left\{ \frac{(2\theta - \text{Sin}2\theta)}{\sin\theta} + 4\cos\theta \right\} + \frac{E_t}{E \sin\theta} \right]$$

and $\text{Sin}\theta = \varepsilon_y/\varepsilon_o \quad \frac{\varepsilon_y R}{a}$.

M_o = moment corresponding to the first onset of yielding on the outside surface = $\sigma_y \pi a^2 t$.

Clearly, for fully elastic behavior, $\theta = \pi/2$, and $M_t = M_o$.

Figure 2-10 shows the variation of the applied moment with the outside fiber strain and also the bend radius R. As shown in the figure, in order to get a final radius of 91.25 inches, the outer fiber strain during bending is 2.37%. The corresponding moment is $1.43\ \sigma_y\ \pi a^2 t$.

The residual stress distribution can now be determined by combining the elastic stress corresponding to ($-M_t$) and the elastic-plastic stress during bending. Figure 2-11 shows the resulting stress distribution.

Figure 2-11 shows that the pipe is subjected to high residual stresses (approaching the yield stress), and that the stress distribution varies around the circumference of the pipe. In particular, it shows tensile stresses on the surface facing the centerline of the vessel. It should be noted that the actual stresses could be higher due to local yielding at locations where

Hertzian contact stresses (between the roller and the pipe) occur during bending. Since this would be most likely to occur on the surface of the sparger facing the center of curvature, higher stresses could be expected at this location.

The residual stresses shown here were calculated for room temperature conditions. However, for reactor operating temperatures ≃550°F, the residual stresses are expected to relax to the yield value at that temperature (18.8 ksi at 550°F).

The conclusions from the evaluation of fabrication stresses presented in this section are summarized below:

1. Stresses due to fabrication could be significant and would exist throughout plant operation.

2. A possible synergistic combination of adverse metallurgical conditions (e.g., sensitization, cold work) and high residual stresses may explain the observed cracking.

3. Since the stresses change sign (become compressive) around the circumference, a crack that initiates in the tensile region can be expected to arrest in the compressive regions.

2.5.2 Installation Stresses

Stresses sufficient and necessary to cause initiation and propagation of cracks by intergranular stress corrosion cracking (IGSCC) can be identified by postulating certain installation variables. Figure 2-12 shows two cases which might be postulated.

In Case 1, it is postulated that differential weld shrinkage occurred during welding of the header pipes to the T-box. The outer bracket would provide a force to cause the header to contact the shroud wall. For simplicity, the arm is assumed to have an arc length of 90°. A 1/8-in. differential weld shrinkage is assumed. The deflection resulting at the header end would be approximately:

$$\frac{1/8}{4.0} = \frac{\Delta}{91.25} \; ; \; \Delta = 2.85 \text{ inch} .$$

Then, from Reference 2-1, Table 13.4, Case 1:

$$\Delta = \frac{WR^3}{4EI} (2\phi - \sin 2\phi) \text{ , where } \phi = 90°F .$$

Solving W = 647 lb, assuming:

R = 91.25 in.

E = 28.3×10^6 ksi

I = 4.79 in.^{4}

Since M = WR

$$\sigma = \frac{WRC}{I} = \frac{647 \times 91.25 \times 2.0}{4.79}$$

$$\sigma = 24700 \text{ psi}$$

$$\sigma \simeq 25000 \text{ psi (elastic)}$$

For Case 2, it is assumed that R is incorrectly fabricated to a radius of 90.25 inches. It is further assumed that the vessel brackets cause a uniform moment on the pipe, thus increasing the radius to 91.25 inches.

The initial inner length is $\pi/2 \times 88.25 = 138.62$. After forming, the inner length is $\pi/2 \times 89.25 = 140.19$:

$$\text{Strain} = \varepsilon = \frac{\Delta \ell_{inner}}{\ell_{inner}} = \frac{140.19 - 138.62}{138.62} = 0.011$$

$$= 1.1\%$$

Using a stress strain curve for Type-304 stainless steel, the resulting secondary stress is found to be 37,000 psi for 1.1% strain.

For the postulated conditions, these two examples show that high deflection limited tensile stresses can occur during installation. These stresses have not been confirmed. In addition, the welding process produces residual stresses in the pipe near the weld. The magnitude and sign of the stresses vary with distance from the weld and depend on pipe size and welding speed. These stresses are likely to vary circumferentially. Maximum tensile residual stresses in the range of 18 ksi to 40 ksi have been measured in weld pipe tests (Reference 2-2).

Installation stresses considered in conjunction with the material consideration discussed later (Section 2.6) may explain the cracks that have been observed. It should be emphasized that the installation stresses postulated above are all deflection-limited secondary stresses that will relax to the elevated temperature yield strength of the material during normal plant operation.

2.5.3 Stresses During Normal Operation

All identified stresses during normal operation were found to be negligible. Loadings that were considered include impingement loads (i.e., flow past the spargers), seismic, pressure, thermal mismatch, stagnant line top-to-bottom temperature gradients, stagnant line throughwall temperature gradients and weight. Stress calculations are given in Appendix A.

It should be noted that, during normal plant operation, there is no core spray flow. The sparger $\Delta P = 0$ and $\Delta T = 0$. Impingement loads are 1.0 lbf/in. on the header arm, resulting in negligible stresses. Weight of the spargers and water is only 1.37 lbf/in., again resulting in negligible stresses. Stagnant line temperature gradient calculations are not provided since the maximum ΔT for top-to-bottom gradients and for through wall gradients were found to be less than 8°F, which would result in insignificant stresses. It should be noted, however, that the ΔT for core spray injection is addressed in Section 2.5.4.

It is concluded that the normal operating loadings do not result in stresses that could explain the crack observed in the Brunswick 2 core spray sparger.

2.5.4 Stresses During Core Spray Injection

Stresses during core spray injection are the design stresses for the spargers. Design loadings include all those discussed in Section 2.5.3 plus those that occur because the system is no longer a passive system. The pressure differential in the sparger at rated flow is approximately 28 psid. The hoop stress in the pipe is about 230 psi. Impingement load stresses are less during spray injection than during normal operation. Thermal stresses due to the through-wall temperature gradient are high and are given by:

$$\sigma_T = \frac{E \cdot \alpha \cdot \Delta T}{2(1-\mu)}$$

These stresses are not a concern for one or a few cycles. The radius of the sparger shrinks when the sparger is cooled, resulting in secondary bending stresses of approximately 3100 psi. The axial stress in the pipe due to ΔP and bracket friction is low--less than 220 psi. Flow through the nozzles results in stresses in the nozzle-to-pipe weld which are low--less than 500 psi. Weight stresses are negligible. Water hammer is not expected because the pipe is essentially an open pipe, and the nozzle opening areas are approximately equal to the pipe internal area, even for the short leg. However, water hammer is addressed in the following section.

2.5.4.1 Water Hammer Loads

Water hammer loads as discussed herein are those hydraulic loads associated with injection of core spray water into a core spray system, where the system piping downstream of the check valve in primary containment is assumed empty (or filled with steam) because of the draining of water from the spargers and/or the flashing of water to steam during depressurization prior to core spray injection.

For the purpose of maximizing injection loads on the core spray spargers, it is assumed that reactor pressure is essentially atmospheric (as for a large LOCA), enabling system flow to increase to runout controlled only by the injection valve opening characteristic. Upon valve opening, the head (H) is available to accelerate the flow, but as the velocity increases, the acceleration head is reduced by friction and local losses. If L_e is the equivalent length of the pipe system, the final velocity V_f is given by application of the energy equation:

$$H = f \frac{L_e}{D} \frac{V_f^2}{2g}$$

The maximum velocity attainable is limited to that at system runout flow (6000 gpm), which produces a velocity of 54 ft/sec in the sparger (at the entrance to the long sparger arm to be more concise; the velocity at the ends is zero).

This is conservative because the velocity of the water first entering the sparger will be less than runout velocity because of the relatively slow opening chracteristics of the injection valve. The injected water fills the pipe line between the injection valve and the sparger at a time prior to full valve opening and therefore, before the final runout velocity is attained.

Assuming the maximum velocity attainable, the resulting momentum load in the sparger is:

$$P_m = \frac{V^2}{144\ gv} = \frac{(54)^2}{(144(32.2)\ (0.0160)} = 39.3\ \text{psi}$$

or

$$F_m = P_m\ A_p = 39.3\ (9.89) = 389\ \text{lb.}$$

where

P_m = momentum pressure (psi);

F_m = momentum load (lb);

V = velocity (ft/sec);

g = gravitational acceleration (32.2 ft/sec^2);

v = specific volume (0.0160 ft^3/lb) (~80°F water); and

A_p = pipe flow area (9.89 in.^{2}) (3-1/2-in. Schedule 40 pipe).

If the end plates at the ends of the spargers were removed, it is obvious there would be no impact load. Now cap the ends and also plug the sparger nozzles. Again, there would be no water impact load because the trapped gas in the line acts as a surge tank.

The actual end condition of the spargers is somewhere in between these two extremes. It is much closer to the open end condition, except that there are several "ends" instead of one end, and they are located along the length of the sparger arms.

The exit flow area of the sparger nozzles is computed as follows:

	Number	Area (in.^{2})	Total Area (in.^{2})
1-in. VNC Nozzle	27	1.018	27.5
3101 Nozzle	25	0.307	7.7
Total Open Flow Area Per Sparger =			35.2

The exit flow area of the nozzles and elbows is actually 78% greater than the flow area of the two sparger arms (2 x 9.89 = 19.78 in.^{2}).

An estimate of pressures induced in the sparger at the end of the filling time of the spargers and piping can be made by considering a sparger with only one open elbow located at the end of each arm. Steam would be pushed ahead of the oncoming front of water, exiting the sparger through the assumed single nozzle. The developed differential pressure to expel the steam would be approximately 7 psid. Adding all sparger elbows and nozzles to this logic clearly demonstrates that the sparger indeed behaves like an open-ended pipe, and conventional water hammer loads of any significant magnitude would not be present. Injection conditions at higher reactor pressure would clearly be bounded by the runout case presented here.

2.6 MATERIALS ASPECTS OF CRACKING

The potential causes of Brunswick 2 core spray sparger cracking are discussed in this section.

2.6.1 Potential Causes of Cracking

The potential metallurgical causes of core spray sparger cracking can be divided into those relevant to cracking in the heat-affected zone (HAZ) of the T-box to sparger arm weld, as well as those related to cracking in the sparger arm remote from the weld. Cracking in both regions is discussed here even though the crack in the Brunswick 2 core spray sparger is located in the HAZ of the weld.

Near the T-box, three possible causes of sparger cracking have been identified. First, sensitization by welding the sparger arms to the tee box is the most likely cause. It is known that IGSCC can result in the presence of this metallurgical condition with sufficient sustained stresses. In piping systems, the weld residual stresses plus sustained primary or secondary stresses equal to the materials yield stress can result in cracking. Moreover, the small amount of cold work inherent in sparger arm fabrication prior to welding could serve to increase cracking susceptibility. When the material is cold worked and subsequently sensitized, the susceptibility to IGSCC is markedly increased for cold work levels less than 20% (Reference 2-3). Carbide precipitation kinetics are markedly increased and some martensite can be formed. It has been shown that the presence of martensite accelerates kinetics of crack initiation and propagation.

Second, fatigue induced by thermal variations in the environment may be the cause of the sparger indications. However, the variations in temperature during operation of the reactor (8°F, see Section 2.5.3) are expected to be small. No evidence of a driving force for thermal fatigue has been identified.

Finally, fatigue resulting from flow-induced vibrations could be hypothesized. However, the natural frequencies of the sparger are high relative to any flow-induced excitation sources (Appendix A.2).

In the arms remote from the T-box by distances greater than 2 inches, welding cannot be considered a major influence on cracking. Sensitization may still be present if the original solution heat treatment was inadequate, either in temperature or quench rates. No direct evidence exists of this condition. Secondly, if cold work from arm bending were followed by local heating, a susceptible condition would more readily exist. Again, no direct evidence exists. Thirdly, surface cold work resulting from arm bending or straightening could hasten crack initiation and subsequent growth could occur from redisual or installation stresses. Finally, fatigue by either of the sources cited above for the T-box area could induce cracking, although there is no confirmed source of fatigue loading.

It is postulated that cold work, both local and overall, associated with the bending could produce cracking remote from the T-box. It is known that high levels of cold work without subsequent sensitization can result in initiation of transgranular stress corrosion cracks which can subsequently propagate in an intergranular fashion (Reference 2-3). For the sparger, the overall cold work could be due to the sparger arm formation alluded to above. The local cold work can result from local smearing of metal during the bending operation. While the overall cold work level is small - about 2%, the local cold work level can be quite high.

A sparger with fabrication history very similar to that at Brunswick 2 was examined and found to have these locally smeared areas. Constant Load and Constant Extension Rate stress corrosion test specimens were fabricated from sparger segments with and without the smears. In addition, specimens containing the cold work smears were subjected to solution heat treatment and also tested. Ferrite scope measurements taken on the smeared areas indicated the presence of about 5% ferrite indicating the presence of a magnetic phase such as martensite. Hardness tests on the smeared areas also revealed high local cold work. Normal hardness and no ferrite were found in the non-smear type specimens. The constant extension rate tests were conducted in 550°F, 8 ppm oxygenated water. Transgranular cracking was noted in specimens containing the cold work smears along with some expected intergranular cracking of the underlying material resulting from the crevice formed by the transgranular crack. No such cracking was found in sparger material without smears or in solution annealed material. Constant load tests resulted in similar results with failure times of the smear specimens 69 to 325 hours as opposed to about 4000 hours on test for the other specimens without failure.

2.6.2 Conclusions of Sparger Cracking

In summary, the most probable cause of core spray sparger cracking at Brunswick 2 is cold work and subsequent sensitization.

2.7 CRACK ARREST ASSESSMENT

An assessment of crack propagation has been prepared for CP&L by a third party for CP&L's use with the USNRC for the Brunswick Steam Electric Plant Unit 2.

2.8 STRUCTURAL INTEGRITY WITH 360° THROUGHWALL CRACK

Even though GE believes that a 360° throughwall crack is improbable, a structural analysis was performed (See Appendix A) which conservatively assumed that the existing crack propagated 360° throughwall. Loads which were considered included all loads applicable to the intact sparger (See Section 2.5.3). The analysis ignored the effect of clamp (or assumed a clamp was not installed).

2.8.1 Normal Operation

Bending stress in the broken sparger arm due to impingement is low -- 868 lb/in^2. During the postulated seismic event, bending stress is calculated to be 2380 lb/in^2. All other operating loads result in negligible stresses.

2.8.2 Core Spray Injection

Stresses on the broken sparger during core spray injection are bounded by the stresses given for the intact sparger (Section 2.5.4). Normal stress will therefore be less than 3320 lb/in^2 in the sparger pipe. In the nozzle-to-pipe weld, the maximum normal and shear stresses are 4270 lb/in^2 and 4400 lb/in^2, respectively. In the welded brackets, bounding normal and shear stresses are 5980 lb/in^2 and 752 lb/in^2, respectively.

2.8.3 Flow Induced Vibration

Flow induced vibration is not a concern for the broken sparger case. The ratio of natural frequency of the broken sparger arm to the vortex shedding frequency is greater than 6, which exceeds the GE design basis by more than a factor of 2.

2.8.4 Conclusions

Stresses during normal operation and during core spray injection were found to be well below allowables. The natural frequency of the assumed broken sparger remains high enough so that flow induced vibration is not a concern. It is concluded that the sparger will lose no pieces and will remain attached to the shroud wall under the conservative assumption that the existing crack propagates 360° throughwall.

2.9 REFERENCES

2-1. Hopkins, Design Analysis of Shafts and Beams, McGraw-Hill Book Company.

2-2. H. H. Klepfer, et al, "Investigation of Cause of Cracking in Austenitic Stainless Steel Piping," NEDO-21000-1, July 1978.

2-3. R. L. Cowan and G. M. Gordon, "Intergranular Stress Corrosion Cracking and Grain Boundary Precipitation of Fe-Ni-Cr Alloys," NEDO-12399, September 1973.

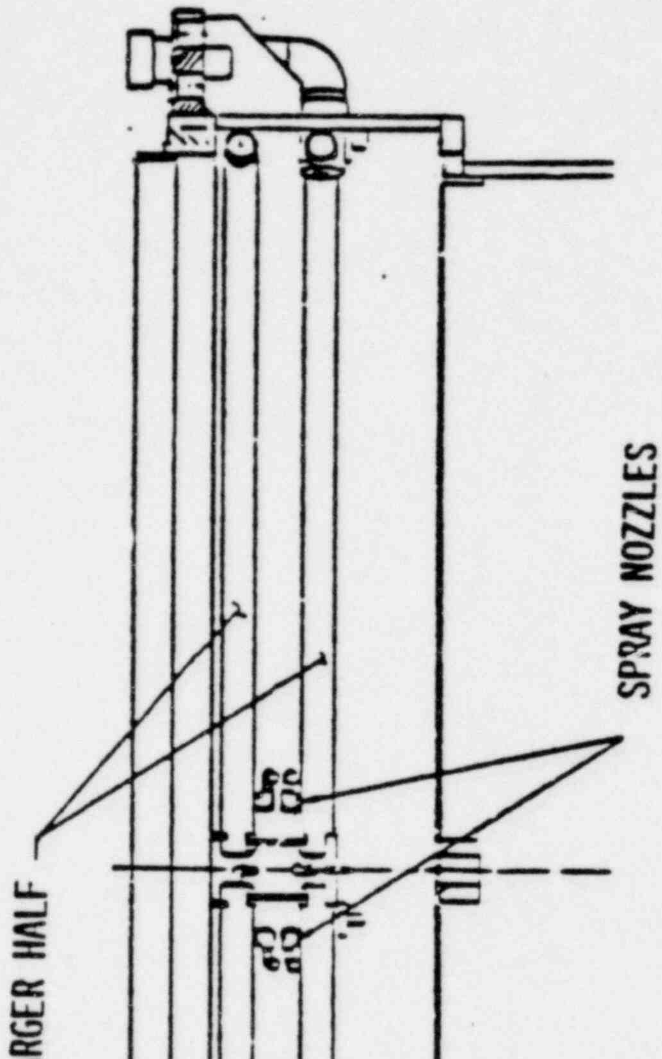

Figure 2-1. Core Spray Sparger - Elevation View

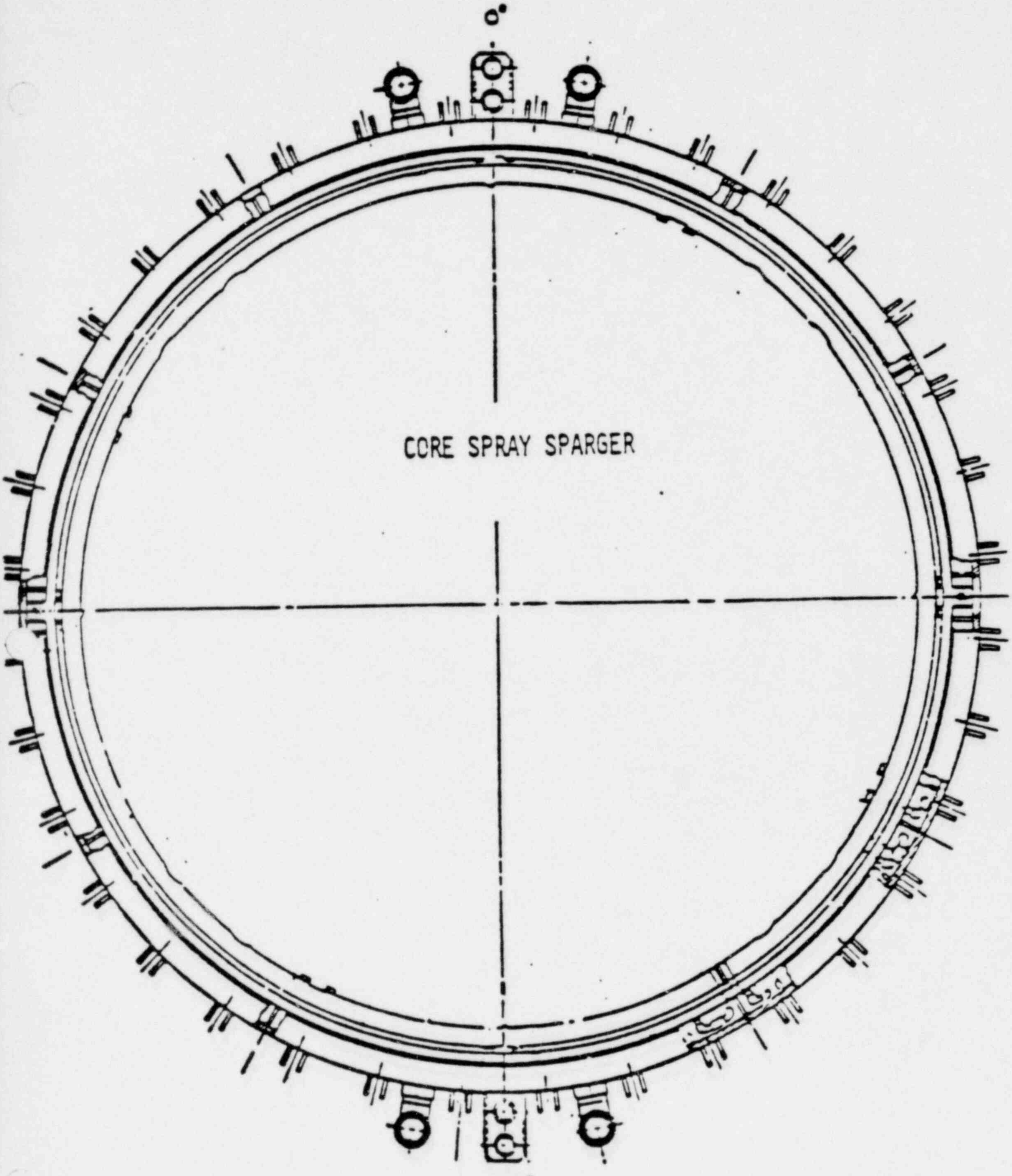

Figure 2-2. Core Spray Sparger - Plan View

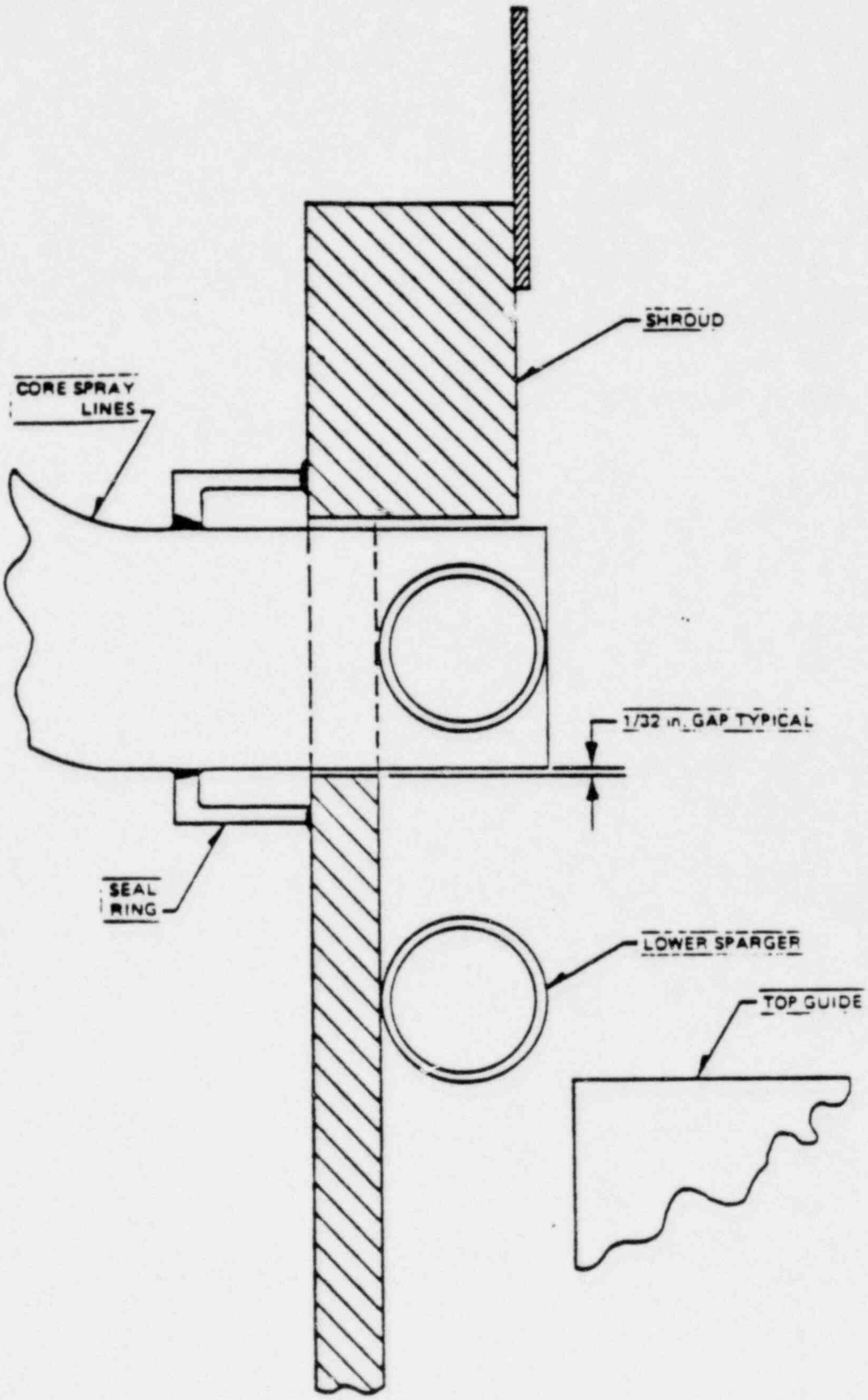

Figure 2-3. Sparger to Shroud Attachment Method

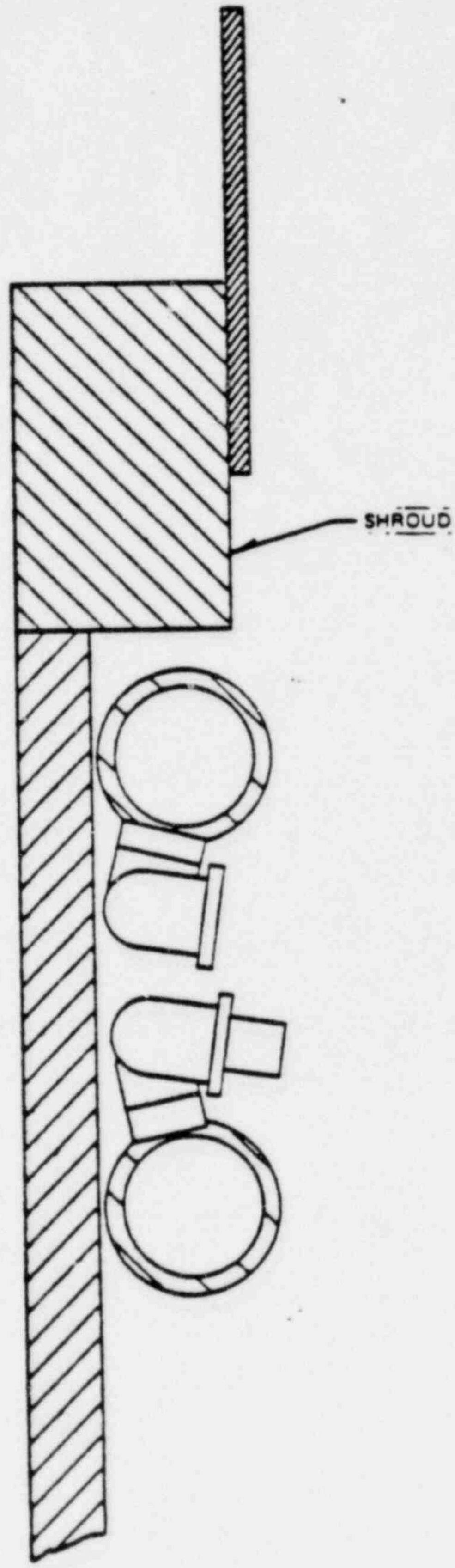

Figure 2-4. Sparger Nozzles

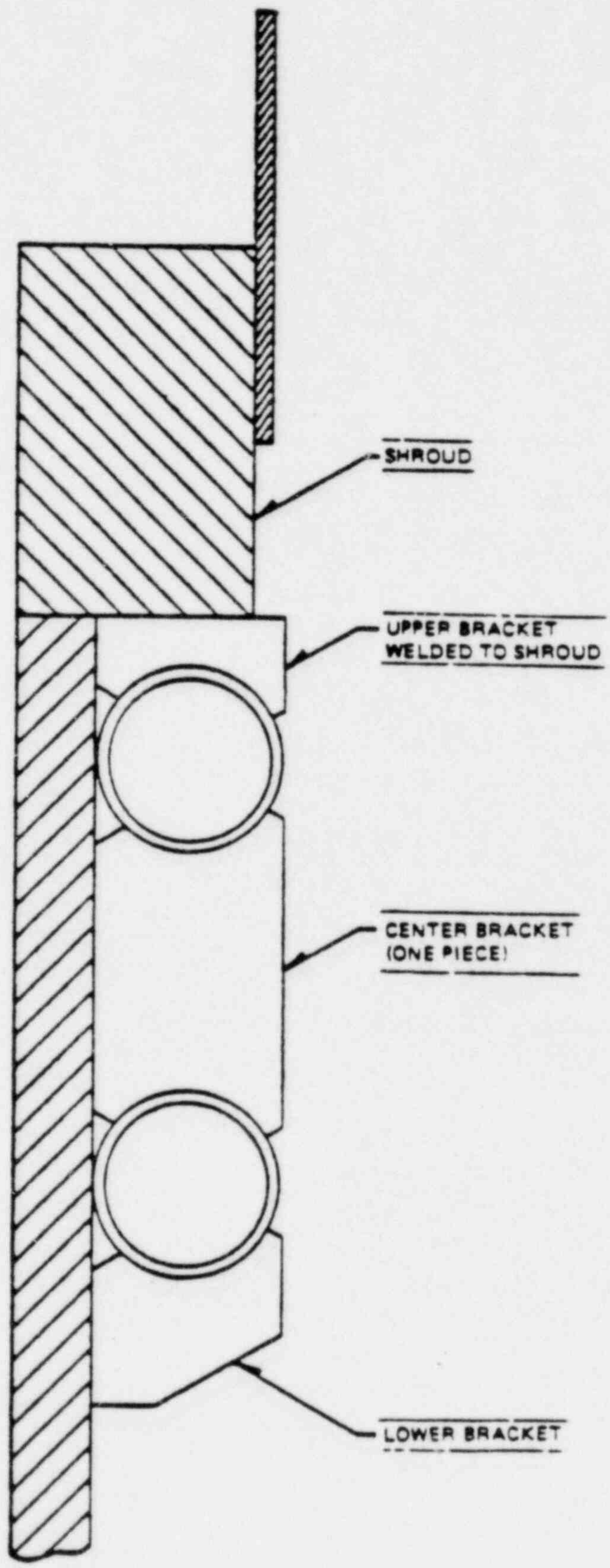

Figure 2-5. Sparger Support Method

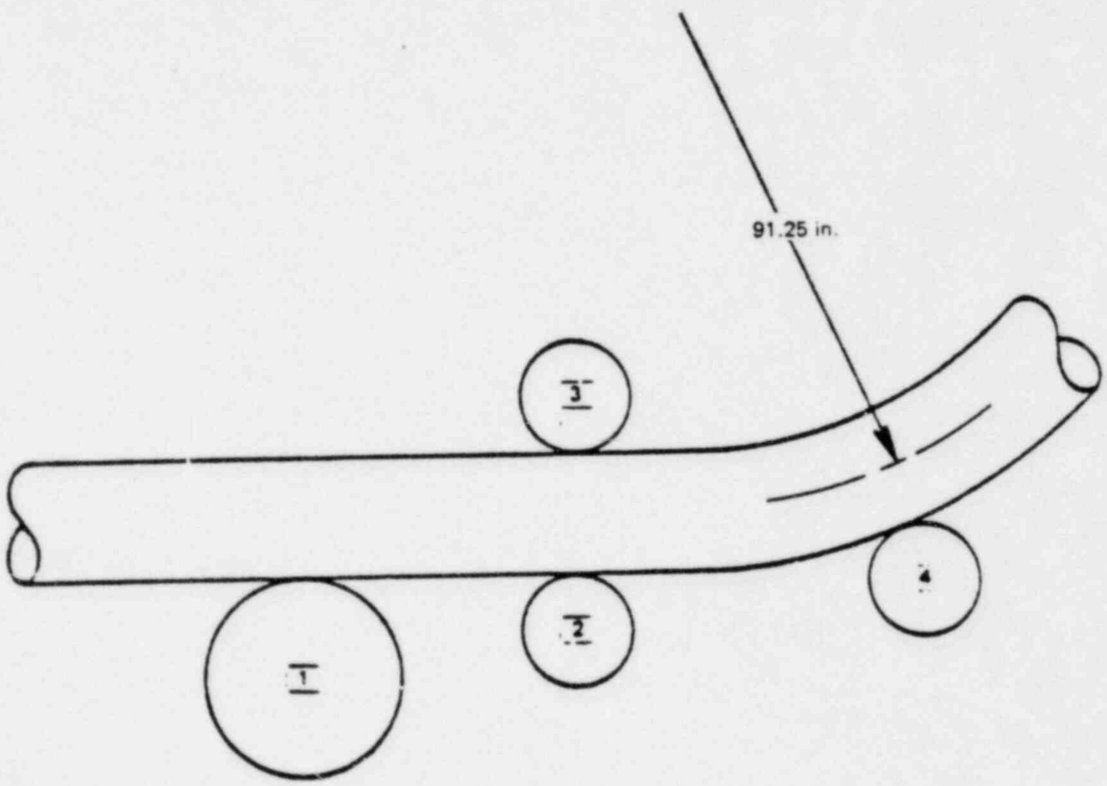

Figure 2-6. Pipe Bending Method

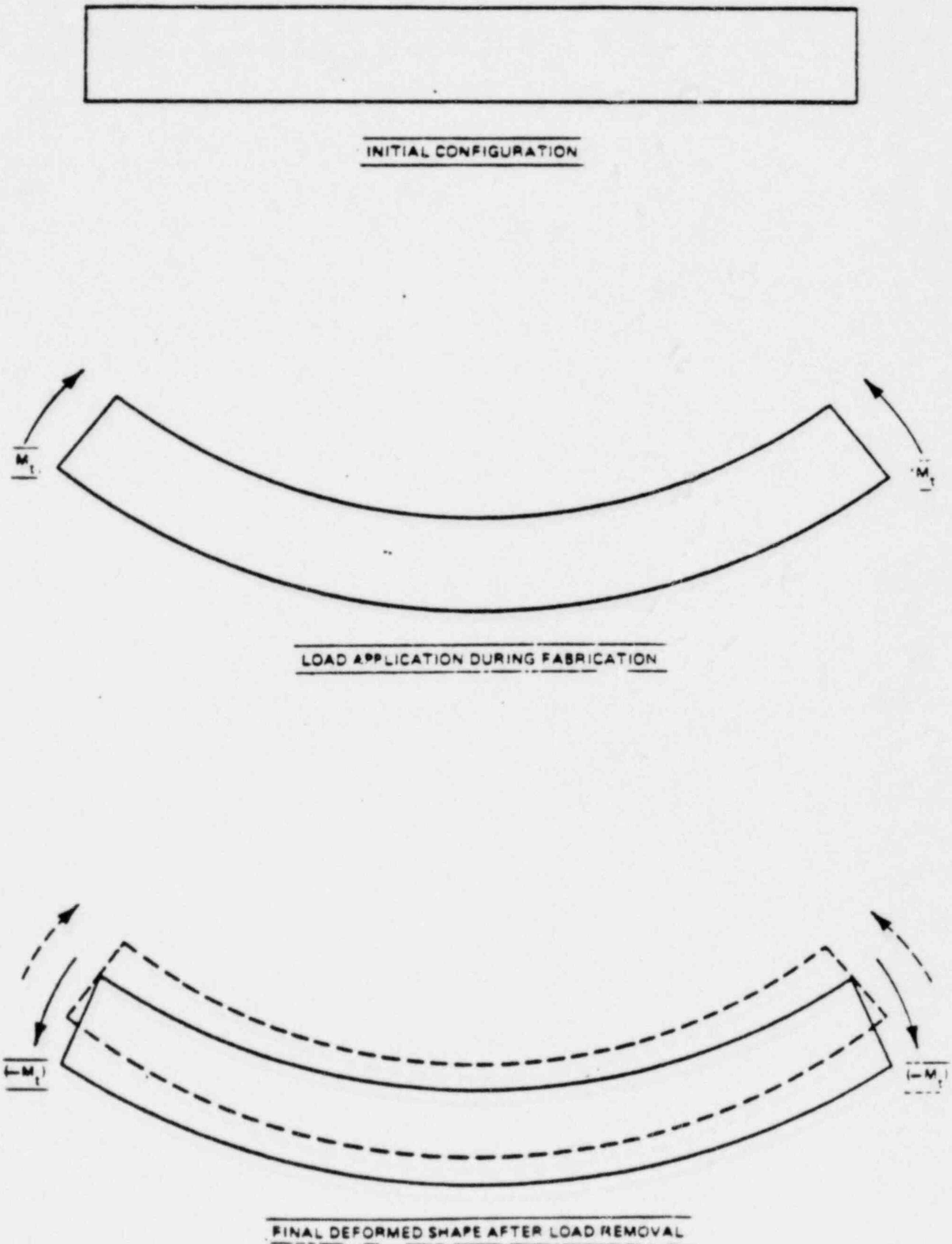

Figure 2-7. Sequence of Events Leading to the Residual Stress Distribution

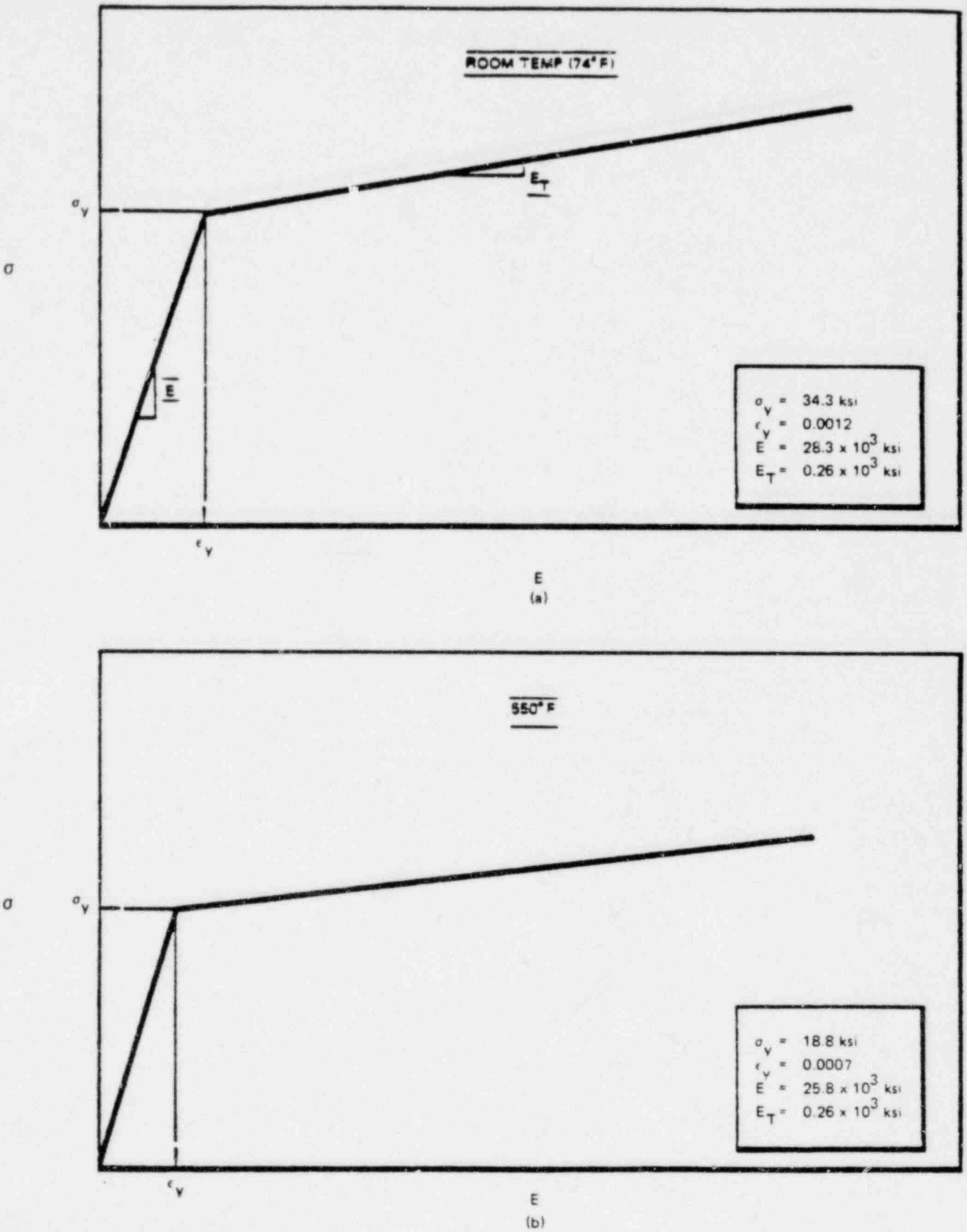

Figure 2-8. Bilinear Stress-Strain Curves for Type-304 Stainless Steel

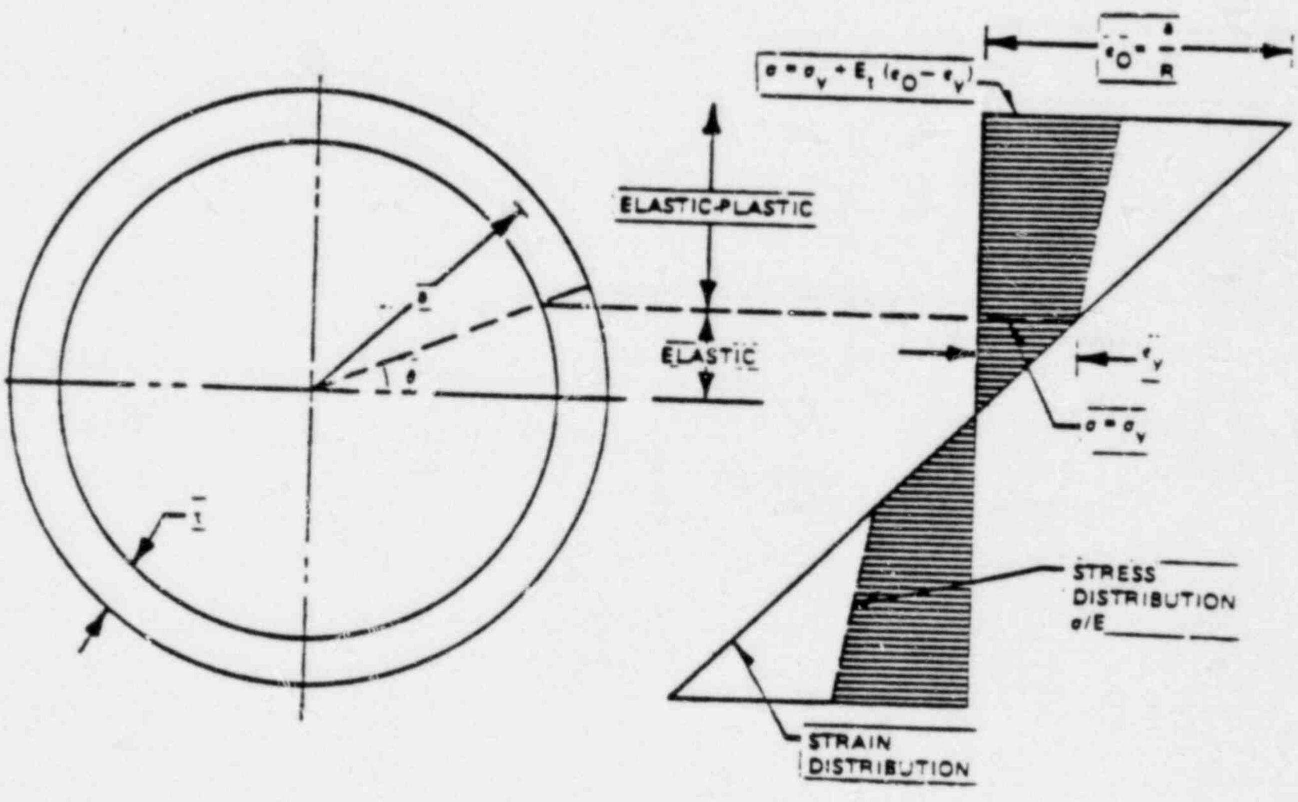

Figure 2-9. Stress and Strain Distribution in the Pipe Under Applied Moment

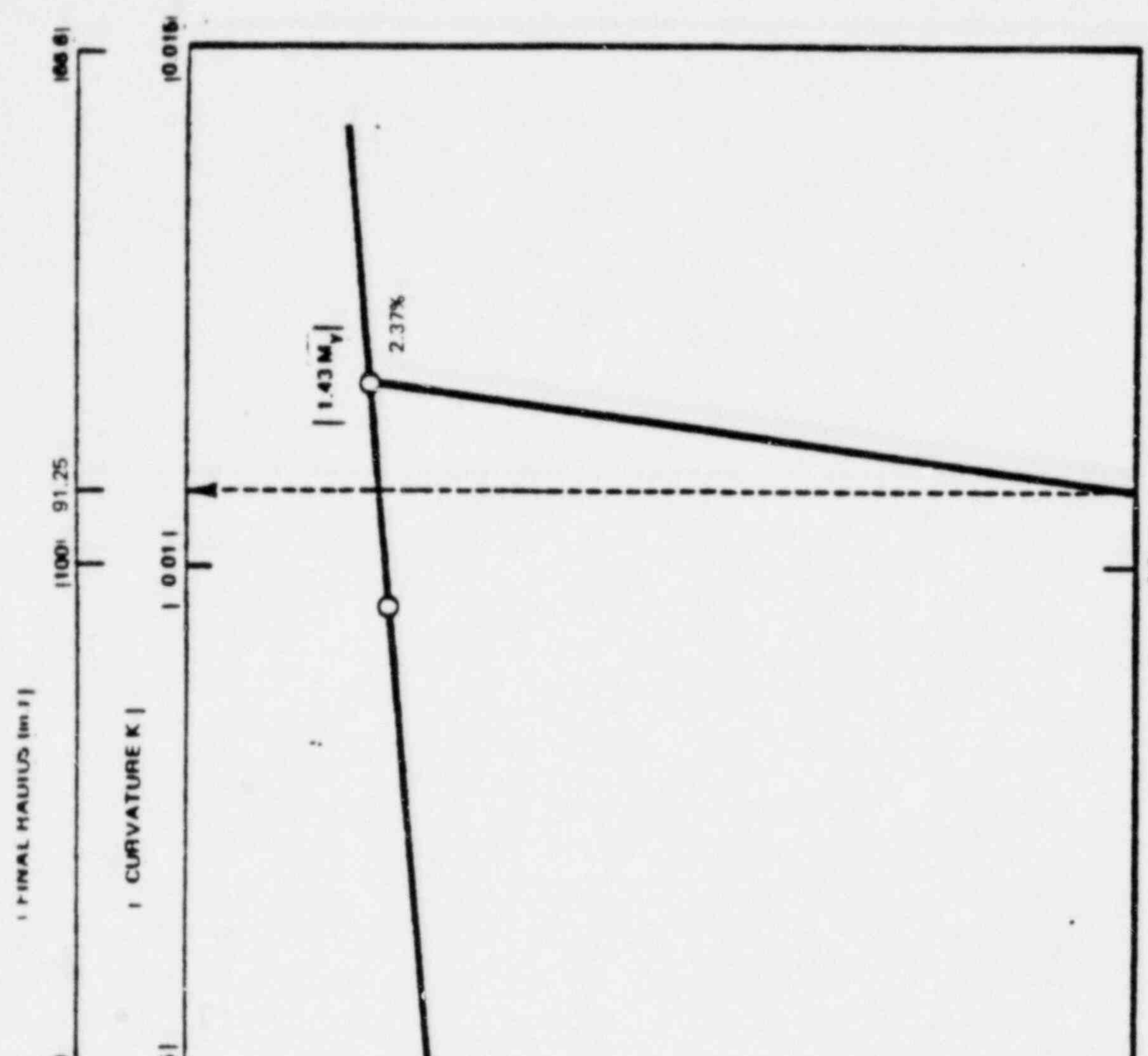

Figure 2-10. Moment Versus Outer Fiber Strain

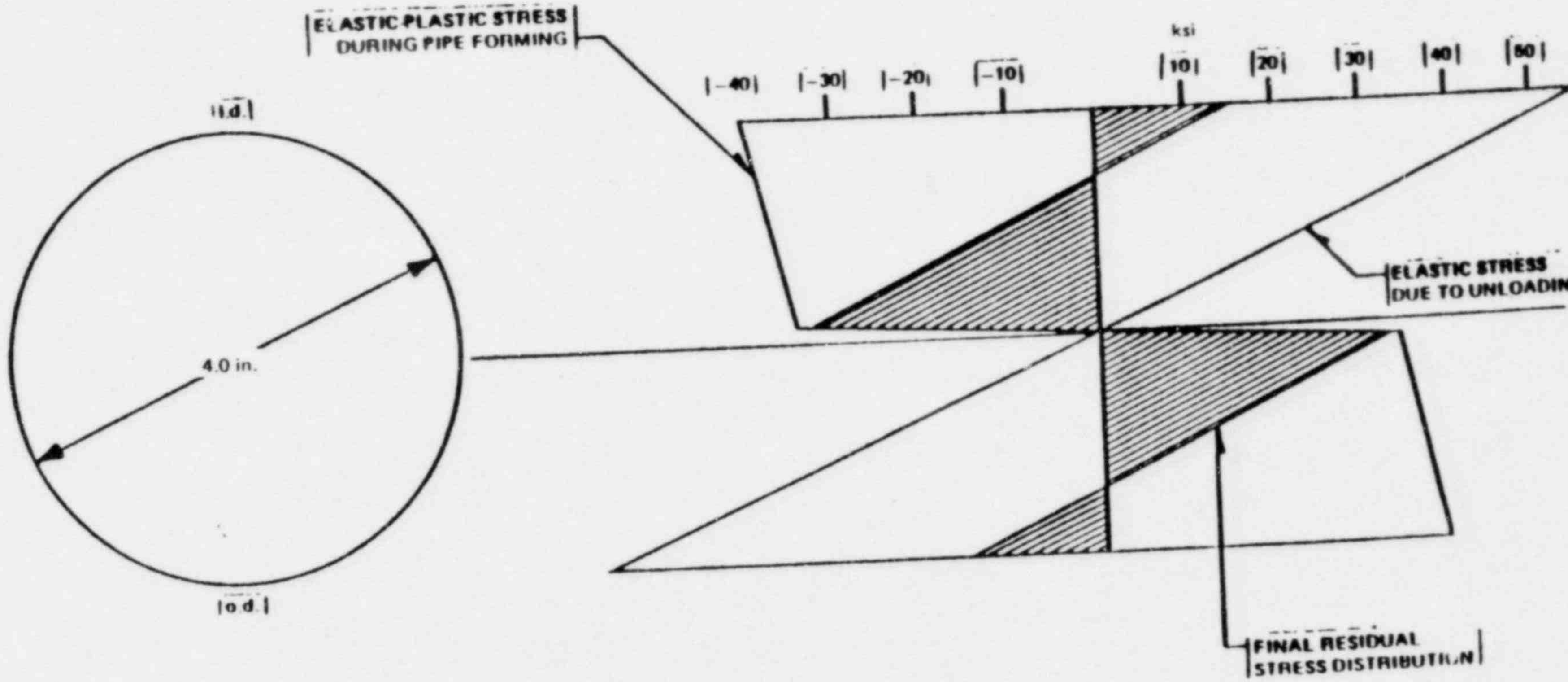

Figure 2-11. Resultant Residual Stress Distribution After Fabrication

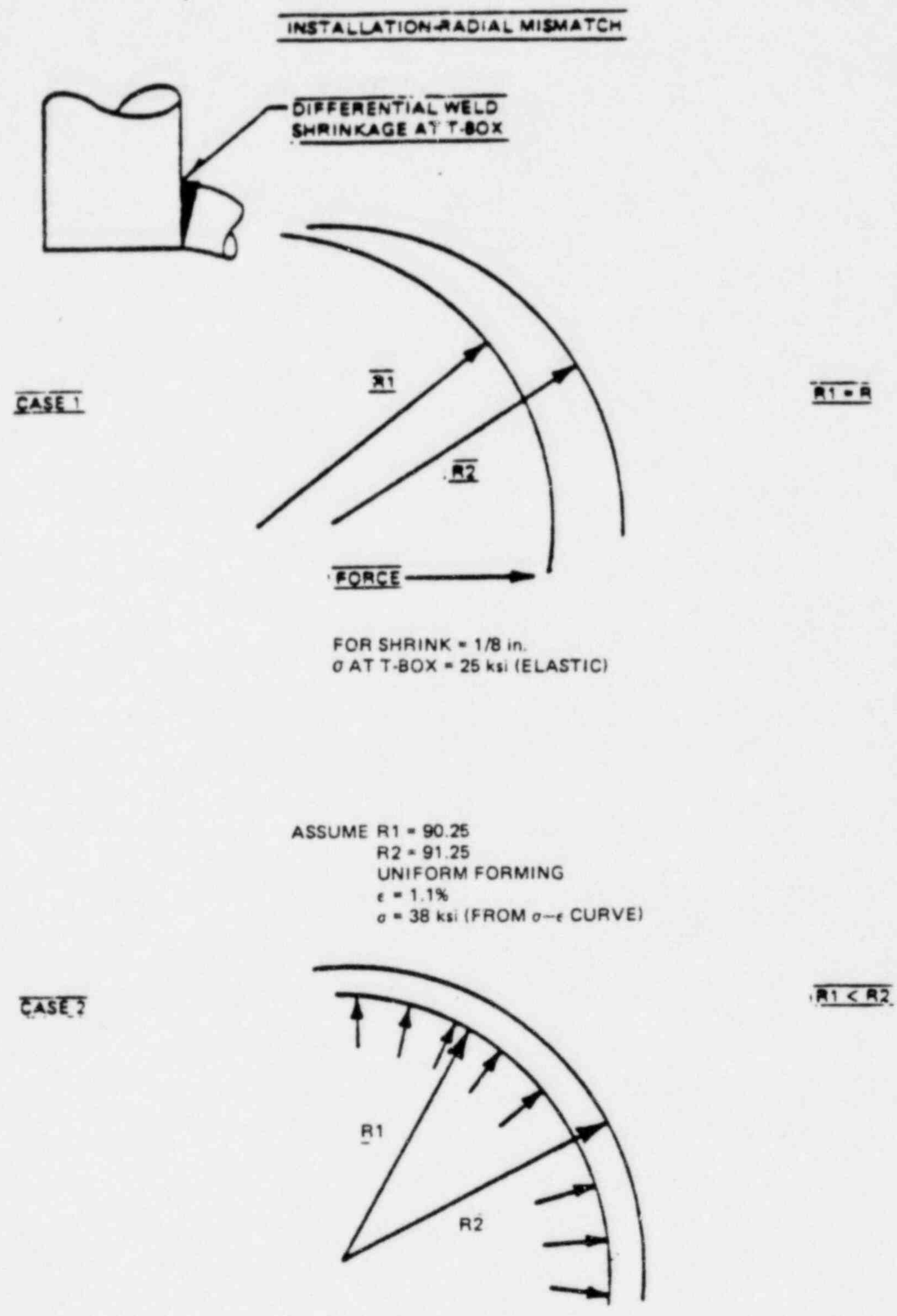

Figure 2-12. Postulated Installation Stresses

3. LOST PARTS ANALYSIS

3.1 INTRODUCTION

Based on the structural analysis given in Section 2, it is expected that the Brunswick 2 core spray sparger will not break and result in loose pieces in the reactor. However, an evaluation of the possible consequences of a potential loose piece is presented in this section.

3.2 LOOSE PIECE DESCRIPTION

Since a piece has not been lost, it cannot be uniquely described. Three different types of loose pieces are postulated in Section 3.4.2: (1) a section of sparger pipe; (2) an outlet nozzle; and (3) a small piece of the sparger. The entire sparger is fabricated of Type-304 stainless steel.

3.3 SAFETY CONCERN

The following safety concerns are addressed in this safety analysis:

1. Potential for corrosion or other chemical reaction with reactor materials.

2. Potential for fuel bundle flow blockage and subsequent fuel damage.

3. Potential for interference with control rod operation.

4. Potential for damage of other reactor internals.

3.4 SAFETY EVALUATION

The above safety concerns for the postulated loose pieces are addressed in this section. The effect of these concerns on safe reactor operation is also addressed.

3.4.1 General Description

The core spray spargers are attached to the inside of the core shroud (Figure 3-1) in the upper plenum. For a piece of the sparger to reach and potentially block the inlet of a fuel assembly, it would have to be carried out of the upper plenum and pass down into the lower plenum. To accomplish this, it would have to be carried by the fluid flow in the upper plenum up through the steam separators then outward to the downcomer annulus, the through the jet pump nozzle into the lower plenum, then make a 180°F turn and be carried upward to the fuel assembly inlet orifices. A part of the sparger cannot reach the fuel assembly inlet orifices by falling down inside the core shroud as the core support plate and the loaded core will prevent this. For a part of the core spray sparger to reach a control rod, it must first traverse the upper plenum from the outer region of the shroud toward the center, then either fall through the restrictive passage between two fuel channels; or fall through an opening between the outside of the peripheral bundles and the core shroud, both of which are unlikely.

Since all parts of the core spray sparger are designed for in-reactor service, there is no possibility that any loose part will cause any corrosion or other chemical reaction with any reactor material.

3.4.2 Postulated Loose Pieces

3.4.2.1 Sparger Pipe

The sparger pipe is 3-1/2 in. Schedule 40 pipe and is attached to the core shroud at seven locations (T-box plus six brackets). The maximum span between the crack and the support is approximately 61.5 inches and between supports is about 65 inches. In order to generate a loose piece of pipe, a minimum of two throughwall cracks would have to propagate 360° around the sparger. The weight of the largest pipe segment would be approximately 84 lb. Because of the slow rate of potential crack propagation and based on previous experience with cracks in core spray spargers, it is judged that pieces will not break off and become loose. However, for purposes of evaluating the probability for loose pieces, which might potentially cause core damage, a conservative estimate of this probability has been chosen at 10^{-3} (see Section 3.5).

A pipe segment could come to rest in any of three locations: (1) the top surface of the top guide outboard of the fuel assemblies; (2) the top surface of the fuel assembly handles; or (3) in an unlikely event, the top surface of the core plate. In all three of these locations, the flow velocity is low and insufficient to lift a segment of the pipe (see Appendix B). Therefore, it will remain at one of these locations and is not expected to lift or rattle around. An 84 lb piece of pipe which falls from the core spray sparger will not harm the core plate, top guide or fuel assembly handles, since these components are designed for much larger loads.

Since the pipe cannot be lifted by the flow and since the pipe cannot fit through either the steam separator or the jet pump, it will not cause any flow blockage at the fuel inlet orifice. Since the pipe is too large to fit between fuel channels, it will not cause any interference with control rod operations.

3.4.2.2 Spray Nozzle

Each spray nozzle consists of two 1-in. elbows fabricated of Type-304 stainless steel, which are welded to the sparger. In order to generate a loose nozzle, a throughwall crack would have to propagate 360° around the nozzle. The weight of each nozzle assembly is approximately 1-3/4 lb. A loose nozzle would most likely come to rest on the top surface of the core plate or on the top surface of the top guide. The flow velocities in these regions are insufficient to lift the nozzle, and it will remain at one of the above mentioned locations (Appendix B).

Since the nozzle cannot be lifted by the flow and since the nozzle cannot fit through the steam separator, it will not cause any flow blockage at the fuel assembly inlet orifices. The nozzle is too large to fit between two fuel channels; thus, it cannot cause any control rod interferences.

3.4.2.3 Small Pieces

In order to generate small pieces of the sparger, both longitudinal and circumferential throughwall cracking must occur. A small piece could be lifted by the flow if it maintained an orientation with its maximum projected area perpendicular to the flow. Due to flow turbulence and assymmetry of the loose part, the part would tend to rotate so that the minimum projected area will be perpendicular to the flow. With this orientation, and based on the velocities in the upper plenum (Appendix B), all parts with a length of greater than approximately 0.4 in. would sink. Thus, most pieces would not be carried by the flow toward the steam separator. However, in the unlikely event that a piece reached the steam separator, it would have to pass through the steam separator turning vane (Figure 3-2). There are eight curved vanes with the outlet of each vane overlapping the inlet of the adjacent vane. The longest straight piece that can fit through the turning vanes is approximately 6 in. long and it must be oriented with the long dimension in the vertical direction. As shown in Figure 3-3, the maximum dimension of such a piece is approximately 6 x 2 x 2 inches. Thus, a piece 0.4 in. can pass through the separator.

The fluid momentum is reduced as the water is removed in passing through the separator. At the separator exit, the fluid momentum is further reduced as the water is removed. At the separator exit, the fluid is almost entirely steam. A typical water content is 1 weight percent. Thus, it is very unlikely that any piece could be carried out of the separator by the steam. If any piece were carried through the separator by the steam, then it could be carried into the downcomer annulus, through the jet pump and enter the lower plenum. A piece that entered the lower plenum would probably be driven by the jet pump flow to the bottom of the reactor pressure vessel where it would be expected to remain. However, a small piece $\leq$0.4 in. could be carried by the flow to the fuel bundle flow inlet orifices. There are three different sized orifices: 1.225, 1.433 and 2.09 inches.

It is extremely unlikely for a piece larger than the 1.225 in. orifice and essentially impossible for a piece larger than the 2.090 in. orifice to be carried through the steam separator. The outside diameter of the sparger is

4.0 in., while the fuel inlet orifices are slightly recessed relative to the surface of the control rod guide tubes (Figure 3-4), which have an outside diameter of 10-3/4 inches. Due to the different radii of curvature, flow would be able to enter the fuel assemblies. Thus, unacceptable flow blockage as defined by Reference 3-1 would require that more than one loose piece be carried to the same inlet orifice. This is based on the size of the piece(s) that, in a highly unlikely circumstance, have the potential of reaching the vessel lower plenum. The probability of unacceptable flow blockage of any fuel orifice is insignificant. This would require multiple pieces at the same orifice at the same time and the probability of several pieces blocking a significant portion of the bundle inlet to cause significant fuel damage is essentially zero (see Section 3.5.1).

Flow velocities near the sparger are lower than those above the fuel assemblies. Thus, it is unlikely that a small piece would be carried over the fuel assemblies (see Appendix B). If the piece were carried over the fuel assemblies and then rotated so that the flow could no longer carry it, the piece would fall on top of a fuel assembly or between fuel assemblies.

Figure 3-5 shows a typical unit cell of four fuel assemblies and one control rod. The control rod moves in the gap between the fuel channels. The gap between fuel channels is 0.75 inch. The length of the gap between the channel spacer and the channel fastener is 2.3 inches. Thus, any piece larger than 2.3 in. by 0.75 in. cannot cause control rod interference. The control rod thickness is 0.312 in. and the diameter of the control rod rollers is 0.520 inches. Thus, pieces smaller than 0.334 in. will fall past the control rod without causing any interference. A piece of precisely the right size could be in contact with the control rod and one or two fuel channels. Such a piece might be detected during the normal control rod exercising. The rods are inserted one notch and withdrawn one notch each day. It is also possible, though unlikely, that a piece might wedge between two fuel channels above the control rod and thus not be detected by normal control rod operations. If the rod were to be inserted, the control rod mechanism has enough force to lift one fuel assembly with the reactor at normal operating pressure. If the fuel assembly were lifted 1 or 2 inches, it would be able to move horizontally at both the bottom and the top, thus almost certainly relieving any interference. The rod would then insert and the fuel assembly would fall back into place. It is not credible that any control rod will fail to insert.

One of the licensing bases of the reactor is that with the highest worth control rod fully withdrawn, the reactor can be safely shut down. Thus unacceptable control rod interference will require multiple precisely-sized pieces interfering simultaneously with control rods that are in close proximity to each other. The probability of this is judged to be insignificant (see Section 3.5.2).

3.5 DISCUSSION OF PROBABILITY

This section provides the basis which supports the conclusions discussed above that the probability of loose parts from the core spray sparger causing a safety concern are negligible.

Based on operating history of BWRs with cracks in the core spray sparger in the last few years, structural evaluation of the core spray sparger cracks, and the fact that no loose parts have been found, the generation of a loose part is believed to be incredible, i.e., the probability to have a loose part of any size as the result of a crack is believed to be very nearly zero. However, for the purpose of this study, a bounding probability for having a loose piece break off of the sparger is assumed to be 10^{-3}.

3.5.1 Fuel Bundle

For a core spray sparger loose piece to reach a fuel bundle and potentially cause some safety concern it would have to be carried out of the upper plenum and pass through the downcomer, jet pumps, down into the lower plenum and then into the core region. However, the probability of a piece being carried out of the upper plenum, through the steam separator, and outward to the downcomer annulus is limited by the minimum projected area (perpendicular to the flow) that can be lifted by the fluid flow and the size of piece that can physically fit through the turning vanes of the separator (see Section 3.4.2.3). Likewise, if a piece were to be carried to the lower plenum, the probability of the piece potentially being carried to the core is also limited by the minimum projected area that can be lifted by the fluid flow in the lower plenum.

As discussed in Section 3.4.2.3, it is physically possible for a piece approximately 6 x 2 x 2 inches to fit through a separator; however, the fluid velocities in the upper plenum are not sufficient to carry this size piece out and hence it would remain there in the upper plenum. The maximum size piece that can be carried out of the upper plenum is limited to approximately 0.4 x 0.4 x 0.4 inches as discussed in Section 3.4.2.3. If this piece were to be carried to the lower plenum, which is unlikely, it could be lifted toward the core because the vertical fluid velocity in the lower plenum is high enough to lift this sized piece. Therefore pieces of this size are used to evaluate the potential of them reaching the core region from the lower plenum (the thickness of the core spray sparger pipe is only 0.226 in.).

Figure 3-6 is a diagram of the path that a potential loose part from the sparger would follow if it were carried out of the upper plenum into the lower plenum and core. For each flow path, a probability is assigned and the cumulative probability is also shown (in brackets). As discussed above, the probability for a part to break off in the upper plenum is conservatively estimated to be $P_1 = 10^{-3}$. Since it is postulated that a piece of this size is small enough to be carried by the upper plenum fluid velocity it is assumed that it will leave the upper plenum, i.e., $P_2 = 1.0$. Once out of the upper plenum it is assumed that the piece travels with the liquid flow out of the separator and is carried out down the downcomer, i.e., $P_3 = 1.0$. There, the piece is likely to come to rest at the jet pump support plate at the bottom of the shroud and remain there (P_6). However, because of the potential for the piece to be ingested into the jet pump flow (P_4), or to be sucked into the recirculation line (P_7) and driven into the jet pump (P_8), it is conservatively estimated that the probability is the sum of the probability for these flow paths, hence $P_9 = P_8 + P_4 = 0.75$. The probabilities, P_4 and P_8, are based on the projected flow areas and biased by the flow velocity ratios in the jet pumps and annulus downcomer for P_4 and by the recirculation suction line and downcomer for P_7. Once in the jet pump it is further assumed that the part will be carried by the flow stream toward the core, hence $P_{10} = 1.0$.

To enter the core region from the lower plenum, the part must first pass through the fuel bundle inlet orifices (P_{11}) (there are three different sized bundle orifices). Once past the orifice, the part must pass through the lower tie plate (P_{12}) and into the fuel bundle (P_{13}).

The path from the lower plenum through a fuel bundle to the upper plenum is restricted by the following flow areas:

1. Inlet orifices; three sizes 1.225, 1.433 and 2.09 inches; flow area between 1.18 and 3.4 sq. inches;

2. Lower fuel bundle tie plate; made up of 49 irregular shaped holes with a total flow area approximately 11 sq. inches;

3. Fuel bundle with 64 rods inside a square channel with a free flow area of approximately 15 sq. inches;

4. Seven grid spacers along the bundle with a free flow area of approximately 13 sq. inches; and

5. Upper tie plate similar to the lower tie plate.

For a part to enter a fuel bundle it would physically have to pass through the lower tie plate which would further limit its size. A part approximately 1/8 x 1/8 inches would either pass completely through the bundle, beginning the cycle over again, or be trapped within the fuel bundle possibly at one of the fuel rod spacers. If it remained trapped at a spacer for a sufficiently long period of time, there is a potential for fretting wear. Extensive fretting may ultimately lead to local fuel rod perforation and possibly some small release of fission products. This is not a safety problem because offgas radiation monitors are designed to detect fission product release in order to limit offsite dose to within the 10CFR100 limit.

For BWR fuel, the smallest and most restrictive flow path is at the fuel bundle inlet flow orifice. The percentage of blocked orifice area must be greater than 75% before a boiling transition condition would be approached for the most limiting, peak power fuel bundle (Reference 3-1). These bundles have the largest orifices. However, for a conservative estimate the potential for flow blockage for the smallest sized orifice is evaluated. To block 75% of the area of the smallest orifice, at least five of the loose pieces must somehow migrate to the same fuel bundle inlet orifice. Five pie es that pass through the inlet orifices and remain trapped within the bundle would block considerably less flow area and hence would be less restric.ive.

It is extremely unlikely to have more than one loose piece, and the probability of more than one piece migrating to the same fuel bundle is also negligible. However, for evaluating this potential it is assumed that the probability for one loose piece to enter a particular fuel bundle is the cumulative probability for a piece from the upper plenum to reach lower plenum. This is called P and later it is set equal to the cumulative probability at P_{10}. There are 560 fuel bundles in the Brunswick-2 core, each with an inlet orifice. The probability of having n loose pieces is P_1^n. The probability of having n loose pieces from the lower plenum simultaneously, partially blocking one given fuel bundle is substantially lower. We estimate this on the number of fuel bundles. Hence, the probability of n pieces at a given fuel bundle is:

$$P_n = (1/560)^{n-1}, \text{ where } n > 1.$$

Therefore, the probability for blockage of a given bundle is:

$$P_{10}^n \cdot (1/560)^{n-1}$$

To block 75% of the minimum inlet orifices (which control the lowest powered fuel bundles) would require at least 5 small pieces somehow arriving and becoming wedged at the inlet orifice simultaneously. To estimate this probability we take n = 5 in the above expression to block 75% of the smallest inlet orifice. As can be seen the probability of one piece entering the lower plenum is 7.5×10^{-4}. When this is used in the above expression for P_{10} and for 75% blockage n = 5, the resulting probabilities are incredibly small.

The probability for n pieces being carried from the upper plenum to the lower plenum and going to the same orifice is shown in Table 3-1 below.

Table 3-2 summarizes the estimated probabilities and the potential consequences related to fuel damage associated with a piece or number of pieces either entering a fuel bundle or potentially blocking a bundle. As shown in this table the potential consequences do not pose any safety concerns and are of extremely low (incredible) probabilities.

Table 3-1

PROBABILITY OF FUEL BUNDLE BLOCKAGE

n	$(1/560)^{n-1}$	P_n
2	$2\text{x}10^{-3}$	$1\text{x}10^{-9}$
3	$3\text{x}10^{-6}$	$1\text{x}10^{-15}$
>3	$<10^{-8}$	$<<10^{-15}$

n = Total number of pieces generated

P_n = Probability that there is at least one orifice which is blocked by two or more pieces up to a total of n.

Table 3-2

SUMMARY OF RESULTS OF THE PROBABILITY STUDY

No. Pieces or Percent Flow Blockage	Probability	Consequences
1 piece	7.5×10^{-4}	May become trapped within a bundle and after extended period could lead to local fuel rod perforation and subsequent fission product release in RPV
<5 pieces	$<10^{-15}$	Same as above
5 pieces 75% blockage	$<<10^{-15}$	Same as above with possibility of local boiling transition and several perforated rods.

3.5.2 Control Rod Mechanism

The probability of forming a small loose piece (small enough to fall down from the sparger to the bypass region) is assumed to be 10^{-3} as previously discussed. Small pieces could be lifted by the flow velocities in the upper plenum and during a hot shutdown condition of the reactor could drop or fall back and possibly pass through the flow area from the upper plenum to the bypass (approximately 18.5 ft^2 total). The total flow area in the upper plenum above the fuel bundles is approximately 182 ft^2. Therefore the probability of such a piece (after being formed) to fall into the bypass region is $18.5/182 \approx 0.1$. The total probability of the piece forming and reaching the bypass is $0.1 \times 10^{-3} = 1 \times 10^{-4}$.

The probability of multiple pieces (i.e., n pieces) reaching a specific control rod guide tube is:

$$P(n) = (10^{-4})^n/(\text{no. guide tubes})^{n-1}.$$

For two pieces (n = 2), $P(2) = (10^{-4})^2/137 \approx 7\text{x}10^{-11}$.

Therefore the probability of multiple pieces reaching the same guide tube (control rod drive) is negligible. The probability of multiple pieces interfering with more than one (or adjacent) control rods is substantially less.

3.6 CONCLUSION

There is no possibility for unacceptable corrosion or other chemical reaction due to a loose piece. The probability of unacceptable flow blockage of a fuel assembly or unacceptable control rod interference is essentially zero. Therefore, it is concluded that there is no safety concern from a loose part perspective.

3.7 REFERENCES

3-1. "Consequences of a Postulated Flow Blockage Incident in a Boiling Water Reactor," October 1977 (NEDO-10174, Rev. 1).

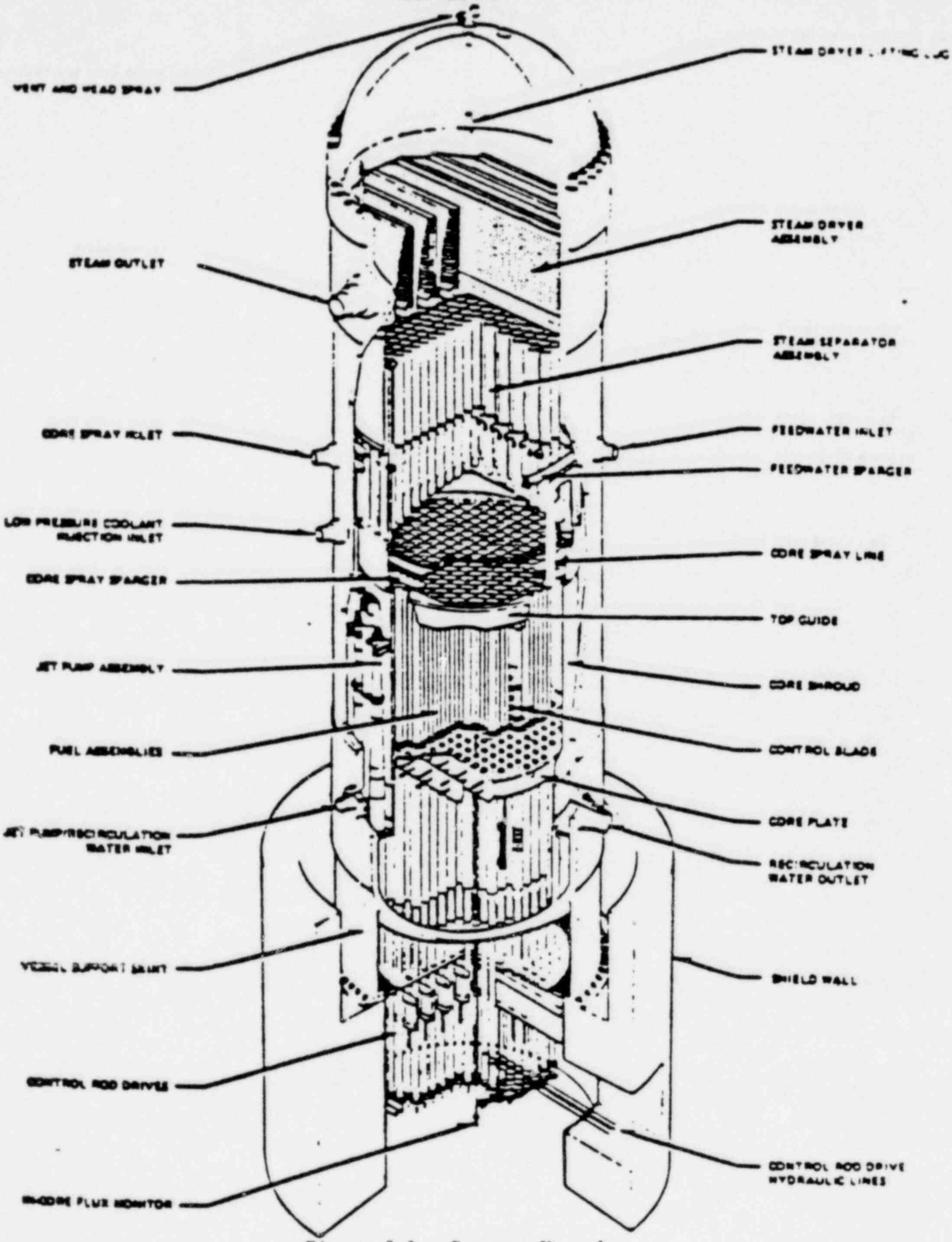

Figure 3-1. Reactor Vessel

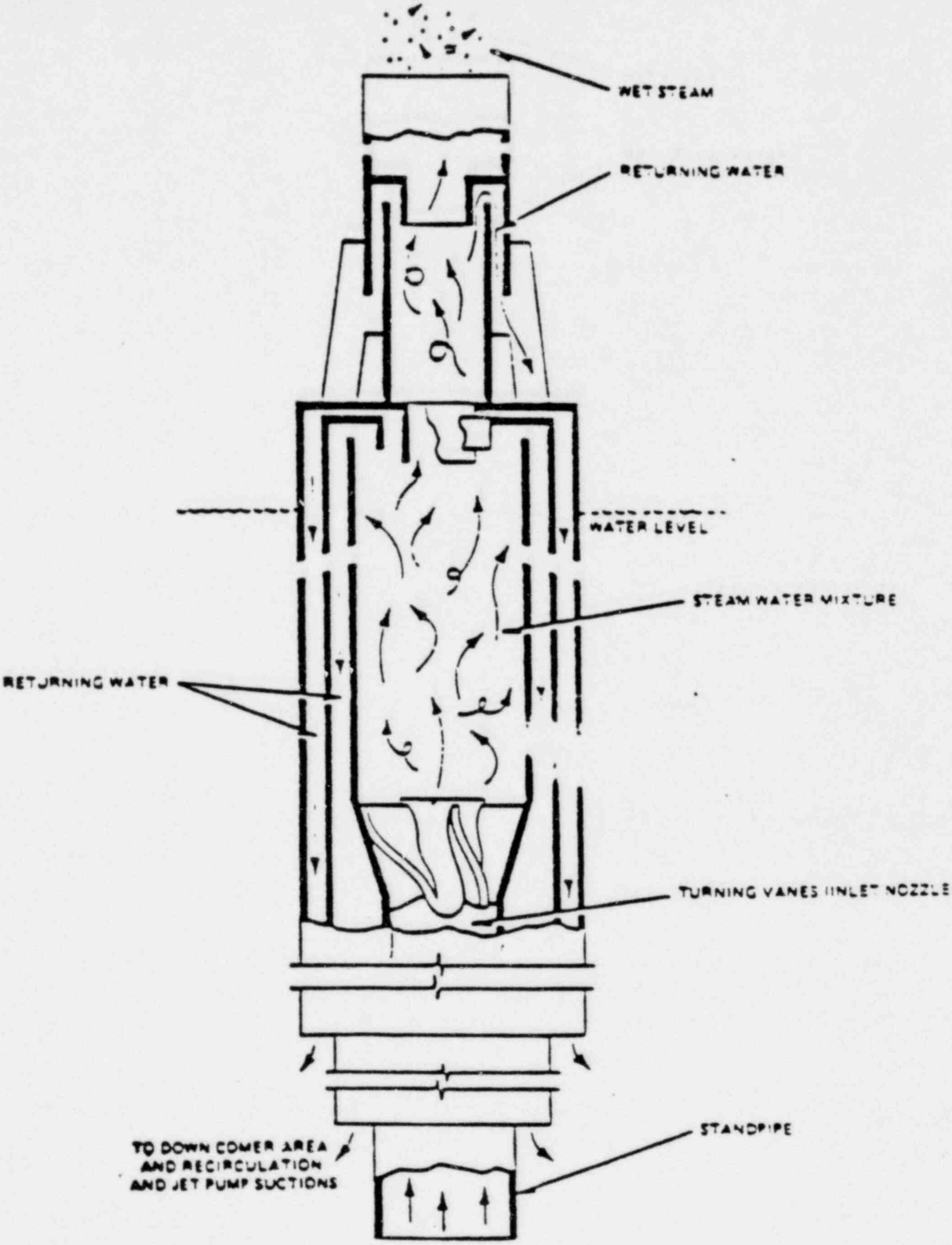

Figure 3-2. Steam Separator

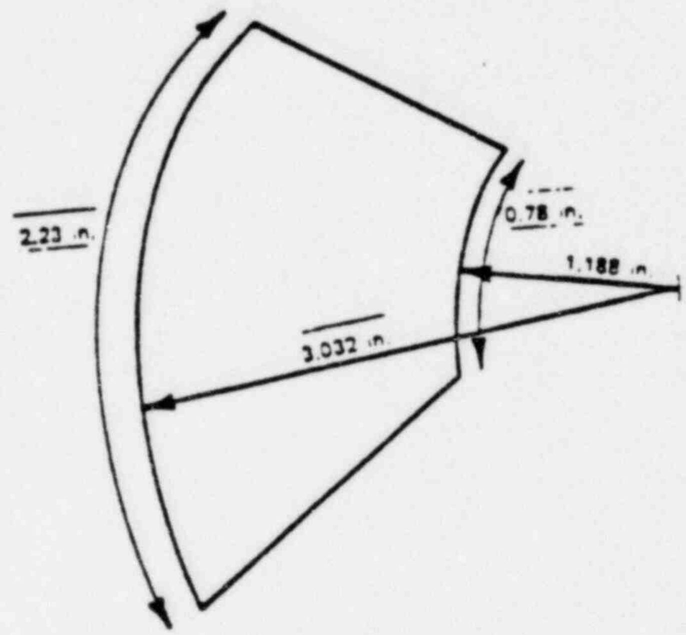

Figure 3-3. Largest Piece That Can Fit Through the Turning Vane (End View)

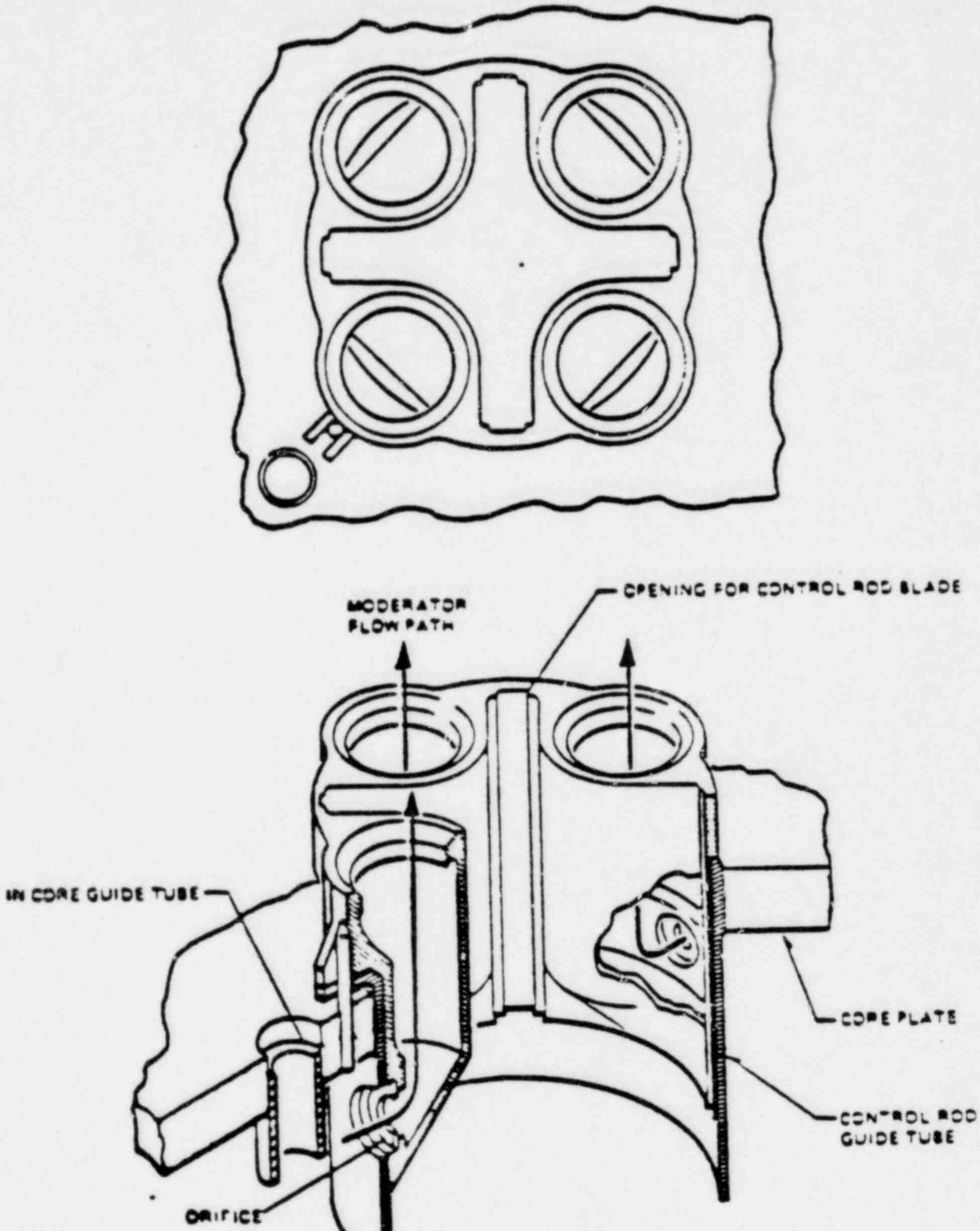

Figure 3-4. Orificed Fuel Support

FUEL ASSEMBLIES & CONTROL ROD MODULE

1. TOP FUEL GUIDE
2. CHANNEL FASTENER
3. UPPER TIE PLATE
4. EXPANSION SPRING
5. LOCKING TAB
6. CHANNEL
7. CONTROL ROD
8. FUEL ROD
9. SPACER
10. CORE PLATE ASSEMBLY
11. LOWER TIE PLATE
12. FUEL SUPPORT PIECE
13. FUEL PELLETS
14. END PLUG
15. CHANNEL SPACER
16. PLENUM SPRING

GENERAL ELECTRIC

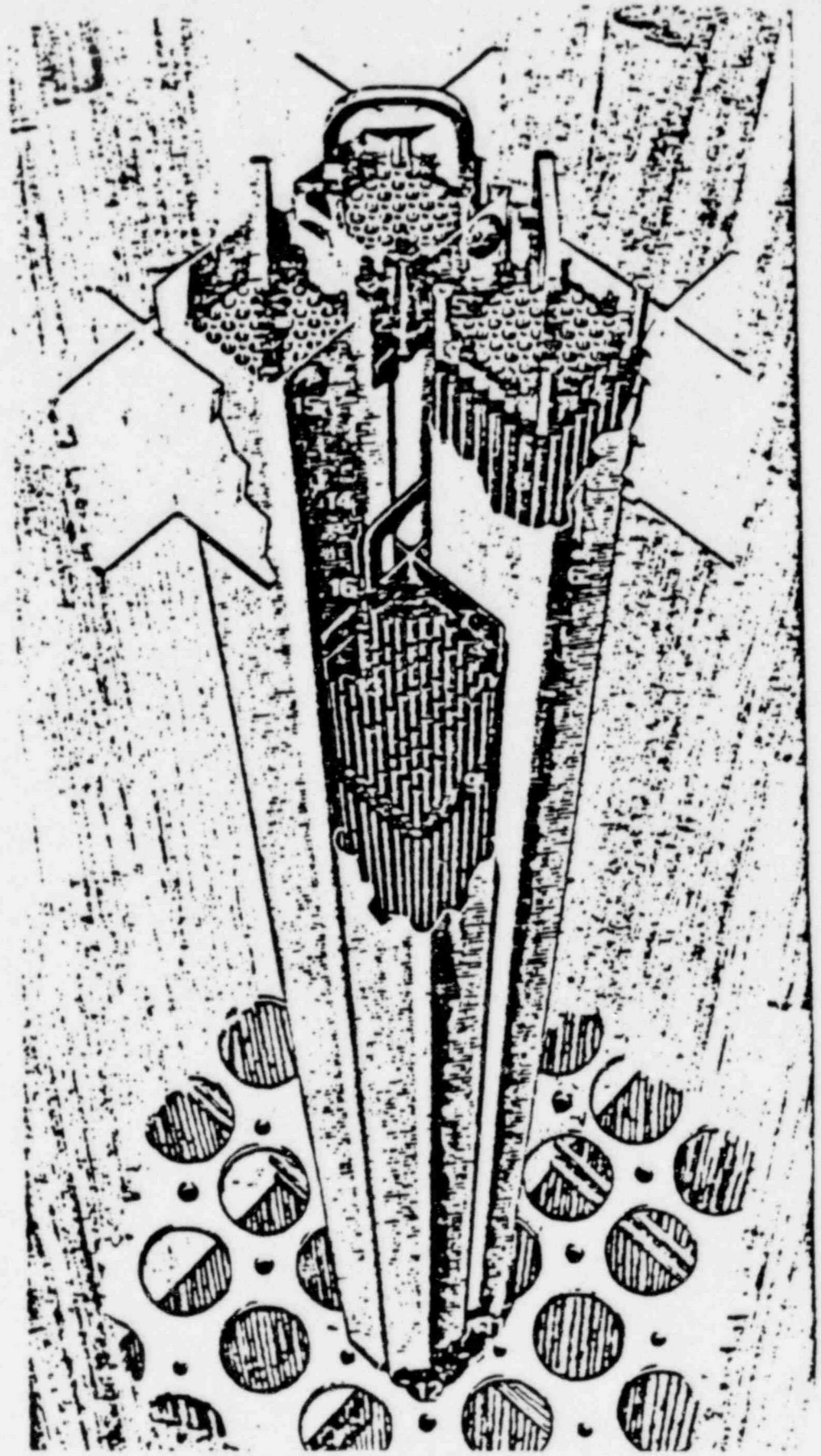

Figure 3-5. Fuel Assemblies and Control Rod Module

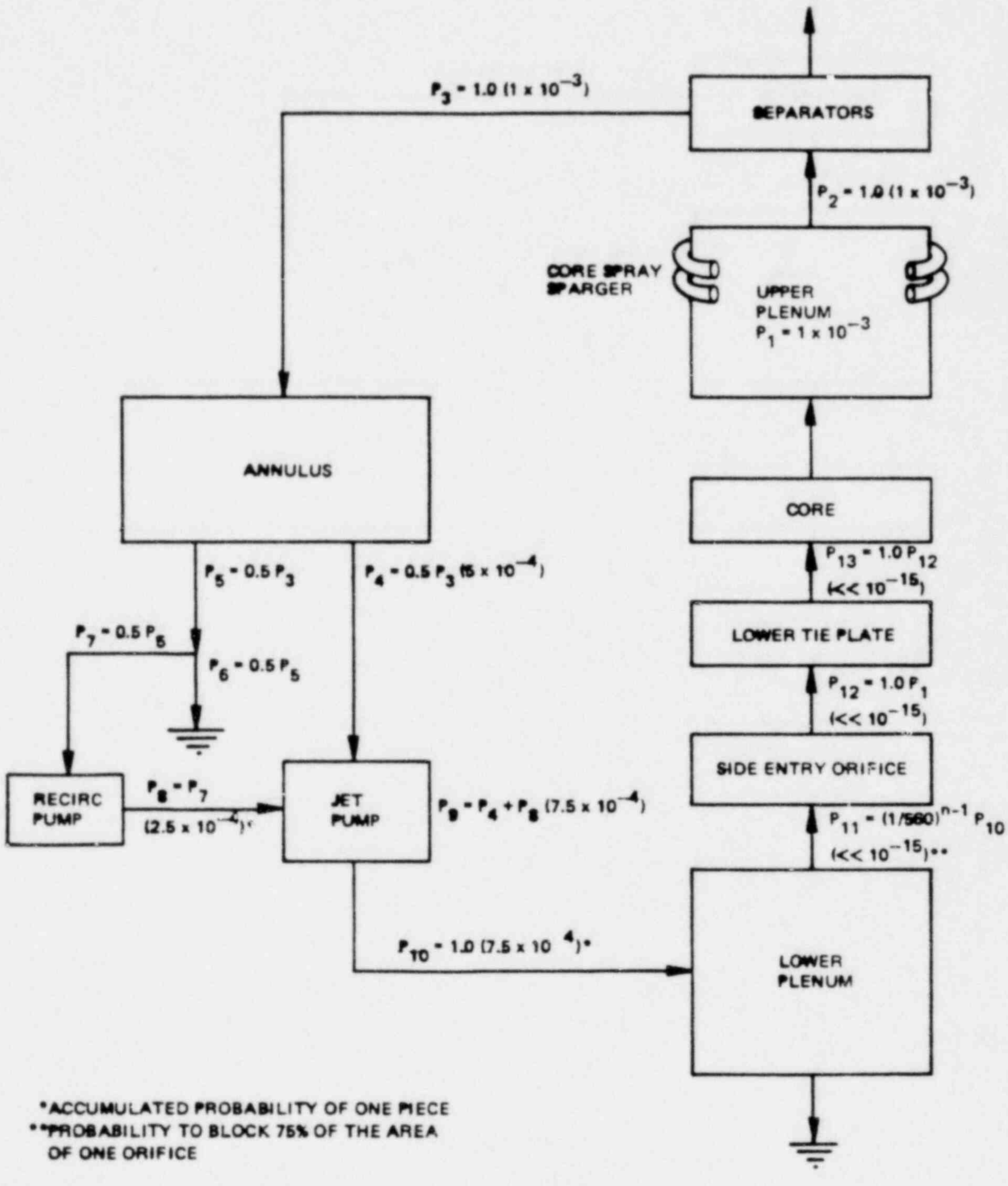

Figure 3-6. Loose Piece Potential Upward Flow Path

4. LOSS-OF-COOLANT ACCIDENT ANALYSIS WITH A CRACK IN ONE CORE SPRAY SPARGER

4.1 INTRODUCTION

A crack in the core spray sparger at the Brunswick 2 plant, located in the upper sparger near the T-Box to sparger weld, has been clamped. The structural integrity of the sparger and the intended cooling function of the spray system are not adversely affected by the presence of the crack. Therefore, no change in Emergency Core Cooling System (ECCS) performance analysis or Maximum Average Planar Linear Heat Generation Rate (MAPLHGR) limits is required. However, at the request of Carolina Power & Light (CP&L), conservative ECCS sensitivity analyses have been performed and are presented here.

This section describes the methods used to evaluate the MAPLHGR requirements to meet 10CFR50 Appendix K for the current Brunswick 2 operating cycle with a cracked core spray sparger. The potential effect of spray distribution on the Peak Cladding Temperature (PCT) of the limiting break size and a single failure is discussed in Section 4.2. The phenomena involved and the inputs to the approved 10CFR50 Appendix K computer codes are discussed in Section 4.3, the results of analyses performed are given in Section 4.4 and 4.5, and the conclusions are presented in Section 4.6.

4.2 LIMITING BREAK SIZE AND SINGLE FAILURE ANALYSIS

For the Brunswick 2 plant, there are no single failures for any break location (other than a core spray line break) that can result in less than one core spray system injecting water into the upper plenum above the reactor core. For a core spray line break, there are always at least three low pressure ECCS pumps injecting water into the reactor vessel, thereby ensuring that this break is not a limiting event. For medium and large break sizes (which depressurize relatively quickly), the most limiting failures are those that result in the least number of ECCS pumps remaining operable (i.e., injecting water into the reactor vessel).

The only two single failure candidates that are potentially limiting for medium to large break sizes are:

A. Diesel Generator Failure - 1 core spray (LPCS) + 1 Low Pressure Coolant Injection (LPCI) + HPCI + the ADS operable;

B. LPCI Injection Valve Failure - 2 core spray (LPCS) + HPCI + the ADS operable.

Since the High Pressure Coolant Injection (HPCI) is steam turbine powered, it is not a significant contributor to mitigating medium to large breaks which depressurize rapidly. Also, since the function of the Automatic Depressurization System (ADS) is to depressurize the reactor as a backup to the HPCI, it contributes little toward mitigating medium and large break LOCAs. Therefore, failure candidates A and B are limiting and each result in a dependence on only two ECCS pumps.

Per the plant specific LOCA analysis (Reference 4-4), failure candidate B (LPCI Injection valve failure) is limiting by a large margin because of the conservative modeling of counter current flow limiting (CCFL) at the fuel assembly upper tie plates. The calculation limits the coolant delivery or downflow from the core spray systems to the fuel bundles and further prolongs core reflooding by neglecting the water held back in the upper plenum.

Both single failure candidates (A and B) were re-examined for large breaks acknowledging the crack in one sparger. The limiting single failure, break size, and location were found not to change. This is because the calculated core uncovery and recovery times and the reactor depressurization rates are insensitive to changes in spray cooling heat transfer, and even with more realistic treatment of CCFL the failure candidate B yields (marginally) the limiting result.

For smaller break sizes, the limiting single failure is the high pressure ECCS (HPCI) since the transient is a relatively slow depressurization event that is dominated by the time required to either reflood the reactor with the high pressure system or the time to depressurize the reactor so that the low pressure systems become effective. Furthermore, the effects of CCFL in limiting coolant delivery to the core are not as large at higher reactor pressures. The small break LOCA transient is, therefore, insensitive to spray distribution because reflooding occurs very rapidly once any one or two of the six low pressure ECCS pumps begin injecting coolant into the reactor vessel.

Therefore, only medium and large break LOCA calculations have any potential for dependence on spray distribution, and detailed LOCA calculations need only be performed for large limiting break sizes with the current limiting single failure.

4.3 PHENOMENA INVOLVED IN THE ANALYSIS OF SPARGER PERFORMANCE

The key phenomena involved in evaluating core cooling performance resulting from the injection of spray through the core spray sparger in the BWR are listed in Table 4-1. The analytical assumptions regarding these phenomena which are important to understanding system performance and the predicted core cooling are also tabulated.

The approved Appendix K models include these phenomena, but the input assumptions used in the standard reload analysis are overly conservative. The extent of this conservatism is evident from Table 4-1 in light of the realistic phenomena observed and tabulated. The bases for the first three of these realistic inputs are derived from a recently completed, jointly sponsored, large scale BWR safety research program between NRC, EPRI and GE (Reference 4-1).

The relevant phenomena do not depend on the distribution of the injected spray through the nozzles but on the injection of coolant into the upper plenum (Reference 4-1). Recently, the NRC staff has evaluated the issues related to the adequacy of the core spray systems in the BWR and their ability to distribute spray water to the core (Reference 4-2). This evaluation was

Table 4-1

KEY PHENOMENA RELATED TO CORE SPRAY COOLING PERFORMANCE

Phenomena	Analytical Assumptions Used in the Current Reload Analysis	Realistic Assumptions
Upper Plenum Inventory	Conservatively assumed to not interact or contribute to core reflood during LOCA transient	Pool of water present throughout transient assures coolant delivery to all fuel bundles (supported by Large Scale Tests)
Counter Current Flow Limiting	Saturated water in upper plenum above core	Some subcooling and less CCFL occurs. A residual pool of water remains during and after core reflooding. (supported by Large Scale Tests)
	No CCFL breakdown	Breakdown of CCFL shortly after spray initiation causes rapid reflooding (supported by Large Scale Tests)
Core heat transfer	Limited spray cooling after blowdown (Appendix K credit only)	Steam cooling contribution as much as 10 times greater than Appendix K spray cooling
Decay Heat	1971 ANS + 20% specified by Appendix K	1979 ANS (GE has submitted a technical basis as a part of the Standard Plant docket which is based on the 1979 ANS decay heat correlation)

in response to concerns that the core spray systems may not distribute any spray to certain regions of the core when injected into an upper plenum steam environment. The staff testimony in Reference 4-2 concluded that the spray distribution adequacy is not a safety concern because the coolant injected into the upper plenum will either disperse uniformly in a pool of water above the core or will flow to the lower plenum producing rapid reflooding. Therefore, the current reload calculation using the plant specific LOCA analysis basis is applicable and conservative despite the presence of any crack(s) in the core spray sparger.

4.4 ANALYSIS RESULTS

The current reload analysis for the limiting LOCA with the most limiting fuel type and exposure combination results in a calculated PCT of 2200°F. This is for 8x8R fuel at an exposure of 20,000 MWd/t and a MAPLHGR of 11.8 KW/ft.

Figure 4-1 shows the heat transfer assumed as a function of time (Curve 1) compared with the realistic heat transfer (Curve 2). A bounding calculation (Curve 3) of the limiting LOCA with approved Appendix K models but with CCFL breakdown input based on observed large scale tests, and no convective core cooling prior to reflooding results in a maximum PCT of less than 1260°F at a MAPLHGR of 11.8 KW/ft. This result demonstrates that the current reload calculation is conservative by more than 940°F. No credit for steam cooling or the improved decay heat correlation are included in this calculation which would further reduce the PCT.

A comparison of the current reload analysis with the conservatively calculated PCT using CCFL breakdown is shown in Curve 4 at the bottom of Figure 4-1. It is clear from this figure that the overly conservative treatment of CCFL results in the unrealistically slow core reflooding time and high calculated PCT in the reload analysis.

4.5 BOUNDING SENSITIVITY CALCULATION

At the request of CP&L, a simplified and conservative sensitivity calculation was also performed with the following assumptions: 1) no credit for upper plenum inventory, 2) no CCFL breakdown, and 3) no cooling contribution from the sparger with the crack before core reflooding. This analysis results in a bounding MAPLHGR reduction of 8.5 percent at 20,000 MWd/T exposure to meet the 2200°F Appendix K limits for all fuel types and exposures.

To perform this bounding calculation, the cooling contribution from the cracked sparger was ignored prior to reflooding. With only the core spray system with the cracked spray sparger operating, the spray heat transfer coefficient was set to zero. For the core spray system with the uncracked sparger operating, the spray heat transfer was set to one half the value used in the reload calculation (Reference 4-3). This is the approved assumption when one spray system is totally inoperable.

GE considers this calculation to be unrealistic and overly conservative but has performed this calculation at the request of CP&L to quantify the sensitivities of the core spray performance to various assumptions.

4.6 CONCLUSIONS

An analysis of one cracked core spray sparger in the Brunswick 2 BWR was performed utilizing the approved Appendix K evaluation models. The results of this analysis demonstrate that with CCFL breakdown (derived from a conservative interpretation of recent large scale tests) the calculated PCT is at least 940°F less than the current reload circulation. Without CCFL breakdown the upper plenum inventory (pool of water) ensures adequate coolant delivery to the core. Therefore, the current reload calculation is applicable and conservative and there is no basis to impose a MAPLHGR penalty on Brunswick 2 for the next or succeeding cycles.

4.7 REFERENCES

4-1. Refill-Reflood Program Task 4.4-CCFL/Refill System Effects Test (30°F Sector) SSTF System Response Test Results, D. G. Schumacher, T. Eckert, J. A. Findlay, General Electric Co., NUREG/CR-2568, EPRI NP-1525, GEAP-24893-2, March 1982.

4-2. Transcript of Testimony before the Atomic Safety and Licensing Board For Long Isand Lighting Co., May 28, 1982 - Docket No. 50-322-OL. NRC Staff Testimony of Summer B. Sun on ECCS Core Spray.

4-3. SER, O. D. Parr (NRC) to G. G. Sherwood (GE), Review of General Electric Topical Report NEDO-20566, Amendment 3, June 13, 1978.

4-4. "Loss-of-Coolant Accident Analysis Report for Brunswick Steam Electric Plant Unit No. 2", NEDO-24053, September 1977.

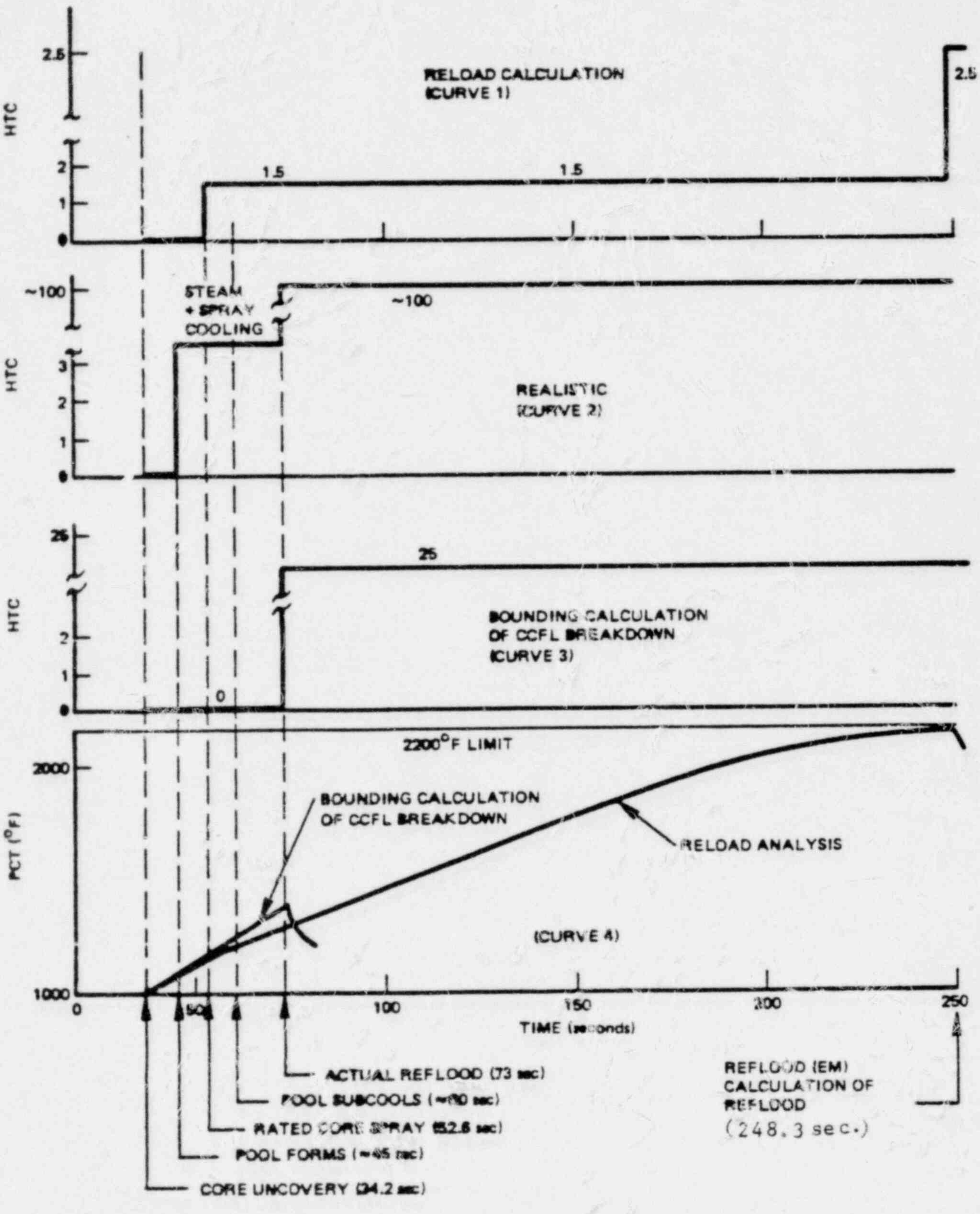

Figure 4-1. Brunswick 2 DBA (Limiting LOCA) Analysis

APPENDIX A

STRUCTURAL ANALYSIS OF THE BRUNSWICK 2 CORE SPRAY SPARGER

TABLE OF CONTENTS

Appendix A

STRUCTURAL ANALYSIS OF THE BRUNSWICK 2 CORE SPRAY SPARGER

SUMMARY

This appendix contains structural analyses that support Sections 2.5.3, 2.5.4, 2.6 and 2.8 of this report and, also, the presentation to the USNRC on June 14 and 15, 1982 reported in Section 1.

Section A.1 contains the calculation of loads during normal plant operation and during the core spray injection event for input into Section A.2, A.3 and A.4 of this Appendix.

Section A.2 contains flow-induced vibration and natural frequency calculations that show that flow-induced vibration is not a problem for the intact sparger condition and for an assumed broken sparger condition.

Section A.3 contains the structural analysis of the core spray sparger in an intact condition. The stresses were found to be low during all identified loading conditions.

Section A.4 contains the structural analysis of the core spray sparger which conservatively assumes a 360° throughwall crack in the larger sparger arm at the T-box. The analysis ignores the effect of a clamp (or assumes no clamp is installed).

The stresses were found to be low during all identified loading conditions.

Section A.5 contains heat transfer calculations that determine the maximum (bounding) temperature differential between the sparger pipe arms and the shroud wall.

Because the calculated stresses were well below the allowables, it was deemed unnecessary to calculate principle stresses and stress intensities. The material properties are given below for comparison purposes.

- Material - 304 SS
- Temperature - 550°F
- Material Properties (ASME Section III)

S_m = 16.9 ksi (upset allowable)

S_y = 18.8 ksi

S_u = 57.3 ksi

$E = 25.75 \times 10^6$ lb/in.^{2}

The structural analysis results of the intact sparger and the broken sparger are summarized below.

SUMMARY OF STRESSES FOR INTACT SPARGER

	Seismic Bending Stress (lb/in.^{2})	Impingement Bending Stress (lb/in.^{2})	Thermal Mismatch Normal Stress (lb/in.^{2})
Sparger Pipe	476	174	3319

	Normal Stress (lb/in.^{2})	Shear Stress (lb/in.^{2})
Nozzle (Weld)	369	101
Lower Bracket (Plate)	3845	954
Lower Bracket (Weld)	3067	617
Middle Bracket (Plate)	1422	31 (avg)
Middle Bracket (Weld)	654	44 (avg)

SUMMARY OF STRESSES FOR BROKEN SPARGER

	Seismic Bending Stress ($lb/in.^2$)	Impingement Bending Stress ($lb/in.^2$)	Thermal Mismatch Normal Stress ($lb/in.^2$)
Sparger Pipe	2380	868	3316

	Normal Stress ($lb/in.^2$)	Shear Stress ($lb/in.^2$)
Nozzle (Weld)	4267	4396
Lower Bracket (Plate)	3031	752
Lower Bracket (Weld)	5974	534
Middle Bracket (Plate)	5210	158 (avg)
Middle Bracket (Weld)	1800	224 (avg)

A.1 DESIGN LOADS

This section contains the calculation of loads on the core spray sparger during normal plant operation and during the core spray injection event. The loads are used in Section A.2 for natural frequency calculations and in Sections A.3 and A.4 for calculating stresses in the intact sparger condition and the assumed broken sparger condition respectively.

A.1.1 Weight of Sparger

3 1/2" sch. 40 pipe

$$W_{pipe} = \frac{\pi}{4}\left(d_o^{\,2} - d_i^{\,2}\right)\rho_{stainless\ steel} \qquad \rho_{ss} = 488\ lb/ft^3$$

$$= \frac{\pi}{4}\left(\left(\frac{4.0}{12}\right)^2 - \left(\frac{3.548}{12}\right)^2\right)(488) = 9.1\ lb/ft$$

$$W_{water} = \frac{\pi}{4} \left(\frac{3.548}{12}\right)^2 \; 62.2 = 4.3 \text{ lb/ft}$$

$$W_{nozzles} \cong 3 \text{ lb/ft}$$

$$W = 9.1 + 4.3 + 3 = 16.4 \text{ lb/ft}$$

$$= \frac{16.4}{12} = \underline{\underline{1.37}} \text{ lb/in.}$$

A.1.2 Impingement Loads (90° Deflection of Flow)

$$F = PA = \frac{\rho \, V^2 \, DL}{g}$$

$$\frac{F}{L} = \frac{\rho \, V^2 \, D}{g}$$

$\rho = 45.87 \text{ lb/ft}^3$ @ 550°F

$D = \frac{4.0}{12}$ ft   V = 5 ft/sec
(conservative value - more realistic value is $\sim$3.5 ft/sec)

$$\frac{F}{L} = \frac{45.87 \, (5)^2 \, (4.0/12)}{32.2}$$

$$\frac{F}{L} = 11.87 \text{ lb/ft} = \underline{\underline{1.0}} \text{ lb/in.}$$

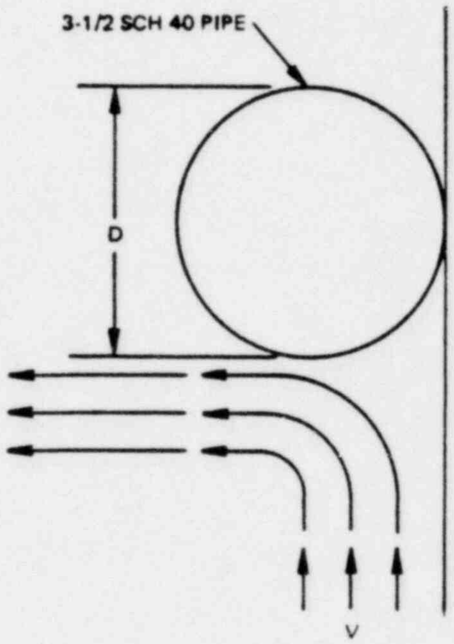

A.1.3 Impingement and Seismic Load

Impingement Only

$W_i = -1.0$ lb/in. (upward)   (Sect A.1.1)

Seismic Only - Assume 1g (conservative)

$W_s = W \pm (1.0)\, W$ $W = 1.37$ lb/in.   (Sect A.1.2)

$W_s = 1.37 - 1(1.37) = \underline{0}$ lb/in. (upward)

$W_s = 1.37 + 1(1.37) = \underline{2.74}$ lb/in. (downward)

Impingement & Seismic

$W_T = -1.0 - 0.0 = \underline{-1.0}$ lb/in. (upward)

$W_T = -1.0 + 2.24 = \underline{1.74}$ lb/in. (downward)

Seismic loading (absolute value) is more severe than seismic plus impingement loading.

A.1.4 Pressure/Flow Loads

Maximum Flow = 6000 gpm (Rated Flow = 4625 gpm) (Section A.5.3)

$$Q = 6000 \text{ gal/min} \times \frac{1 \text{ min}}{60 \text{ sec}} \times \frac{\text{ft}^3}{7.48 \text{ gal.}}$$

$$= 13.37 \text{ ft}^3\text{/sec}$$

- Maximum pressure in sparger arm

$$\Delta P_{measured} = 28 \text{ psig @ } 4491 \text{ gpm}$$

$$\Delta P_{max} = 28 \left(\frac{6000}{4491}\right)^2 = \underline{50.0} \text{ psig}$$

- Pressure load on sparger segment

$$F = \Delta PA \qquad A = \frac{\pi}{4}\ d_i^{\ 2} = \frac{\pi}{4}(3.548)^2 = 9.89 \text{ in.}^2$$

$$F_{max} = 50.0\ (9.89) = \underline{495 \text{ lb}}$$

- Maximum nozzle flow

The one inch VNC nozzle has the highest flow and will produce the greatest nozzle thrust.

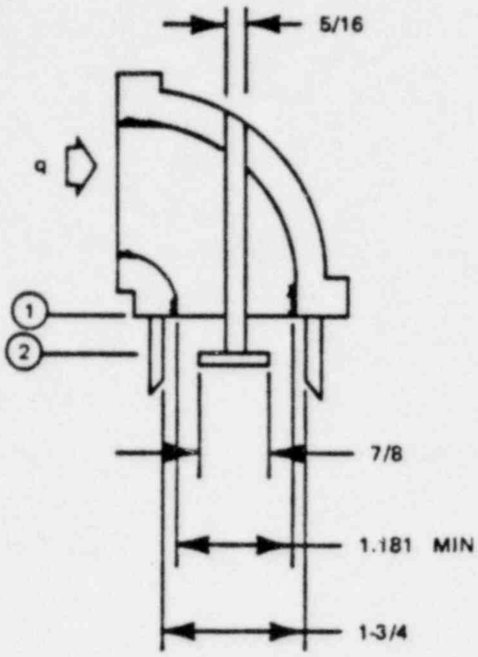

$$A_1 = \frac{\pi}{4}\,(1.181^2 - 0.313^2) = 1.018 \text{ in.}^2 \text{ (min.)}$$

$$A_2 = \frac{\pi}{4}\,(1.75 - 0.875^2) = 1.804 \text{ in.}^2$$

$$\rho = 62.2 \text{ lb/ft}^3 \text{ @ } 80°\text{F}$$

$$q_{max} = 64 \text{ gpm @ } 4491 \text{ gpm}$$

$$q_{max} = 64\left(\frac{6000}{4491}\right) = 85.5 \text{ gpm}$$

$$W_{max} = \frac{85.5(62.2)}{60(7.48)} = 11.85 \text{ lb/sec}$$

$$V_{max} = \frac{W_{max}}{\rho A} = \frac{11.85(144)}{62.2(1.018)} = \underline{26.95} \text{ ft/sec @ exit from nozzle}$$

A.1.5 <u>Nozzle Thrust Loads</u>

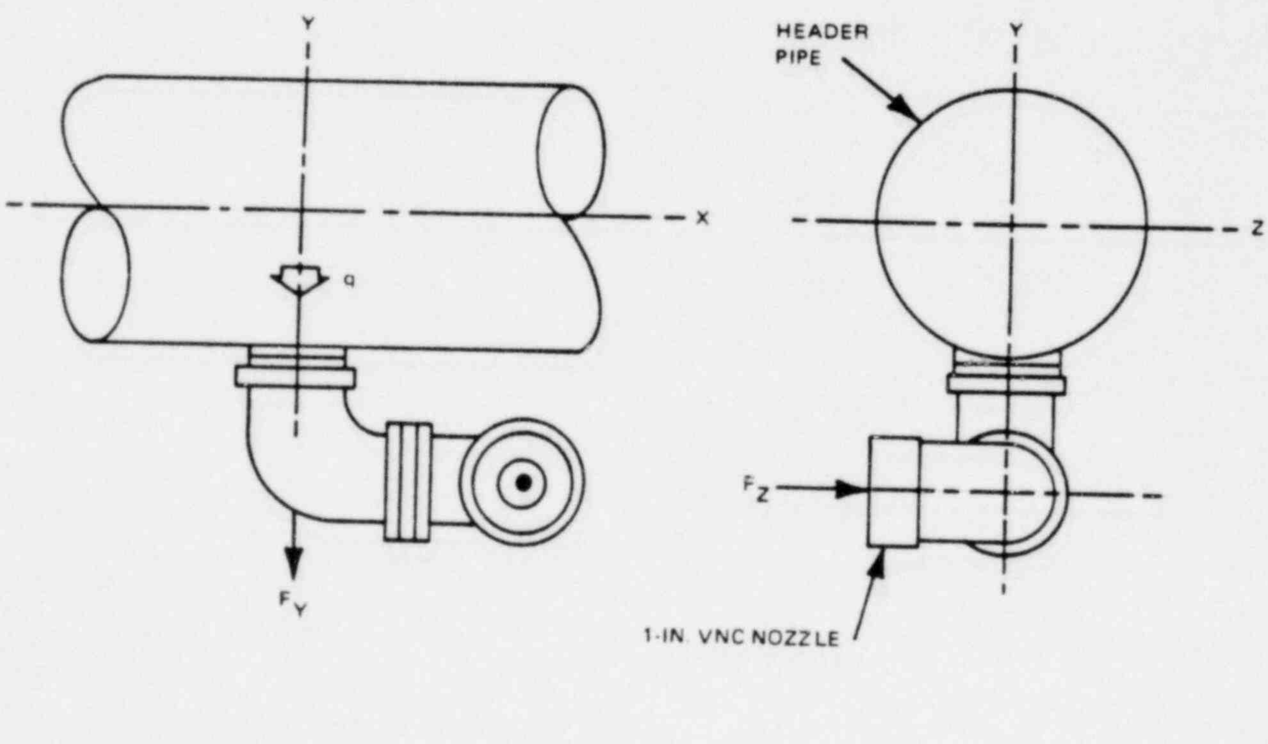

$$F_y = \Delta PA + \frac{\rho V^2 A}{g}$$

$$\Delta P = 28 \text{ @ 4491 gpm test flow}$$

$$\Delta P = 28\,(6000/4491)^2 = 50.0 \text{ psi @ mount}$$

$$A = \frac{\pi}{4} d^2$$

where

d = 1.181 in (minor diameter of 1" straight internal threads)

$$A = \frac{\pi}{4}(1.181)^2 = 1.095 \text{ in}^2$$

$$V = \frac{W_{max}}{\rho A} = \frac{11.85\ (144)}{62.2\ (1.095)} = 25.05 \text{ ft/sec @ exit from HEADER}$$

$$F_y = 50(1.095) + \frac{62.2\ (25.05)^2\ (1.095)}{32.2\ (144)} = \underline{63.97} \text{ lb}$$

$$F_z = \frac{\rho V^2 A}{g} + \cancelto{0}{\Delta PA} \qquad V = 26.95 \text{ ft/sec @ EXIT FROM NOZZLE}$$

$$F_z = \frac{62.2\ (26.95)^2\ (1.018)}{32.2\ (144)} = \underline{9.92 \text{ lb}}$$

A.1.6 Thermal Expansion Mismatch Loads - Intact Sparger

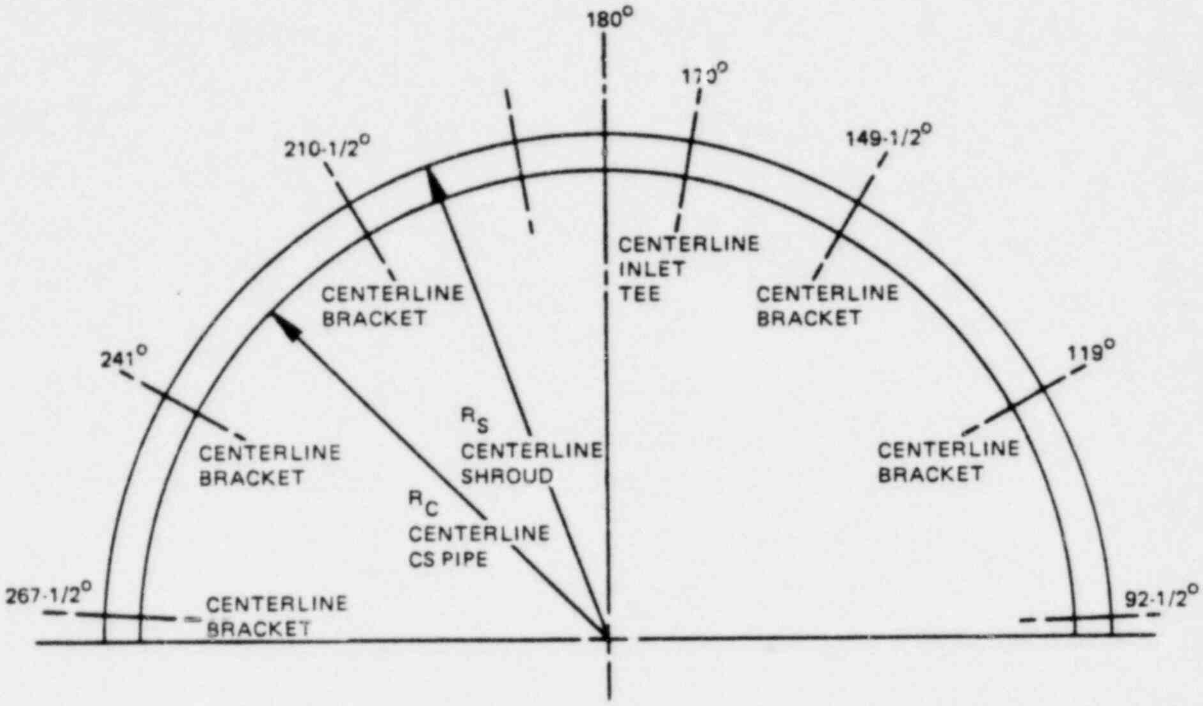

$$R_s = \frac{186\frac{1}{2}}{2} + \frac{1.5}{2} = 94 \text{ in.}$$

$$R_c = \frac{186\frac{1}{2}}{2} - \frac{4.0}{2} = 91.25 \text{ in.}$$

SHROUD TEMPERATURE = 550°F
CS PIPE TEMPERATURE = 200°F } See Section A.5-1

$\therefore \Delta T = 350°F$

$\Delta R = \alpha R \Delta T$ — For 304 STAINLESS STEEL, $\alpha = 9.6 \times 10^{-6}$ in/in.-°F

$R = \frac{186.5}{2} = 93.25$ in. at shroud-to-pipe interface

$$R_{90^\circ} = 9.6 \times 10^{-6}\ (93.25)\ (350^\circ) = 0.313 \text{ in.}$$

(For 90° arc)

FOR SEGMENT:

Assume $\Delta R = \Delta R_{90^\circ}\ (1-\cos\theta) = 0.313\ (1-\cos\theta)$

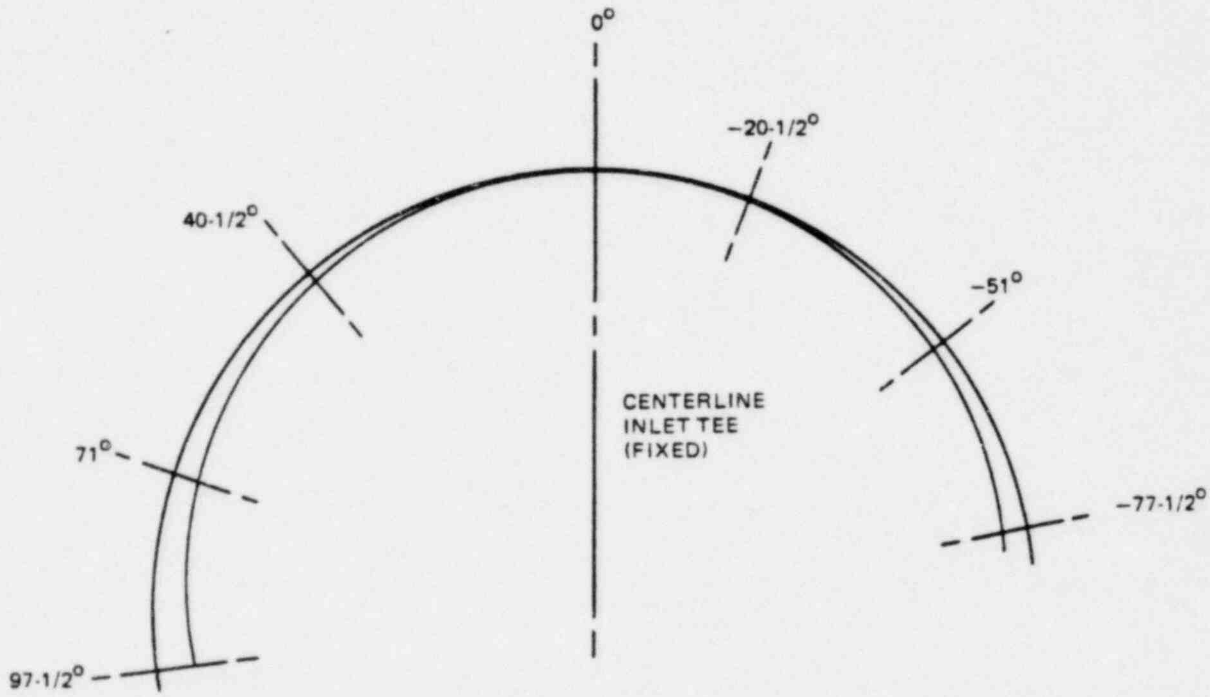

$\Delta R_{40\frac{1}{2}^\circ} = 0.313\ (1 - \cos 40\tfrac{1}{2}^\circ) = \underline{0.075 \text{ in.}}$

$\Delta R_{71^\circ} = 0.313\ (1 - \cos 71^\circ) = \underline{0.211 \text{ in.}}$

$\Delta R_{97\frac{1}{2}^\circ} = 0.313\ (1 - \cos 97\tfrac{1}{2}^\circ) = \underline{0.354 \text{ in.}}$

$\Delta R_{-20\frac{1}{2}^\circ} = 0.313\ (1 - \cos 20\tfrac{1}{2}^\circ) = \underline{0.0198 \text{ in.}}$

$\Delta R_{-51^\circ} = 0.313\ (1 - \cos 51^\circ) = \underline{0.166 \text{ in.}}$

$\Delta R_{-77\frac{1}{2}^\circ} = 0.313\ (1 - \cos 77\tfrac{1}{2}^\circ) = \underline{0.245 \text{ in.}}$

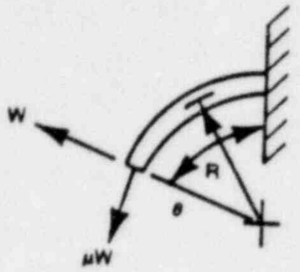

Assume the ΔR is resisted only by each bracket support in turn:

$$\Delta R = \frac{WR^3}{4EI}(2\theta - \sin 2\theta) - \frac{\mu WR^3}{4EI}(\cos 2\theta - 4\cos\theta + 3)$$

$$W = \frac{4EI\Delta R}{R^3\,(2\,\theta - \sin 2\theta - \mu\cos 2\theta + 4\mu\cos\theta - 3\mu)}$$

$$E = 28 \times 10^6 \text{ lb/in.}^2 \qquad R = R_c = 93.25 - 2.0 = 91.25$$

$$I = \frac{\pi}{64}(4.0^4 - 3.548^4) = 4.79 \text{ in.}^4$$

$$\mu = 0.2 \quad \text{(coefficient of friction)}$$

$$W = \frac{4\,(28 \times 10^6)\,(4.79)\,\Delta R}{(91.25)^3\,(2\theta - \sin 2\theta - 0.2\cos 2\theta + 0.8\cos\theta - 0.6)}$$

$$W = \frac{706\,\Delta R}{(2\theta - \sin 2\theta - 0.2\cos 2\theta + 0.8\cos\theta - 0.6)}$$

$$W_{40\frac{1}{2}^\circ} = \frac{706\,(0.075)}{0.403} = \underline{131 \text{ lb}}$$

$$W_{71^\circ} = \frac{706\,(0.211)}{1.68} = \underline{89 \text{ lb}}$$

$$W_{97\frac{1}{2}^\circ} = \frac{706\,(0.354)}{3.15} = \underline{79 \text{ lb}}$$

$$W_{20\frac{1}{2}^\circ} = \frac{706\,(0.0198)}{0.0579} = \underline{241 \text{ lb}}$$

$$W_{-51^\circ} = \frac{706\ (0.116)}{0.747} = \underline{110\ \text{lb}}$$

$$W_{-77\frac{1}{2}^\circ} = \frac{706\ (0.245)}{2.04} = \underline{85\ \text{lb}}$$

A.1.7 Thermal Expansion Mismatch Loads - Broken Sparger

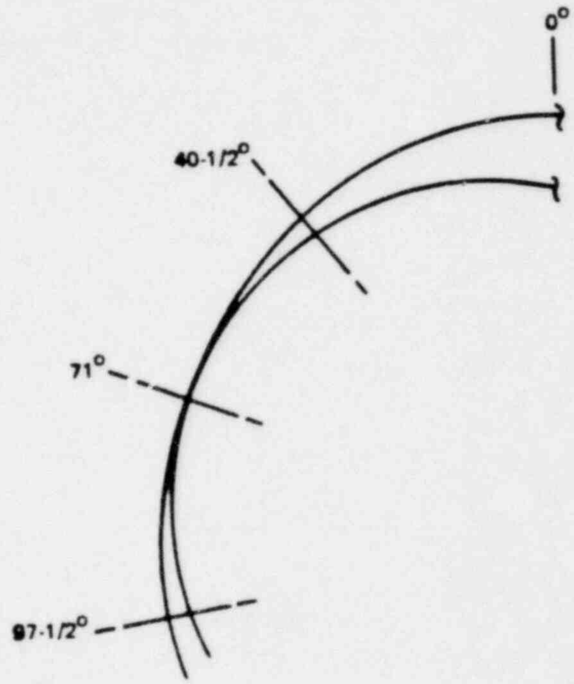

1. Assume break in sparger at T-Box during core spray injection.

2. Assume ΔT at sparger-to-shroud = 350°F (maximum - see Section A.1.6).

$\Delta R = \alpha\ R\ \Delta T$

$\alpha = 9.6 \times 10^{-6}$ in./in.-°F (304-SS)

$R = 93.25$ in. at shroud-to-pipe interface

$\Delta R_{90^\circ\ arc} = 9.6 \times 10^{-6}\ (93.25)\ (350^\circ) = 0.313$ in.

Assume $\Delta R_\theta = \Delta R_{90^\circ\ arc}\ (1 - \cos\theta)$

Take 70° bracket as $\theta = 0^\circ$

Then: $40\frac{1}{2}^\circ$ bracket is at $\theta = 40\frac{1}{2} - 71 = -30\frac{1}{2}^\circ$.

$97\frac{1}{2}^\circ$ bracket is at $\theta = 97\frac{1}{2} - 71 = 26\frac{1}{2}^\circ$.

$\Delta R_{-30\frac{1}{2}^\circ} = 0.313\ (1 - \cos 30\frac{1}{2}^\circ) = 0.0433$ in.

$\Delta R_{26\frac{1}{2}^\circ} = 0.313\ (1 - \cos 26\frac{1}{2}^\circ) = 0.0329$ in.

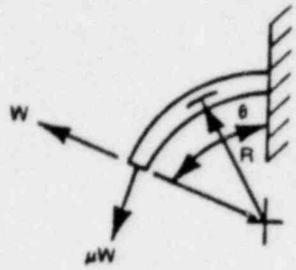

Assume that the 71° bracket is fixed and that the corresponding ΔR is resisted by the brackets to each side of it:

$$\Delta R = \frac{WR^3}{4EI}(2\theta - \sin 2\theta) - \frac{\mu WR^3}{4EI}(\cos 2\theta - 4\cos\theta + 3)$$

$$W = \frac{4EI\Delta R}{R^3\,(2\theta - \sin 2\theta - \mu\cos 2\theta + 4\,\mu\cos\theta - 3\mu)}$$

$E = 28 \times 10^6$ lb/in.^{2} $\qquad R = R_c = 93.25 - 2.0 = 91.25$

$$I = \frac{\pi}{64}(4.0^4 - 3.548^4) = 4.79 \text{ in.}^4$$

$\mu = 0.2$ (coefficient of friction)

$$W = \frac{4\,(28 \times 10^6)\,(4.79)\,\Delta R}{(91.25)^3\,(2\theta - \sin 2\theta - 0.2\cos 2\theta + 0.8\cos\theta - 0.6)}$$

$$= \frac{706\ \Delta R}{(2\theta - \sin 2\theta - 0.2\cos 2\theta + 0.8\cos\theta - 0.6)}$$

$$W_{-30\frac{1}{2}^\circ} = \frac{706 \times 0.0433}{(2\pi \times 30.5/180 - \sin 61^\circ - 0.2\cos 61^\circ + 0.8\cos 30.5^\circ - 0.6)}$$

= 168 lb

$$W_{26\frac{1}{2}^\circ} = \frac{706 \times 0.0329}{(2\pi \times 26.5/180 - \sin 53^\circ - 0.2\cos 53^\circ + 0.8\cos 26.5^\circ - 0.6)}$$

= 190 lb (maximum)

A.2 FLOW INDUCED VIBRATION - NATURAL FREQUENCY

GE Design Basis requires that the natural frequency f_n is equal to or greater than three (3) times the vortex shedding frequency.

A.2.1 Flow Induced Vibration

The vortex shedding frequency, f_n, is given by

$$\frac{f_v D}{V} = 0.21$$

V = velocity past shroud wall = 5 ft/sec (Conservative value - more realistic value is ~3.5 ft/sec)

D = sparger pipe diameter = $\frac{4.0}{12}$ ft

$$f_v = \frac{0.21\ (5)}{(4/12)} = \underline{\underline{3.15}}\ \text{Hz}$$

A.2.2 Natural Frequency

The sparger natural frequency is now calculated for four different cases. The first two cases are bounding for the intact sparger. The last two cases are for the broken sparger.

Case 1 - Intact Sparger

Calculate the natural frequency of the sparger by examining the longest segment between support brackets. Assume this section has a uniform load w per unit length, both ends simply supported.

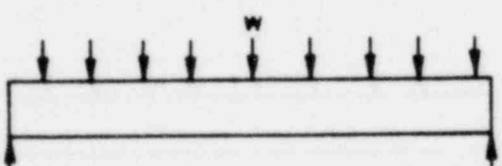

$$f_n = \frac{K_n}{2\pi} \sqrt{\frac{EIg}{wL^4}}$$

$$K_n = 9.87$$

$E = 25.75 \times 10^6$ lb/in.^{2} $\qquad$ $I = 4.79$ in.^{4}

$L = \frac{40.5}{180} \times \pi \times 91.25 = 65.4$ in. (distance from T-box centerline to the first bracket)

$W = 1.37$ lb/in.

$$f_n = \frac{9.87}{2\pi} \sqrt{\frac{25.75 \times 10^6 \ (4.79) \ (32.2) \ (12)}{1.37 \ (64.5)^4}} = 70.4 \text{ Hz}$$

$$\text{Ratio} = \frac{f_n}{f_v} = \frac{70.4}{3.15} > 3$$

Case 2 - Intact Sparger (Missing Bracket)

Calculate the natural frequency of the sparger by examining the longest segment between support brackets ignoring an intermediate support. Values other than L are same as previous case.

$$L = \frac{71}{180} \times \pi \times 91.25 = 113$$

$$f_n = 70.4 \left(\frac{64.5}{113}\right)^2 = 22.9$$

$$\text{Ratio} = \frac{f_n}{f_v} = \frac{22.9}{3.15} > 3$$

Case 3 - Broken Sparger

Calculate the natural frequency of the unsupported sparger segment. Assume the segment acts as a cantilever and has a uniform load w (force/unit length).

NOTE: Length of unsupported segment is taken 3" from T-box centerline to account for location of crack.

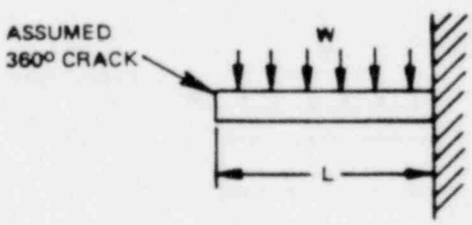

$$f_n = \frac{k_n}{2\pi} \sqrt{\frac{EIg}{wL^4}}$$

$$k_n = 3.52$$

$$E = 25.75 \times 10^6 \text{ lb/in.}^2$$

$I \quad = 4.79 \text{ in.}^4$

$L_{max} = [40\tfrac{1}{2} \, (\pi/180) \times 91.25] - 3 = 64.5 - 3 = 61.5 \text{ in.}$
(∼distance from crack to bracket)

$w \quad = 1.37 \text{ lb/in.}$ (Section A.1.1)

$$f_n = \frac{3.52}{2\pi} \sqrt{\frac{25.75 \times 10^6 \, (4.79) \, (32.2) \, (12)}{1.37 \, (61.5)^4}} = 27.6 \text{ Hz}$$

$$\text{Ratio} = \frac{f_n}{f_v} = \frac{27.6}{3.15} > 3$$

Case 4 - Broken Sparger (Include Effect of Two Near Brackets)

Rayleigh's Method:

The total kinetic energy of the system is zero at the maximum displacement but is maximum at the static equilibrium point. On the other hand, the total potential energy is maximum at the maximum displacement but is zero at the static equilibrium point. From conservation of energy:

$$(K.E.)_{max} = (P.E.)_{max}$$

$$\sum \frac{Wy^2 \; w_n^{\,2}}{g} = \sum Wy$$

where

W = weight, lb

y = deflection, in.

g = gravitational constant = 386 in./sec^2

w_n = natural frequency, radians/sec

The deflection of the member is obtained by successive graphical integrations starting with the shear diagram.

The loading diagram is shown below. The reaction loads are calculated to develop the shear diagram. The slope at the left end (R_1) is calculated to initialize the slope (dy/dx) diagram.

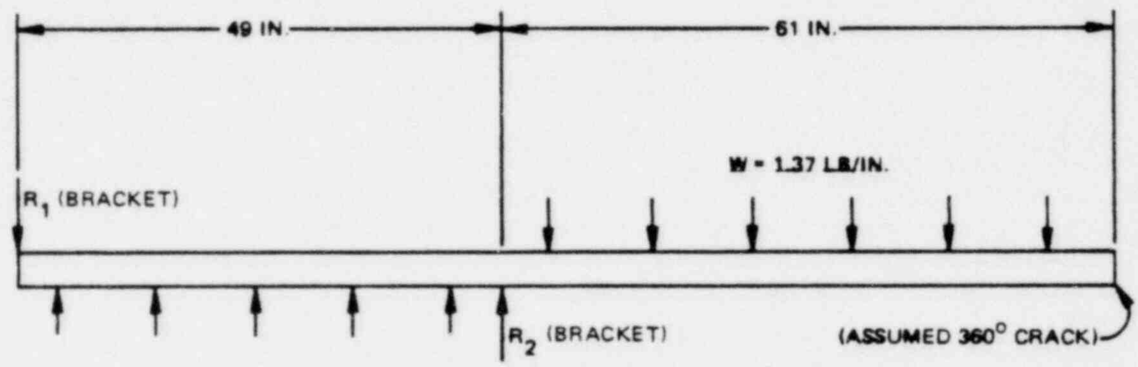

LOADING

$$\Sigma M_1 = 0 \quad 49\ R_2 = 1.37\ (61)\ (49 + 61/2) - \frac{1.37\ (49)^2}{2}$$

$$R_2 = 102.0 \text{ lb}$$

$$\Sigma M_2 = \quad 49\ R_1 = \frac{1.37\ (49)^2}{2} + \frac{1.37\ (61)^2}{2}$$

$$R_1 = 85.6 \text{ lb}$$

$$85.6 - 1.37\ (49) - 102.0 + 1.37\ (61) = 0 \quad \text{(Check)}$$

Slope at R_1:

$$\theta_1 = \frac{1}{24}\ \frac{w\ \ell_1^{\ 3}}{EI} + \frac{1}{6}\ \frac{M_2\ \ell_2}{EI} \qquad M_2 = \frac{1.37\ (61)^2}{2} = 2549 \text{ in.-lb}$$

$$\theta EI = \frac{w\ \ell_1^{\ 3}}{24} + \frac{M_2\ \ell_2}{6} = \frac{1.37\ (49)^3}{24} + \frac{2549\ (61)}{6} = 32630 \text{ lb-in.}^2$$

The shear diagram is now constructed. It is then graphically integrated to construct the moment diagram.

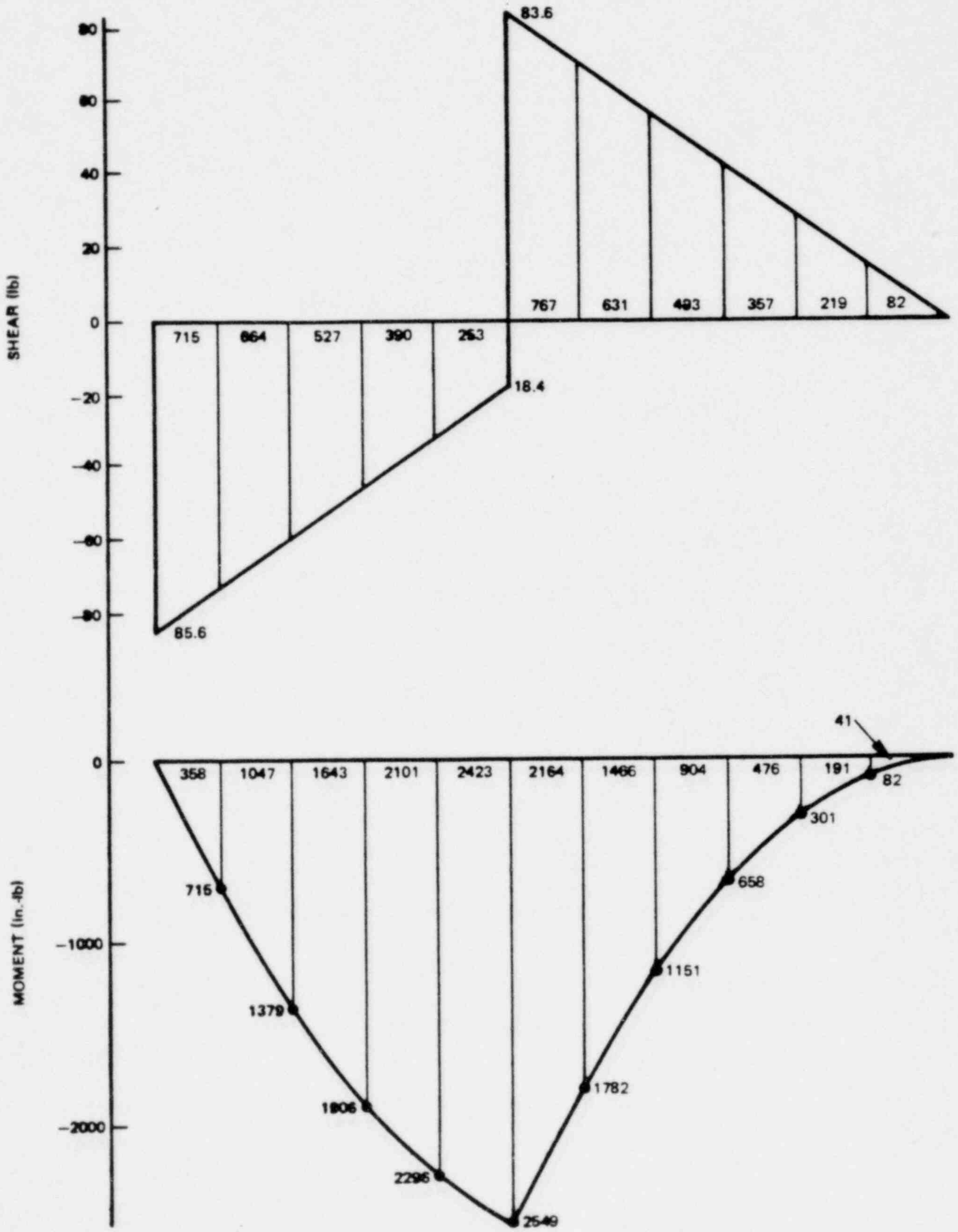

The slope (dy/dx) diagram is now constructed by graphical integration of the moment diagram.

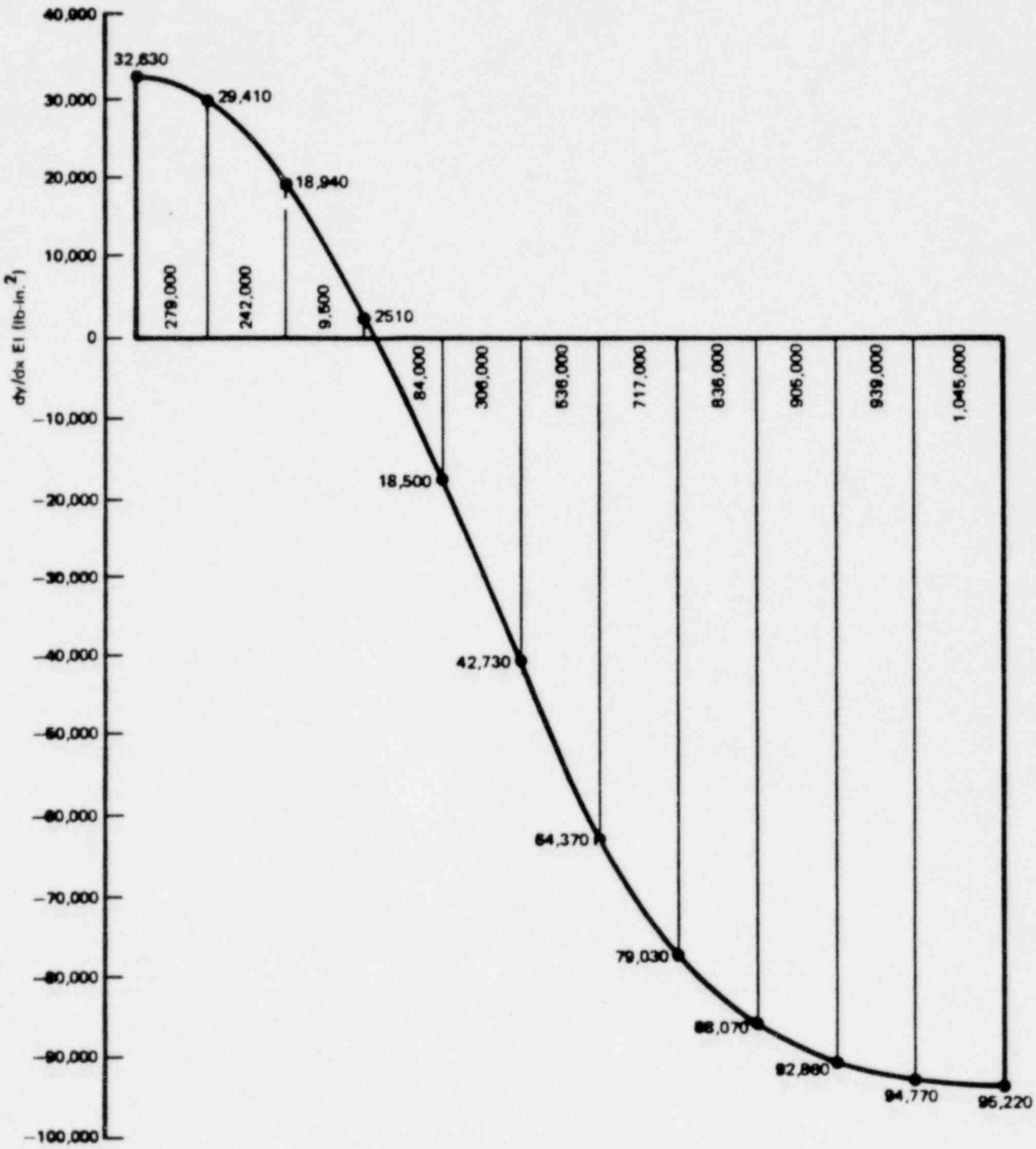

Graphical integration of the slope diagram yields deflections. The deflections must be adjusted so that the deflection at both brackets is zero.

	(lb-in.^2)	(in.)		
	yEI (X100)	y (10^{-3})	Length (in.)	Adjusted y (10^{-2})
Left End Bracket	0	0	0	0
	2790	2.26	9	1.91
	5210	4.23	19	3.49
	6260	5.08	30	3.91
	5420	4.40	39	2.88
Bracket	2360	1.91 (Must be zero)	49	0
	-3000	-2.43	59	-4.73
	-10170	-8.25	69	-10.94
	-18530	-15.03	79	-18.11
	-27580	-22.37	89	-25.84
	-36970	-29.98	99	-33.84
Right End	-47420	-38.46	110	-42.75

$EI = 123.3\ (10^6)\ \text{lb-in.}^2$

$\text{Adjustment} = \frac{1.91}{49}\ 0.001\ \text{in/in. length}$

The deflection diagram is now constructed.

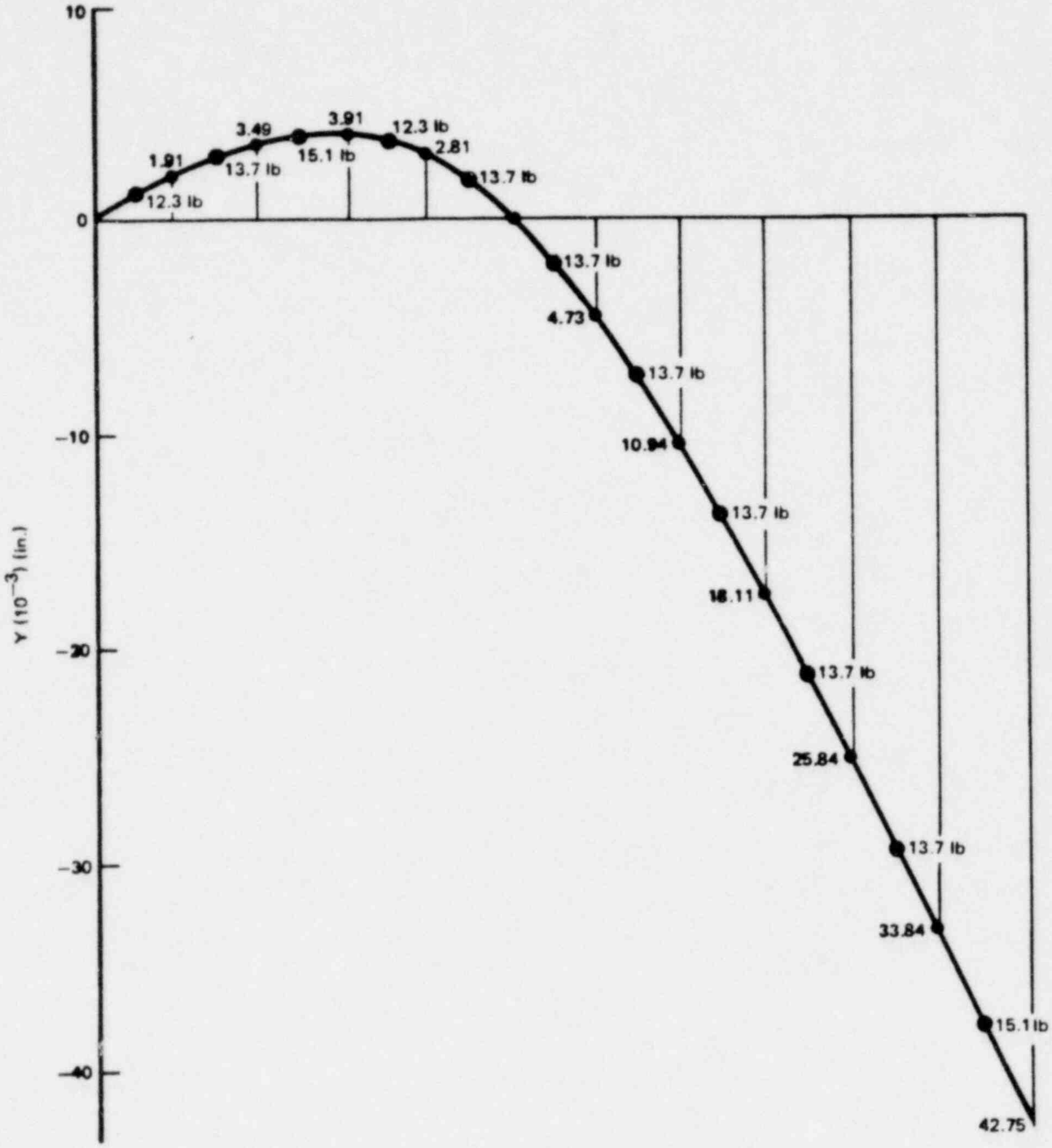

The weight of the member is now distributed as shown above. The natural frequency can now be determined.

$$\Sigma Wy^2 = [12.3\ (0.95)^2 + 13.7\ (2.7)^2 + 15.1\ (3.8)^2 + 12.3\ (3.5)^2 + 13.7\ (1.8)^2 + 13.7\ (2.1)^2 + 13.7\ (7.5)^2 + 13.7\ (14.0)^2 + 13.7\ (21.7)^2 + 13.7\ (29.9)^2 + 15.1\ (38.0)^2\ ]\ (10^{-6})$$

$$= 0.04454 \text{ lb-in.}^2$$

$$\Sigma Wy = [12.3\ (0.95) + 13.7\ (2.7) + 15.1\ (3.8) + 12.3\ (3.5) + 13.7\ (1.8) + 13.7\ (2.1) + 13.7\ (7.5) + 13.7\ (14.0) + 13.7\ (21.7) + 13.7\ (29.9) + 15.1\ (38.0)]\ (10^{-3})$$

$$= 1.778 \text{ lb-in.}$$

$$w_n^2 = (386)\left(\frac{1.725}{0.04252}\right) = 15425$$

$$w_n = 124.2 \text{ rad/sec}$$

$$f_n = \frac{w_n}{2\pi} = \frac{124.2}{2\pi} = 19.8 \text{ Hz}$$

$$\text{Ratio} = \frac{f_n}{f_v} = \frac{19.8}{3.15} = 6.3 > 3$$

A.2.3 Conclusions

1. The natural frequency of the intact sparger, even when a bracket is assumed missing, is greater than three (3) times the vortex shedding frequency. Therefore, fatigue resulting from flow-induced vibrations cannot be hypothesized as a cause of cracking. Also, the loads used to calculate stresses for the intact sparger condition (see Section A.3) do not require amplification.

2. The natural frequency of a broken sparger (assumed 360° throughwall crack near the tee-box) is greater than three (3) times the vortex shedding frequency. Therefore, flow-induced vibration under this assumed condition will not be a problem and the loads used to calculate stresses for the assumed broken sparger condition (see Section A.4) do not require amplification.

A.3 STRESSES FOR UNBROKEN SPARGER

This section contains the calculation of stresses in the intact sparger condition during normal plant operation and during the core spray injection event. During normal plant operation, there is no core spray flow. The sparger $\Delta P = 0$ and $\Delta T = 0$. Impingement loads and weight loads are low and are bounded by the postulated seismic event.

Design loads during core spray injection are the design loads for the sparger. Thermal mismatch between the cold sparger (due to injection) and the hot shroud produce significant loads on the sparger pipe arms and on the brackets. Pressure and thrust loads produce stresses in the pipe arm and nozzles.

A.3.1 Pipe Stresses

A.3.1.1 Seismic and Impingement

For simplicity assume continuous beam - three equal spans.

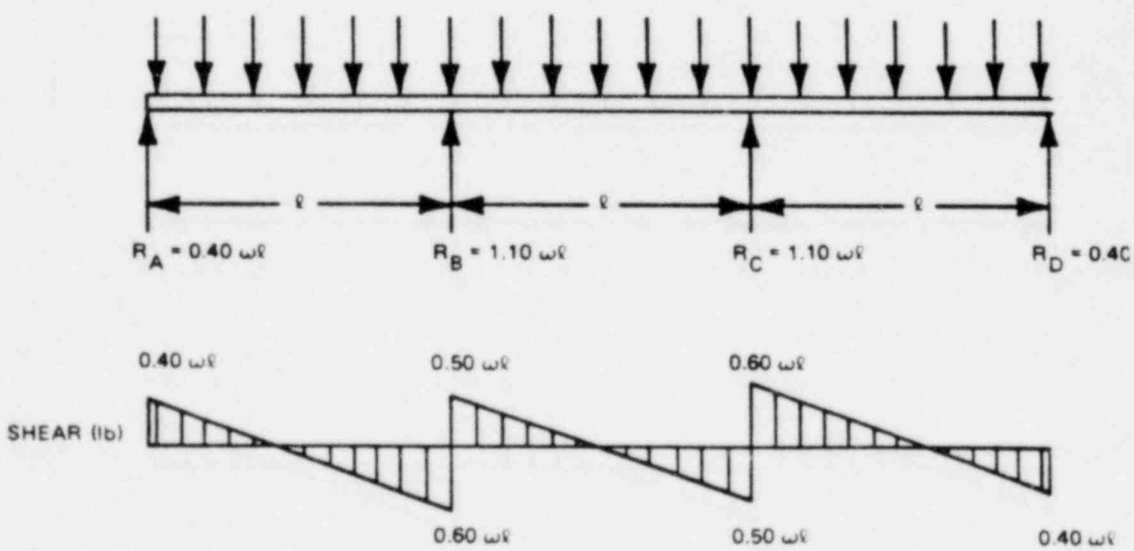

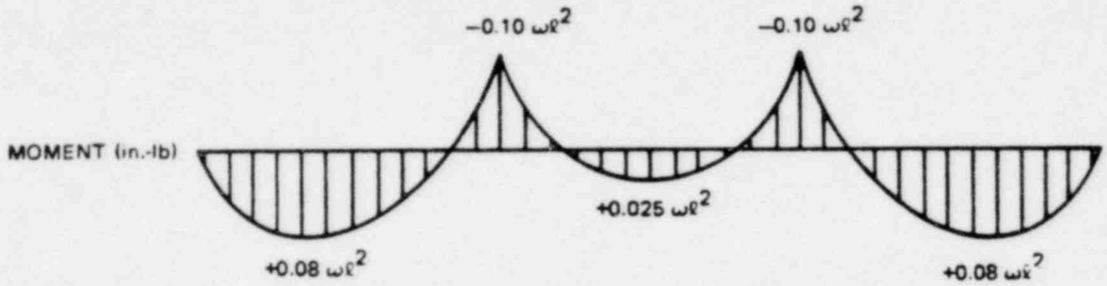

$\ell = \frac{40.5}{180} \times \pi \times 91.25 = 64.5$ in. (Assume maximum span length for conservatism)

$M_{max} = 0.1\ (2.74)\ (64.5)^2 = \underline{1140}$ in.-lb

$\sigma = \frac{Mc}{I}$ $\quad I = 4.79 \quad c = \frac{4.0}{2} = 2.0$ in.

$\sigma_{max} = \frac{1140\ (2.0)}{4.79} = \underline{476}$ lb/in.^{2} (Seismic)

$\sigma_{max} = 476 \left(\frac{1.0}{2.74}\right) = \underline{173.7}$ lb/in.^{2} (Impingement)

A.3.1.2 Differential Pressure

$\Delta P_{max} = 50.0$ psi

$R_o = 2.0$ in.

$R_i = 3.548/2 = 1.774$

$t_{nom.} = 0.226$

$t_{min} = 0.226 - 2$ [(0.003) corrosion allowance] = 0.220 in.

- Hoop Stress

$\sigma = \frac{P\ R_i}{t} = \frac{50.0\ (1.774)}{0.220} = \underline{404}$ lb/in.^{2}

• Axial Stress

$$\sigma = \frac{P\ R_i}{2t} = \frac{404}{2} = \underline{202}\ \text{lb/in.}^2$$

A.3.1.3 Mismatch Due to Thermal Expansion

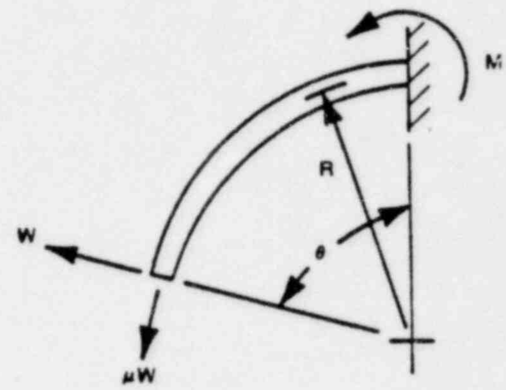

$$m = WR \sin\theta - \mu\ WR\ (1 - \cos\theta)$$

$$= WR\ [\sin\theta - \mu\ (1 - \cos\theta)]$$

Assume $\mu = 0.2$ (See Section A.1.6) $R = 94.25$

• 40½° Bracket

$$M_{40\frac{1}{2}°} = 131\ (91.25)\ [\sin 40.5° - 0.2\ (1 - \cos 40.5°)]$$

$$= \underline{7191}\ \text{in.-lb}$$

• 71° Bracket

$$M_{71°} = 89\ (91.25)\ [\sin 71° - 0.2\ (1 - \cos 71°)]$$

$$= \underline{6583}\ \text{in.-lb}$$

• 97½° Bracket

$$M_{97\frac{1}{2}°} = 79\ (91.25)\ [\sin 97\tfrac{1}{2}° - 0.2\ (1 - \cos 97\tfrac{1}{2}°)]$$

$$= \underline{5517}\ \text{in.-lb}$$

• -20½° Bracket

$$M_{-20\frac{1}{2}°} = 241\ (91.25)\ [\sin 20\tfrac{1}{2}° - 0.2\ (1 \cos 20\tfrac{1}{2}°)]$$

$$= \underline{\underline{7423}}\ \text{in.-lb (maximum)}$$

- $-51°$ Bracket

$$M_{-51°} = 110\ (91.25)\ [\sin 51° - 0.2\ (1 - \cos 51°)]$$

$$= \underline{7056}\ \text{in.-lb}$$

- $-77\tfrac{1}{2}°$ Bracket

$$M_{-77\frac{1}{2}°} = 85\ (91.25)\ [\sin 77\tfrac{1}{2}° - 0.2\ (1 - \cos 77\tfrac{1}{2}°)]$$

$$= \underline{6357}\ \text{in.-lb}$$

Sum of Stresses Attributable to Core Spray Injection:

$$\sigma_{max} = \sigma_{bending} + \sigma_{bracket\ friction} + \sigma_{\Delta P}$$

$$= \frac{Mc}{I} + \frac{\mu W}{A_p} + \frac{Pr}{2t}$$

$$c = \frac{4.0}{2} = 2\ \text{in.},\quad I = 4.79\ \text{in.}^4,\quad \mu W = 0.2\ (241)$$

$$A_p = 2.68\ \text{in.}^2,\quad \frac{Pr}{2t} = 202\ \text{lb/in.}^2\ \text{(Section A.3.1.2)}$$

$$\sigma_{max} = \frac{7423\ (2.0)}{4.79} + \frac{0.2\ (241)}{2.68} + 202$$

$$= 3099 + 18 + 202$$

$$= \underline{\underline{3319}}\ \text{lb/in.}^2$$

A.3.2 Nozzle Stress

A.3.2.1 Nozzle Thrust

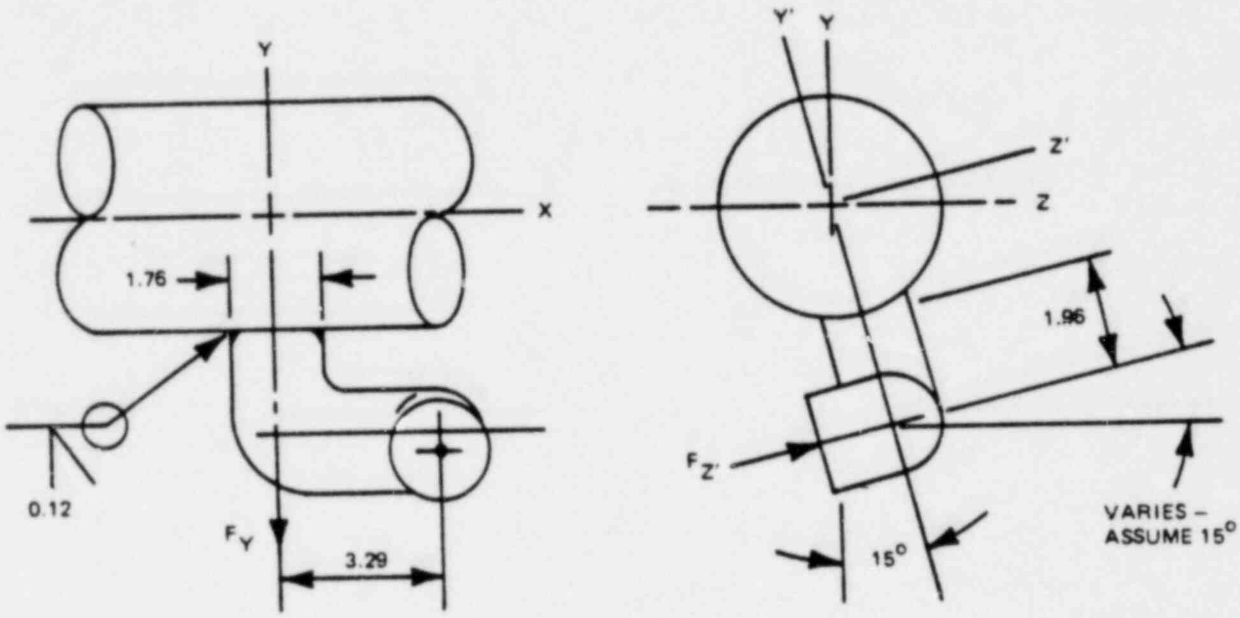

Weld Properties:

$$I = \frac{\pi}{64}\ (1.76^4 - 1.52^4) = 0.209\ \text{in.}^4$$

$$K = \frac{\pi}{32}\ (1.76^4 - 1.52^4) = 0.418\ \text{in.}^4$$

$$A = \frac{\pi}{4}\ (1.76^2 - 1.52^4) = 0.618\ \text{in.}^2$$

$$C = \frac{1.76}{2} = 0.88\ \text{in.}$$

$$t = 0.12\ \text{in.}$$

$$r = \frac{1.76}{2} = 0.88\ \text{in.}$$

$F_y = 64$ lb $\qquad F_{z'} = 9.9$ lb (Section A.1.5)

$P = 50$ psi (Section A.1.4)

The resulting loads at the weld are:

$$F_{axial} = F_y = 64 \text{ lb}$$

$$F_{shear} = F_{z'} = 9.9 \text{ lb}$$

$$T_{torsion} = 3.29 \; F_{z'} = 3.29 \; (9.9) = 32.6 \text{ in.-lb}$$

$$M_{moment} = 1.96 \; F_{z'} = 1.96 \; (9.9) = 19.4 \text{ in.-lb}$$

The stresses are conservatively calculated as:

$$\sigma_y = \pm \frac{M_m c}{I} + \frac{F_a}{A} + \frac{Pr}{2t}$$

$$= \pm \frac{19.4 \; (0.88)}{0.209} + \frac{64}{0.618} + \frac{50 \; (0.88)}{2 \; (0.12)}$$

$$= \pm 81.7 + 103.6 + 183$$

$$\sigma_y = \underline{369} \text{ lb/in.}^2, \quad 205 \text{ lb/in.}^2$$

$$\tau_{xy} = \frac{T_T c}{K} + \alpha \frac{F_s}{A} \qquad \alpha = 2 \text{ (thin wall cylinder)}$$

$$= \frac{(32.57)(0.88)}{0.418} + 2 \; \frac{9.9}{0.618}$$

$$= 60 + 32$$

$$\tau_{xy} = \underline{101} \text{ lb/in.}^2$$

A.3.3 Bracket Stresses

A.3.3.1 Lower Bracket Stresses Due to Thermal Expansion

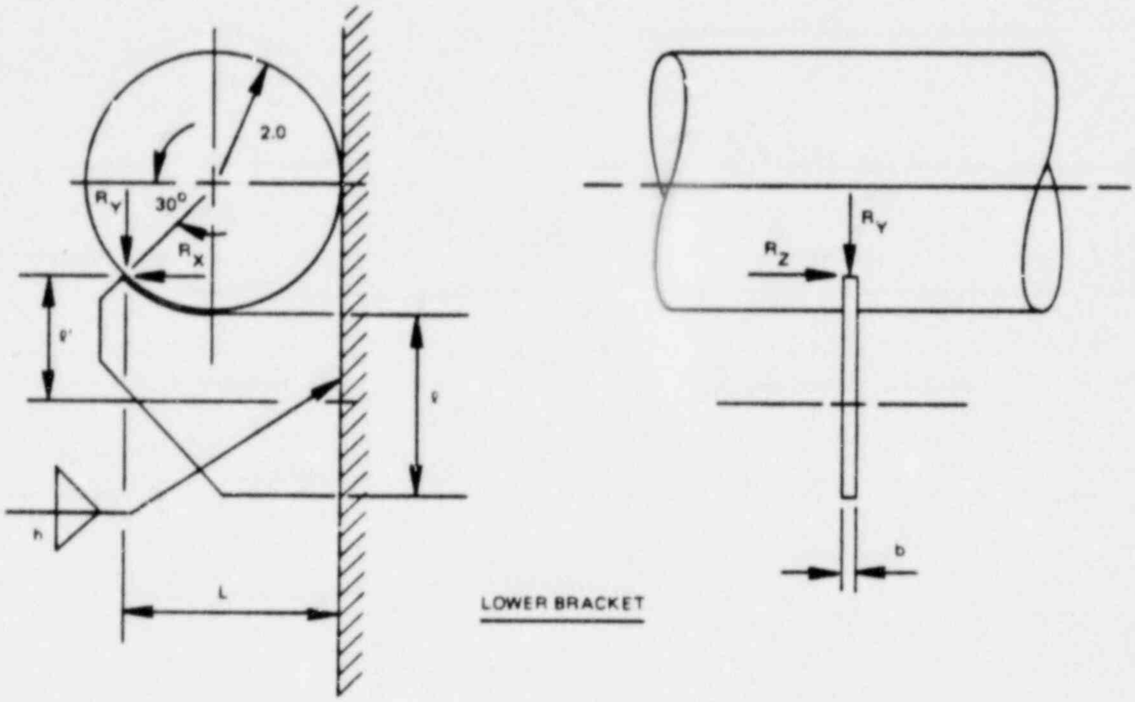

$\ell = 4.0 - 2.0 = 2.0$ in.

$L = 2.0\ (1 + \cos 30°) = 3.73$ in.

$\ell' = \frac{2.0}{2} + (1 - \sin 30°)\ (2.0) = 2.0$ in.

$b = 0.5$ in.

$h = 0.25$ in.

$R_x = 241$ lb

$R_z = \mu\ R_x = 0.2\ (241) = 48.2$ lb

$R_y = 0$

(Section A.1.6)

Maximum shear stress in the fillet weld is

$$\tau = \frac{\sqrt{2}}{2} \quad \frac{R_x + R_z}{h\ell} + \frac{\sqrt{2}}{2} \quad \frac{M}{(b + h)\ (\ell \cdot h)\ h}$$

where

$$M = \ell' \ R_z$$

$$\tau = \frac{\sqrt{2}}{2} \quad \frac{(241 + 48.2)}{0.25 \quad (2.0)} + \frac{\sqrt{2}}{2} \quad \frac{(2.0)\ 48.2}{(0.5 + 0.25)\ (2.0 - 0.25)\ (0.25)}$$

$$\tau = 409 + 208 = \underline{\underline{617}} \text{ lb/in.}^2$$

Maximum normal stress in weld is:

$$\sigma_{max} = \frac{\sqrt{2}}{2} \quad \frac{R_x}{h\ell} = \frac{R_z}{h\ell\ (b+h)} \quad \sqrt{2L^2 + \frac{(b+h)^2}{2}} \quad + \frac{3\ \sqrt{2}\ M}{h\ell^2}$$

where

$$M = \ell' \ R_x$$

$$\sigma_{max} = \frac{\sqrt{2}}{2} \quad \frac{(241)}{0.25\ (2.0)} + \frac{3\ \sqrt{2}\ (2.0)\ (241)}{0.25\ (2.0)^2}$$

$$- \frac{48.2}{0.25\ (2.0)\ (0.5 + 0.25)} \quad \sqrt{2\ (3.73)^2 + \frac{(0.5 + 0.25)^2}{2}}$$

$$\sigma_{max} = 341 + 2045 + 681.4 = \underline{\underline{3067}} \text{ lb/in.}^2$$

Maximum normal stress in plate is ...

$$\sigma_{max} = \frac{R_x}{A} + \frac{\ell' R_x C_{xy}}{I_{xy}} + \frac{L R_z C_{zx}}{I_{zx}}$$

$$A = 0.5\ (2.0) = 1.0 \text{ in.}^2$$

$$I_{xy} = \frac{b\ell^3}{12} = \frac{0.5\ (2.0)^3}{12} = 0.333 \text{ in.}^4$$

$$C_{xy} = \frac{2.0}{2} = 1.0 \text{ in.}$$

$$I_{zx} = \frac{\ell b^3}{12} = \frac{2.0\ (0.5)^3}{12} = 0.02083 \text{ in.}^4$$

$$C_{zx} = \frac{0.5}{2} = 0.25 \text{ in.}$$

$$\sigma_{max} = \frac{241}{1.0} + \frac{(2.0)\ (241)\ (1.0)}{0.3333} + \frac{3.73\ (48.2)\ (0.25)}{0.02083}$$

$$= 241 + 1446 + 2158$$

$$\sigma_{max} = \underline{\underline{3845}} \text{ lb/in.}^2$$

Maximum shear stress in plate

$$\tau = \frac{R_x + R_z}{b\ell} + \frac{\ell' R_z\ (3\ell + 1.8b)}{\ell^2\ b^2}$$

$$= \frac{241.0 + 48.2}{0.5\ (2.0)} + \frac{(2.0)\ (48.2)\ (3 \times 2.0 + 1.8 \times 0.5)}{(2.0)^2\ \ (0.5)^2}$$

$$\tau = 289.2 + 665 + \underline{\underline{954}} \text{ lb/in.}^2$$

A.3.3.2 Middle Bracket Stresses Due to Thermal Expansion

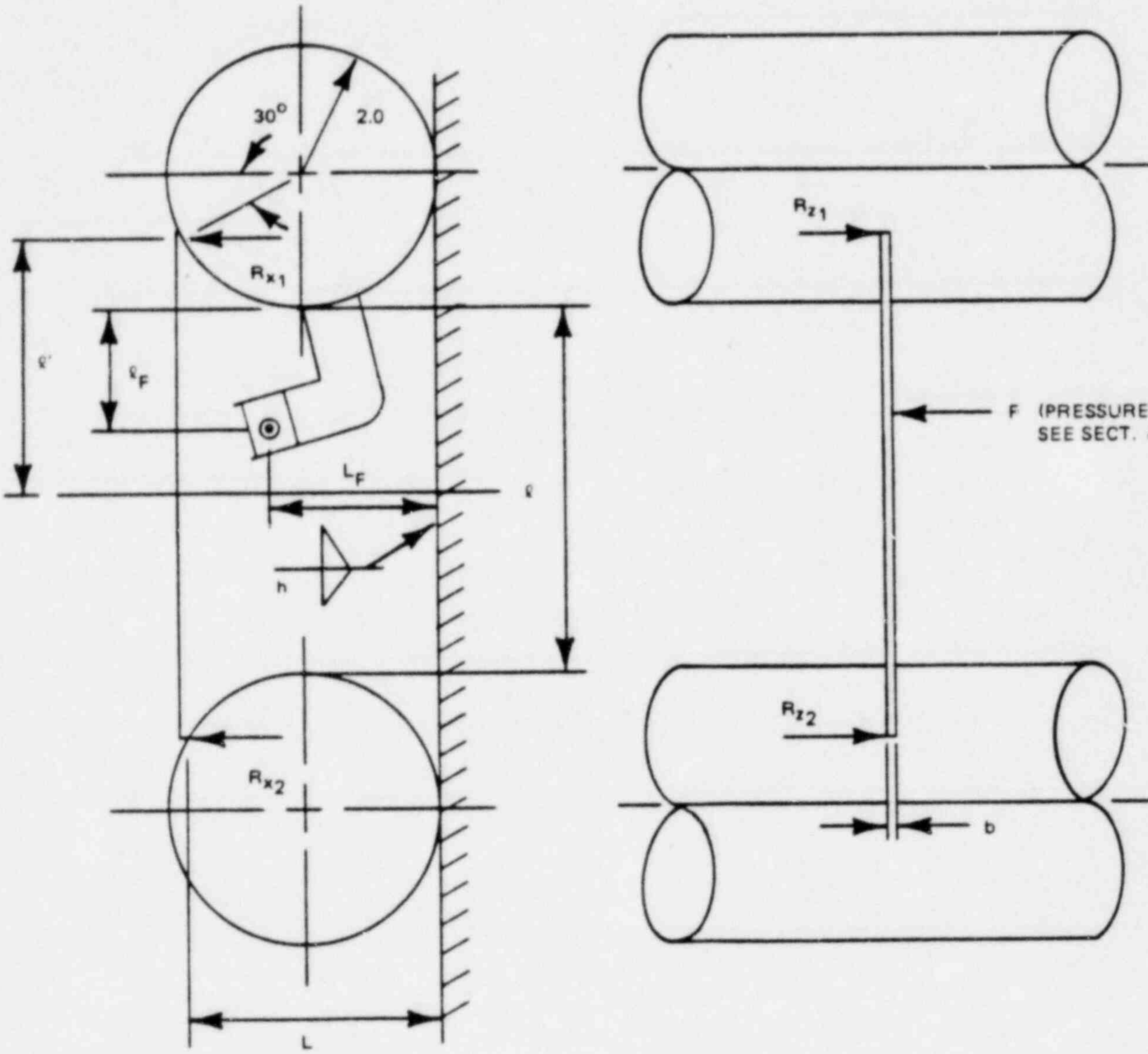

$\ell = 10.25 - 2\ (2.0) = 6.25$ in. $\quad b = 0.5$ in.

$\ell' = \frac{6.25}{2} + (1 - \sin 30°)\ (2.0) = 4.13$ in. $\quad h = 0.25$ in.

$L = (1 + \cos 30°)\ (2.0) = 3.73$ in.

$\ell_F = (2.0 + 1.96) \cos 15° + (1.50 + 1.18) \sin 15° - 2.0$

$$\ell_F = 2.52$$

$$L_F = 2.0 - (2.0 + 1.96) \sin 15° + (1.50 + 1.18/2) \cos 15°$$

$$L_F = 2.99 \text{ in.}$$

(NOTE: ℓ_F, L_F used in Section A.4.3.3)

Assume

$$R_{x1} = R_{x_2} = 241 \text{ lb} \qquad \text{(Section A.1.5)}$$

$$R_{z1} = R_{z_2} = 0.2\ (241) = 48.2$$

Shear Stress

$$\tau_{AVG} = \frac{\sqrt{2}}{2} \left(\frac{R_{z_1} + R_{z_2}}{h\ell} \right) = \frac{\sqrt{2}}{2} \frac{96.4}{(0.25)\ (6.25)}$$

$$\tau_{AVG} = \underline{\underline{44 \text{ lb/in.}^2}} \text{ (weld)}$$

$$\ell_{AVG} = \frac{(R_{z_1} + R_{z_2})}{b\ell} = \frac{96.4}{0.5\ (6.25)}$$

$$\ell_{AVG} = \underline{\underline{31 \text{ lb/in.}^2}} \text{ (Bracket)}$$

Normal Stress

$$\sigma = \frac{\sqrt{2}}{2} \frac{R_{x_1} + R_{x_2}}{h\ell} \pm \frac{R_{z_1} + R_{z_2}}{h\ell\ (b+h)} \sqrt{2L^2 + \frac{(b+h)^2}{2}}$$

$$\sigma = \frac{\sqrt{2}}{2}\,\frac{241\ (2)}{0.25\ (6.25)} \pm \frac{2\ (48.2)}{0.25\ (6.25)\ (0.5 + 0.25)} \times$$

$$\sqrt{2\ (3.73)^2 + \frac{(0.5 + 0.25)^2}{2}}$$

$$= 218.1 \pm 436$$

$$\sigma = \underline{\underline{654}}\ \text{lb/in.}^2,\quad -218\ \text{lb/in.}^2\quad \text{(WELD)}$$

$$\sigma = \frac{R_{x_1} + R_{x_2}}{b\ell} \pm \frac{(L - h)\ (R_{z_1} + R_{z_2})\ C}{I}$$

$$c = 0.25\ \text{in.}\quad I = 0.0651\ \text{in.}^4$$

$$\sigma = \frac{2\ (241)}{0.5\ (6.25)} \pm \frac{(3.73 - 0.25)\ (96.4)\ (0.25)}{0.0651}$$

$$= 154 \pm 1288$$

$$\sigma = \underline{\underline{1442}}\ \text{lb/in.}^2,\quad -1134\ \text{lb/in.}^2\quad \text{(BRACKET)}$$

A.4 STRESSES FOR BROKEN SPARGER

This section contains the calculation of stresses during normal plant operation and during the core spray injection event. The analysis conservatively assumes a 360° throughwall crack in the longer pipe arm at the T-box and ignores the effect of a clamp (or assumes no clamp is installed). The analysis includes all the loading conditions identified in Section A.3. In addition, the stresses in the middle bracket due to the pressure load are calculated. (A nozzle will contact the middle bracket in order to axially restrain the broken sparger arm when it is pressurized). Stresses in both the middle bracket and the lower bracket (assumes lower sparger cracks) are calculated in order to bound the condition.

A.4.1 Pipe Stress Due to Seismic Load

Assume uniformly loaded beam with three supports, end moment M_3 and force P_3 and the 3rd support.

using theorem of three moments...

$$\frac{M_1 \ell_1}{I_1} + 2\,M_2 \left(\frac{\ell_1}{I_1} + \frac{\ell_2}{I_2}\right) + \frac{M_3 \ell_2}{I_2} = \frac{\omega_1\ \ell_1^{\ 3}}{4I_1} + \frac{\omega_2\ \ell_2^{\ 3}}{4I_2}$$

$$M_1 = 0 \quad I_1 = I_2 \quad \omega_1 = \omega_2$$

$$2M_2\left(\frac{\ell_1 + \ell_2}{I}\right) + \frac{M_3\ \ell_2}{I} = \frac{\omega\ (\ell_1^{\ 3} + \ell_2^{\ 3})}{4I}$$

$$M_2 = \frac{\frac{\omega}{4}\ (\ell_1^{\ 3} + \ell_2^{\ 3}) - M_3\ \ell_2}{2\ (\ell_1 + \ell_2)} - - -$$

M_3 is caused by the contilevered section of pipe between the support bracket and the break

$$M_3 = \frac{\omega \ell_3^{\ 2}}{2}$$

Likewise,

P_3 is caused by the cantilevered section

$$P_3 = \omega \ell_3$$

For Seismic

ω = 2.74 lb/in. $\quad \ell_1 = 26\frac{1}{2} \times \left[\frac{\pi}{180} \times 91.25\right] = 26.5 \times 1.5926 = 42.2$

ℓ_2 0½ x 1.59 = 48.6 in.

$$\ell_3 = 40\tfrac{1}{2} \times 1.59 = 64.5 \text{ in.}$$

$$P_3 = 2.74\ (64.5) = \underline{\underline{177 \text{ lb}}}$$

$$M_3 = \frac{2.74(64.5)^2}{2} = \underline{\underline{5700}} \text{ in-lb}$$

$$M_2 = \frac{\frac{2.74}{4}\ (42.2^3 - 48.6^3) - 5700\ (48.6)}{2\ (42.2 + 48.6)}$$

$$= \underline{-809} \text{ in-lb}$$

$$\sigma = \frac{Mc}{I} \qquad I = 4.79 \text{ in.}^4 \qquad c = \frac{4.0}{2} = 2.0 \text{ in.}$$

$$\sigma_{max} = \frac{5700\ (2.0)}{4.79} = \underline{2380} \text{ lb/in.}^2$$

$$\tau_{max} = 2\ \frac{F}{A} = 2\ \frac{201}{2.68} = \underline{150} \text{ lb/in.}^2$$

For impingement

$$\omega_i = |-1.0| = 1.0 \text{ lb/in.}$$

$$P_3 = 177\ (1.0/2.74) = \underline{65} \text{ lb.}$$

$$M_3 = 5700\ (1.0/2.74) = \underline{2080} \text{ in-lb.}$$

$$M_2 = -809\ (1.0/2.74) = \underline{-295} \text{ in.-lb.}$$

$$\sigma_{max} = 2080\ (2.0/4.79) = \underline{868} \text{ lb/in.}^2$$

- Determine reaction loads for seismic only

$\Sigma M_2 = 0$ For segment 2:

$$R_3 = P_3 + \frac{\omega_s \ \ell_2}{2} + \frac{M_s}{\ell_2} - \frac{M_2}{\ell_2}$$

$$= 177 + \frac{2.74\ (48.6)}{2} + \frac{5700}{48.6} - \frac{(-809)}{48.6}$$

$$= \underline{377.5}\ \text{lb}$$

$\Sigma M_2 = 0$ For Segment 1:

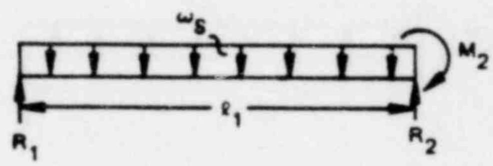

$$R_1 = \frac{\omega_s \ \ell_1}{2} - \frac{M_2}{\ell_1}$$

$$= \frac{2.74\ (42.2)}{2} - \frac{(-809)}{42.2}$$

$$= \underline{77.0}\ \text{lb}$$

$\Sigma M_1 = 0$ For Segment 1, $\Sigma M_3 = 0$ For Segment 2:

$$R_2 = \frac{\omega_s \ \ell_1}{2} + \frac{M_2}{\ell_1} + \frac{\omega_s \ \ell_2}{2} + \frac{M_2}{\ell_2} - \frac{M_3}{\ell_2}$$

$$= \frac{(2.74)\ (42.2)}{2} + \frac{(-809)}{42.2} + \frac{(2.74)\ (48.6)}{2} + \frac{(-809)}{48.6} - \frac{5700}{48.6}$$

$$= \underline{-28.7}\ \text{lb}$$

$$\left.\begin{aligned} R_1 + R_2 + R_3 &= \underline{426} \\ (2.74)\ (\ell_1 + \ell_2 + \ell_3) &= \underline{\underline{426}} \end{aligned}\right\} \text{CHECK}$$

A.4.1.1 Mismatch Due to Thermal Expansion

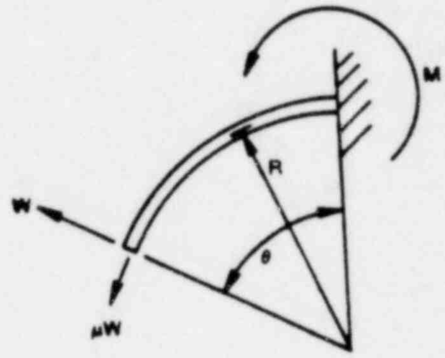

$$M = WR \sin\theta - \mu WR\,(1 - \cos\theta)$$

$$= WR\,(\sin\theta - \mu\,(1 - \cos\theta))$$

Assume

$\mu = 0.2 \quad R = 91.25$

(See Section A.1.7)

μ = coef, of friction

$$M_{-30.5°} = 168\,(91.25)\,(\sin 30.5° - 0.2\,(1 - \cos 30.5°))$$

$$= \underline{7356} \text{ in.-lb.}$$

$$M_{26.5°} = 190\,(91.25)\,(\sin 26.5° - 0.2\,(1 - \cos 26.5°))$$

$$= \underline{7372} \text{ in.-lb (maximum)}$$

$$\sigma_{max} = \sigma_{BENDING} + \sigma_{BRACKET\ FRICTION} + \frac{Pr}{2t}$$

$$= \frac{Mc}{I} + \frac{\mu W}{Ap} + \frac{Pr}{2t}$$

$$c = 4.0/2 = 2.0 \text{ in.}, \quad I = 4.79 \text{ in.}^2$$

$$\mu W = 0.2\,(190), \qquad Ap = 2.68 \text{ in.}^2$$

$$\frac{Pr}{2t} = 202 \text{ lb/in.}^2 \quad \text{(Section A.3.1.2 - BOUNDING VALUE)}$$

$$\sigma max = \frac{7372\,(2.0)}{4.79} + \frac{0.2\,(190)}{2.68} + 202$$

$$= \underline{\underline{3316}} \text{ lb/in.}^2$$

A.4.2 Nozzle Stresses Due to Pressure Load

Assume 360° break, nozzle loaded by bracket.

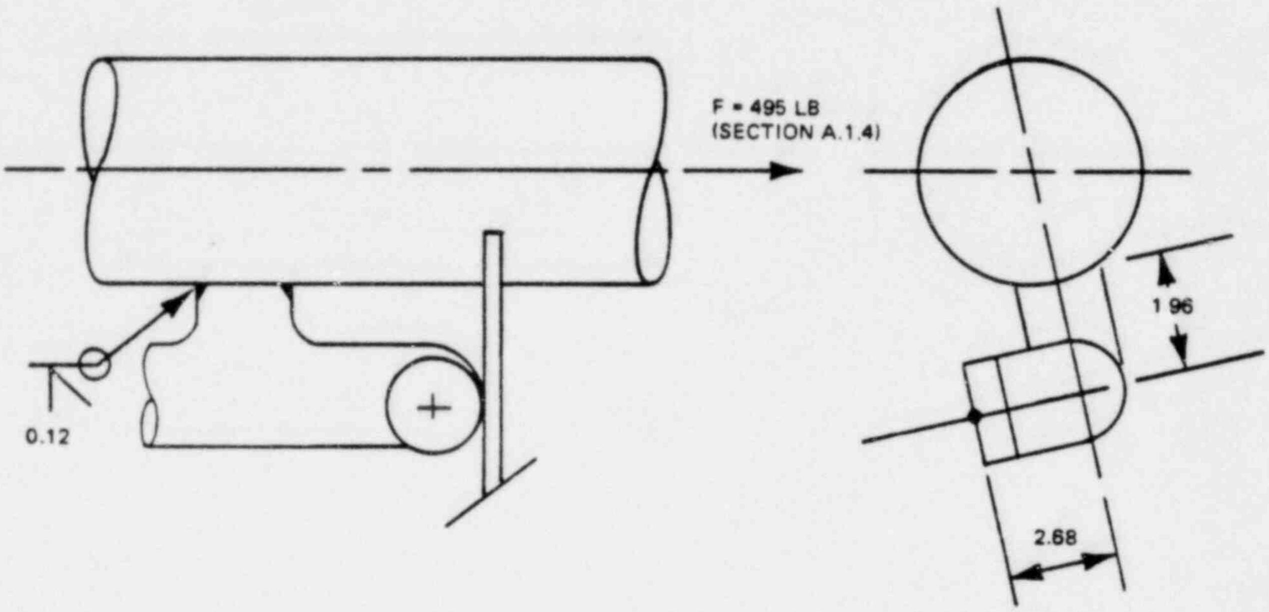

The resulting loads at the weld are.

$$F_{SHEAR} = F = 495 \text{ lb}$$

$$T_{TORSION} = 2.68\ F = 2.68\ (495) = 1327 \text{ in.-lb.}$$

$$M_{MOMENT} = 1.96\ F = 1.96\ (495) = 970 \text{ in.-lb}$$

The stresses are conservatively calculated as...

$$\sigma_y = \pm \frac{M_m c}{I} + \frac{Pr}{2t}$$

$$= \pm \frac{970\ (0.88)}{0.209} + \frac{50\ (0.88)}{2\ (0.12)}$$

P = 50 psig (see Section A.1.4)
For Weld Properties, see Section A.3.2.1

$$= \pm 4084 + 183$$

$$\sigma_y = -3901 \text{ lb/in.}^2 , \underline{\underline{4267}} \text{ lb/in.}^2$$

$$\tau_{xy} = \frac{T_T c}{k} + \alpha \frac{F_s}{A} \qquad \alpha = 2.0$$

$$= \frac{1327 (0.88)}{0.418} + 2 \frac{495}{0.618}$$

$$= 2794 + 1602$$

$$\tau_{xy} = \underline{\underline{4396}} \text{ lb/in.}^2$$

A.4.3 Bracket Stresses

A.4.3.1 Lower Bracket Stress Due to Seismic Loading

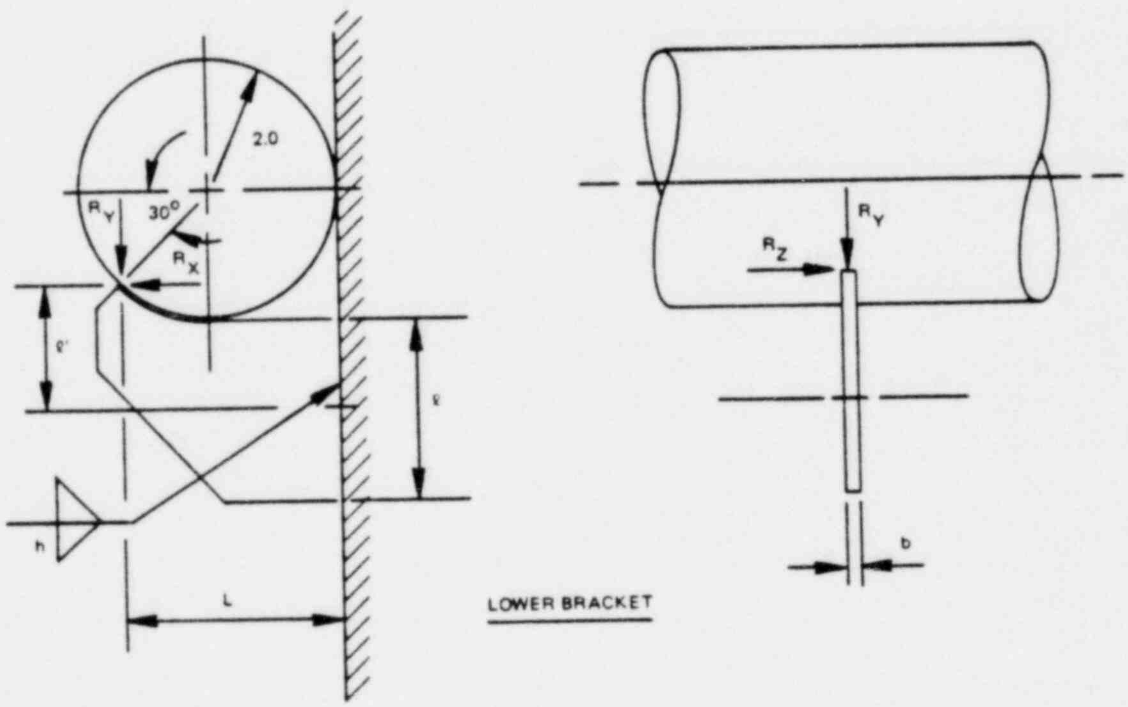

$\ell = 4.0 - 2.0 = 2.0$ in. $\quad L = 2.0 (1 + \cos 30°) = 3.73$ in.

$\ell' = \frac{2.0}{2} + (1 - \sin 30°)(2.0) = 2.0$ in.

$b = 0.5$ in. $\quad h = 0.25$ in.

$$R_y = 377.5 \text{ lb} \qquad R_x = 0 \qquad R_z = 0$$

(Section A.1.3)

(conservatism - uses highest bracket load at weakest bracket)

The stress in the fillet weld is ...

$$\tau_{AVG} = \frac{\sqrt{2}}{2}\frac{R_y}{h\ell} = \frac{\sqrt{2}}{2}\frac{(377.5)}{0.25\ (2.0)} = \underline{\underline{534}} \text{ lb/in.}^2$$

$$\sigma_{BENDING} = \frac{3\sqrt{2}\ M}{h\ \ell^2} = \frac{3\sqrt{2}\ \ L\ R_y}{h\ \ell^2}$$

$$= \frac{3\sqrt{2}\ (3.73)\ (377.5)}{(0.25)\ (2)^2} = \underline{\underline{5974}} \text{ lb/in.}^2$$

A.4.3.2 Lower Bracket Stress Due to Thermal Expansion

$$R_x = 190 \text{ lb} \qquad R_z = \mu R_x = 0.2\ (190) = 38 \text{ lb}$$

(Section A.1.7) $\quad R_y = 0$

Maximum shear stress in the fillet weld is...

$$\tau = \frac{\sqrt{2}}{2}\ \frac{R_x + R_z}{h} + \frac{\sqrt{2}}{2}\ \frac{M}{(b+h)\ (\ell-h)\ (h)}$$

where

$$M = \ell'\ R_z$$

$$\tau = \frac{\sqrt{2}}{2}\frac{190 + 38}{0.25\ (2.0)} + \frac{\sqrt{2}}{2}\frac{(2.0)\ 38}{(0.5 + 0.25)\ (2.0 - 0.25)\ (0.25)}$$

$$\tau = 322.4 + 163.8 = \underline{\underline{486}} \text{ lb/in.}^2$$

Maximum normal stress in weld is ...

$$\sigma_{max} = \frac{\sqrt{2}}{2}\frac{R_x}{h\ell} + \frac{R_z}{h\ell\ (b+h)} \sqrt{2L^2 + \frac{(b+h)^2}{2}} + \frac{3\ \sqrt{2}\ m}{h\ \ell^2}$$

where

$$M = \ell'\ R_x$$

$$\sigma_{max} = \frac{\sqrt{2}}{2}\frac{(190)}{0.25\ (2.0)} + \frac{3\ \sqrt{2}\ (2.0)\ (190)}{0.25\ (2.0)^2}$$

$$+ \frac{52.8}{0.25\ (2.0)\ (0.5 + 0.25)} \sqrt{2\ (3.73)^2 + \frac{(0.5 + 0.25)^2}{2}}$$

$$\sigma_{max} = 268.7 + 1612.2 + 746.5 = \underline{\underline{3360}} \text{ lb/in.}^2$$

Maximum normal stress in plate is...

$$\sigma_{max} = \frac{R_x}{A} + \frac{\ell'\ R_x\ C_{xy}}{I_{xy}} + \frac{L\ R_z\ C_{zx}}{I_{zx}}$$

$$A = 0.5\ (2.0) = 1.0 \text{ in.}^2$$

$$I_{xy} = \frac{b\ell^3}{12} = \frac{0.5\ (2.0)^3}{12} = 0.333 \text{ in.}^4$$

$$C_{xy} = \frac{2.0}{2} = 1.0 \text{ in.}$$

$$I_{zx} = \frac{\ell\ b^3}{12} = \frac{(2.0)\ (0.5)^3}{12} = 0.02083$$

$$C_{zx} = \frac{0.5}{2} = 0.25$$

$$\sigma_{max} = \frac{190}{1.0} + \frac{(2.0)\ (190)\ (1.0)}{0.3333} + \frac{3.73\ (38)\ (0.25)}{0.02083}$$

$$= 190.0 + 1140.0 + 1701.1$$

$$\sigma_{max} = \underline{\underline{3031}}\ \text{lb/in.}^2$$

Maximum Shear Stress in Plate

$$\tau = \frac{R_x + R_z}{b\ell} + \frac{\ell'\ R_z\ (3\ell + 1.8b)}{\ell^2\ b^2}$$

$$= \frac{190 + 38}{0.5\ (2.0)} + \frac{(2.0)\ (38)\ (3\text{x}\ 2.0 + 1.8\ \text{x}\ 0.5)}{(2.0)^2\ (0.5)^2}$$

$$= 228 + 524 = \underline{\underline{752}}\ \text{lb/in.}^2$$

A.4.3.3 Middle Bracket Stress Due to Pressure Load

(Refer to Figure, Section A.3.3.2)

$F = 495$ lb (Section A.1.4)

Shear Stress (Neglect Torsion - Small)

$$\tau_{AVG} = \frac{\sqrt{2}}{2}\frac{F}{h\ell} = \frac{\sqrt{2}}{2}\frac{(495)}{0.25\ (6.25)} = \underline{\underline{224}}\ \text{lb/in.}^2 \quad \text{(WELD)}$$

$$\tau_{AVG} = \frac{F}{b\ell} = \frac{495}{0.5\ (6.25)} = \underline{\underline{158}}\ \underline{\text{lb/in.}^2} \qquad \text{(BRACKET)}$$

Stress Due to Bending

$$\sigma_{max} = \frac{F}{h\ell\ (b+h)} \sqrt{2L_F{}^2\ \frac{(b+h)^2}{2}}$$

$$= \frac{495}{0.25\ (6.25)\ (0.5 + 0.25)} \sqrt{2\ (2.99)^2 + \frac{(0.5 + 0.25)^2}{2}}$$

$$\sigma_{max} = \underline{\underline{1800}}\ \text{lb/in.}^2 \quad \text{(WELD)}$$

$$\sigma_{max} = \frac{Mc}{I} \qquad c = \frac{0.5}{2} = 0.25\ \text{in.}$$

$$I = \frac{\ell\ b^3}{12} = \frac{6.25\ (0.5)^3}{12} = 0.0651\ \text{in.}^4$$

$$M = (L_F - h)\ F$$

$$\sigma_{max} = \frac{(2.99 - 0.25)\ (495)\ (0.25)}{0.0651} = \underline{\underline{5210}}\ \text{lb/in.}^2 \quad \text{(BRACKET)}$$

A.5 CORE SPRAY SPARGER TEMPERATURE CALCULATIONS

This section contains heat transfer calculations that determine the maximum (bounding) temperature differential between the pipe arm and the shroud.

A.5.1 Temperature Difference - Bracket to Pipe

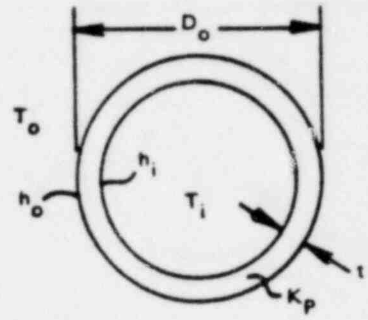

$$\left.\begin{array}{lll} h_i & = & 5145 \text{ Btu/hr-ft}^2\text{-°F} \\ h_o & = & 390 \text{ Btu/hr-ft}^2 \text{ - °F} \\ k & = & 10 \text{ Btu/hr-ft-°F} \end{array}\right\} \text{(Section A.5.2)}$$

D_o = 4.0 in. t = 0.226 in. D_i = 3.548 in.

T_i = water in sparger = 80°F

T_o = water outside = 550°F

$$A_i = \pi\left(\frac{3.548}{12}\right)(1) = 0.9289 \text{ ft}^2 \text{ (1 ft long section)}$$

$$A_o = \pi\left(\frac{4.80}{12}\right)(1) = 1.0472 \text{ ft}^2 \text{ (1 ft long section)}$$

$$A_p = \pi\left(\frac{4.0 + 3.548}{2\ (12)}\right)(1) = 0.9880 \text{ ft}^2 \text{ (1 ft long section)}$$

The thermal resistance, R is

$$\frac{1}{R} = \frac{1}{\frac{1}{A_i h_i} + \frac{1}{A_o h_o} + \frac{t}{A_p k}}$$

$$Q = \frac{T_o - T_i}{\frac{1}{A_i h_i} + \frac{1}{A_o h_o} + \frac{1}{A_p k}}$$

$$\Delta T_{\text{FILM OUTSIDE}} = Q \frac{1}{A_o h_o} = \frac{\frac{1}{A_o h_o} \quad (T_0 - T_1)}{\frac{1}{A_i h_i} + \frac{1}{A_o h_o} + \frac{t}{A_p k}}$$

$$\Delta T_{\text{FILM INSIDE}} = \frac{\frac{1}{A_i h_i} \quad (T_0 - T_1)}{\frac{1}{A_i h_i} + \frac{1}{A_o h_o} + \frac{t}{A_p k}}$$

$$x = \frac{1}{A_i h_i} + \frac{1}{A_o h_o} + \frac{t}{A_p k}$$

$$x = \frac{1}{(0.9289)\ 5145} + \frac{1}{(1.0472)\ 390} + \frac{0.226/12}{0.9880\ (10)}$$

$$x = 0.000209 + 0.002449 + 0.001906 = 0.004564$$

$$\Delta T_{\text{FILM OUTSIDE}} = \frac{0.002449\ (550-80)}{0.004564} = 252°\text{F}$$

Outside metal temp = 550 - 252° = 298°F

$$\Delta T_{\text{FILM INSIDE}} = \frac{0.000209\ (550-80)}{0.004564} = 21.5°\text{F}$$

Inside metal temp = 80 + 21.5 = 101.5°F

Average sparger (pipe) temperature = $\frac{298 + 101.5}{2}$ = 200°F

$$\Delta T_{\text{SHROUD TO PIPE}} = 550 - 200 = \underline{\underline{350°\text{F}}}$$

In practice, the core spray pumping system cannot inject into the reactor until the pressure reaches about 300 psia where T_{SAT} = 417°F. In this case, the $\Delta T_{BRACKET\ TO\ PIPE}$ is less than 337°F (417-80)*. Thus the above calculation bounds the inadvertent injection case. It also bounds the case of core spray operation during LOCA for the same reason.

Conservatisms in the calculation are:

1. Bounding for reason described above
2. Assumes steady state conditions ($Q_o = Q_p = Q_i$)
3. Neglects heat conduction to clamp from pipe.
4. Assumes runout flow.

A.5.2 Heat Transfer Coefficients

A. Inside sparger arm (near tee box)

Assume AVG film temperature = 90°F (Check: (101.5+80)/2 = 91°)

$$D_o = 3.548/12 \text{ ft} \quad + \quad A_{FLOW} = \frac{\pi}{4}(3.548/12)^2 = 0.0687 \text{ ft}^2$$

$$\rho = 62.1 \text{ lb/ft}^3 \qquad Q_{RO} = 6000 \text{ gpm (Section A.5.3)}$$

$$\nu = 0.833\ (10^{-5}) \text{ ft}^2\text{/sec}$$

$$\omega_{TOTAL} = 6000 \text{ gpm (1 min/60 sec) (ft}^3\text{/7.48 gal) (62.1 lb/ft}^3)$$

$$= 830 \text{ lb/sec}$$

*$\Delta T_{FILM\ INSIDE}$ and ΔT_{PIPE} are ignored.

$$\omega_{\text{Long Side Arm}} = 830\ (100/360) = 231\ \text{lb/sec}$$

$$V = \frac{\omega}{A\rho} = \frac{231}{0.0687\ (62.1)} = 54.1\ \text{ft/sec}$$

$$Nu = 0.023\ Re^{0.8}\ Pr^{1/3}$$

$$Re = \frac{3.548}{12}\left(\frac{54.1}{0.833\ (10^5)}\right) = 1.92 \times 10^6$$

$$Pr = 5.20\ @\ 90°F$$

$$Nu = 0.023\ (1.92 \times 10^6)^{0.8}\ (5.20)^{1/3} = 4237$$

$$\frac{hD}{k} = Nu$$

where:

$$D = \frac{3.548}{12}\ \text{ft}$$

$$k = 0.359\ \text{Btu/hr-ft-°F}\ @\ 90°F$$

$$\therefore h_1 = \frac{4237\ (0.359)}{\frac{3.548}{12}} = \underline{5145\ \text{Btu/hr-ft}^2\text{-°F}}$$

B. Outside of Sparger Arm

Assume Average Velocity is 2 ft/sec

Assume Average Film Coef. Temperature = 425°F (Check: (550+298)/2 = 424°F)

Assume Heat Transfer is like a cylinder in Cross Flow

$$\nu = 0.166 \times 10^{-5} \ ft^2/sec \ @ \ 425°F$$

$$k = 0.374 \ Btu/ft\text{-}hr\text{-}°F$$

$$Pr = 0.927$$

$$\frac{h_o D_o}{k} = [0.35 + 0.56 \ (Re)^{0.5}] \ Pr^{0.31}$$

$$D_o = \frac{4}{12} \ ft$$

$$R_e = \frac{2 \ (4)}{12 \ (0.166) \ (10^{-5})} = 4.02 \times 10^5$$

$$h_o = \frac{0.374}{(4/12)} \ [0.35 + 0.56 \ (4.02 \times 10^5)^{0.5}] \ 0.927^{0.31}$$

$$\therefore h_o = 390 \ Btu/hr\text{-}ft^2\text{-}°F$$

A.5.3 Pump Head/Runout

Rated Flow = Q_R = 4625 gpm @ 128 psia

Shut-off Head = 380 psia

$$P = P_{SH} - CQ^2$$

$$128 = 380 - C \ (4625)^2$$

$$C = \frac{380-128}{(4625)^2} = 1.178 \times 10^{-5}$$

@ P = 14.7,

$$Q_{RO} = \sqrt{\frac{P_{SH} - P}{1.178\ (10^{-5})}} = 5570\ \text{gpm}$$

For conservatism, assume runout flow to be 6000 gpm

A.6 REFERENCES

Roark, R. J., "Formulas for Stress and Strain", McGraw Hill, Fourth Edition, 1965.

Hopkins, R. B., "Design Analysis of Shafts and Beams", McGraw Hill.

"Machinery's Handbook", The Industrial Press, 16th Edition, 1959.

Blevins, R.D., "Flow-Induced Vibration", Van Nostrand Reinhold Co., 1977.

Kreith, "Principles of Heat Transfer", International, 1969.

Welty, et. al., "Fundamentals of Momentum, Heat and Mass Transfer", John Wiley, 1969.

Shields, C. M., Wade, G. E., "Core Spray Distribution Report No. 16, 218 Standard Plant", NEDE 13006-3.

GE Drawing 730E854, "Shroud".

Appendix B
FLOW VELOCITY CALCULATIONS

This appendix describes the calculations for the flow velocities supporting statements in Section 3.4.2.1 of the text.

B.1 FLOW VELOCITY IN BYPASS REGION

Assumptions:

1. The plant is operating at rated power (2513 MWt) and flow 77.0×10^6 lb/hr.

2. The flow in the bypass regions is homogeneous.

3. The bypass flow fraction is 12% (9.24×10^6 lb/hr).

4. The water in the bypass regions is saturated.

5. There is no down flow in the bypass region. This assumption is discussed later.

There are two parallel flow paths in the bypass region--one is between the fuel channels, and the other is between the core shroud and the outermost fuel assemblies. The flow areas for these paths are shown schematically in Figure B-1. The simple analysis that follows will give an estimate of the relative flow velocity in the neighborhood of the spray sparger.

Path 1 is between the core shroud and the outermost fuel channels. The flow area along path 1 changes from A_1, between the bottom and top of the active fuel, to A_5 at the top guide to A_6 immediately above the top guide:

A_1 = 3758 in.^{2},

A_5 = 1172 in.^{2},

$A_6 = 7157 \text{ in.}^2$

Path 2 is between the fuel channels. The flow area along path 2 changes from A_2 to A_3 at the top guide to A_4 above the fuel channels:

$A_2 = 3118 \text{ in.}^2$,

$A_3 = 1486 \text{ in.}^2$,

$A_4 = 20160 \text{ in.}^2$

From the geometry and the flow areas, the loss coefficient, K, for path 1 is approximately 1.0 and for path 2 is approximately 1.1. Therefore, for equal pressure drop:

$$\frac{(K_1 W_1^2)}{A_5^2} = \frac{K_2 W_2^2}{A_3^2}$$

$$\frac{(1.0) W_1^2}{1172} = \frac{(1.1) W_2^2}{1486}$$

$$W_1 = 0.93 W_2$$

But, $W_1 + W_2 = 9.24 \times 10^6$.

Therefore,

$W_1 = 4.5 \times 10^6$ lb/hr

The velocity is the bypass region between the core spray sparger and the fuel assemblies is then:

$$V = W_1/\rho A_5 + 4.5 \times 10^6/[3600 \times 45.8 \times (1172/144)] = 3.4 \text{ ft/sec.}$$

The fluid in this region is primarily saturated liquid.

The upward fluid velocity in the periphery of the core bypass region is therefore conservatively estimated to be 3.4 ft/sec. The maximum sized piece that can be lifted from this vicinity in the upper plenum is approximately 0.4 inches in length (Reference 3-1).

B.2 FLOW VELOCITY AT BOTTOM OF BYPASS (TOP SURFACE OF CORE PLATE)

$$V = (W_{Total\ Bypass})/\rho A$$

Since

$$W_{Total\ Bypass} = 9.24 \times 10^6 \text{ lb/hr}$$

$$A = \pi/r\ (D^2 - Nd)^2$$

D = inside diameter of shroud - 174.5 in.

N = number of control rod guide tubes = 137

d = outside diameter of control rod guide tube = 10.75 in.

ρ = density = 45.8 lb/ft^3

Then

$$V = (0.24 \times 10^6/(3600 \times 45.8 \times \pi\ (174.5^2 - 137\ (10.75)^2)/(4 \times 144))$$

$$V = 0.70 \text{ ft/sec}$$

From Reference 3-1, a core spray nozzle cannot be lifted with this velocity and therefore the nozzle will remain at the bottom of the bypass.

B.3 FLOW VELOCITY AT THE TOP OF THE FUEL ASSEMBLY HANDLES

$$W_{Total} = 77 \times 10^6 - 9.24 \times 10^6 = 67.76 \times 10^6 \text{ lb/hr}$$

$$A = na$$

n = number of fuel assemblies = 560

a = area associated with each fuel assembly $\cong (6)^2 = 36 \text{ in.}^2$

The nominal single phase velocity is:

$$V = (W_{Total})/\rho A$$

Therefore,

$$V = (67.76 \times 10^6)/(3600 \times 45.8\ (560 \times 36/144)) = 2.93 \text{ ft/sec.}$$

At this location, the fluid is a mixture of steam and water. Therefore, to estimate the lifting force due to the mixture, a two-phase friction multiplier is used:

$$\phi^2 m = 1 + x\ (\rho_f/\rho_g - 1)$$

where:

$$x = \text{quality} = \frac{\text{mass flow rate of steam}}{\text{total mass flow rate}}$$

$$x = (10.5 \times 10^6)/(77 \times 10^6) = 0.136$$

with,

$$\rho_f = 45.8 \text{ lb/ft}^3$$

$$\rho_g = 2.35 \text{ lb/ft}^3$$

$$\phi^2 = 1 + 0.136\ (45.8/2.35 - 1) = 3.51$$

The total lifting force on a section of core spray pipe per unit length is:

$$F = C_D\ A\ \rho_f\ \phi^2\ V^2/(2g)$$

with

C_D = drag coefficient = 1.2

A = area (4.0 in. x 1 (ft/ft))/12 (in/ft) = 0.333 ft^2/ft

Then the maximum weight than can be lifted is:

$$F = 1.2 \times 0.333 \times 45.8 \times 3.51 \times (2.93)^2/(2 \times 32.2) = 8.6\ lb/ft$$

The buoyant weight of the sparger segment is about 11 lb/ft. Therefore, the sparger pipe segment will not be lifted by the upward velocity lifting force.

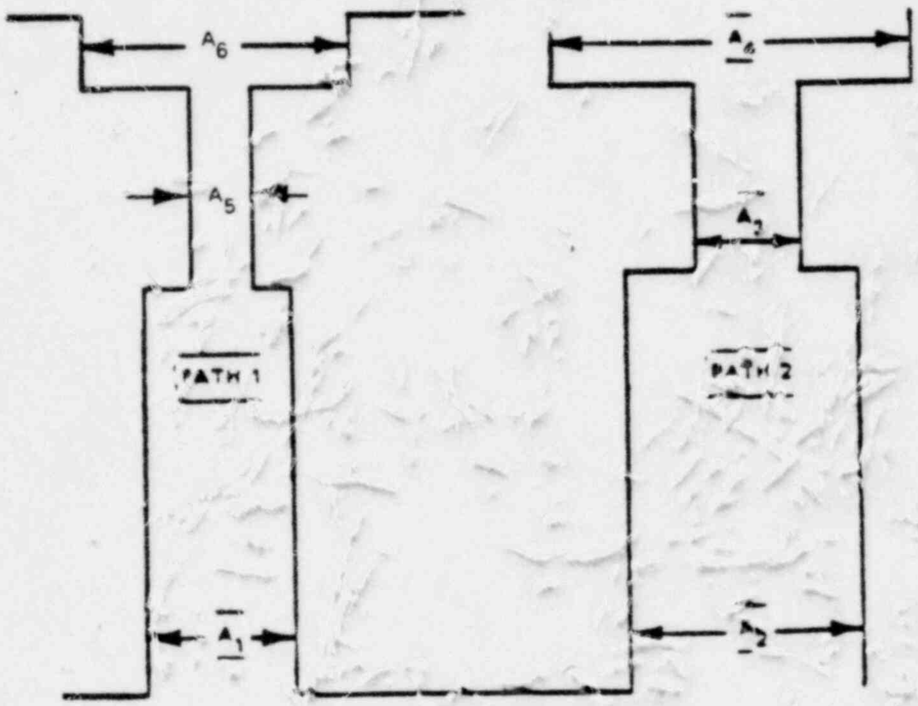

Figure B-1. Flow Paths